



University of
Salford
MANCHESTER

APPLICATION OF THE ROUND-TRIP THEORY TO ELECTRO-DYNAMIC SOURCES OF VIBRATION

Master of Science by Research Thesis

Acoustics Research Centre, The University of Salford, Greater Manchester

Author

JAMES R. EVANS

Supervisor

PROF. ANDY MOORHOUSE

A thesis submitted in partial fulfilment of the requirements for the degree of Master of
Science by Research

March 2021

PREFACE

SECTION	TITLE
i	Abstract
ii	Contents
iii	Symbols, Values & Constants
iv	List of Tables & Figures
v	Acknowledgements

i – Abstract

The Round-Trip Identity, developed by Moorhouse & Elliott at The University of Salford allows the reconstruction of mechanical frequency response functions at remote locations on a test structure, without the need to physically measure at that location. This makes the identity a powerful tool in the field of modal analysis, as it may be applied to structures where measurement at a desired location may be practically difficult or impossible.

This work aims to extend the applications of the Round-Trip Identity, which was originally applied to solely mechanical systems. Work by Moorhouse & Elliott in 2013 suggested that the identity could be applied to any system that is linear and time invariant. Electro-mechanical systems can be found throughout the modern world. This project investigates potential electro-mechanical extensions of the identity, which would allow application of the identity to these hybrid systems.

A thorough summary of electrical network theorems and modal analysis theories is presented. Theories from both fields are subsequently combined to derive the electro-mechanical Round-Trip Identity.

The first objective of this study was to verify the mechanical Round-Trip identity. Following this, an electro-mechanical version of the identity is derived.

A series of increasingly complex experiments is presented that aim to verify the electro-mechanical Round-Trip Identity, the simplest case being a single degree of Freedom on a simply supported beam.

The design of further experiments that would aim to verify the identity for more complex, multi degree of freedom systems is proposed. These relate to the analysis of plates and electric motors.

Finally, recommendations are made for how the identity could be further developed and implemented in an industrial context.

ii – Contents

PREFACE	2
i – Abstract	3
ii – Contents	4
iii - Symbols, Values & Constants.....	9
iv - List of Tables & Figures	10
v - Acknowledgements	12
PART 1: RESEARCH CONTEXT, EXISTING WORKS & THEORY	13
Part 1 Outline	13
1.1 - Introduction & Research Context	14
1.1.1 - Research Context.....	14
1.1.2 - Thesis Aims & Objectives	14
1.1.3 - Thesis Outline.....	14
1.2 – Review of Practical & Theoretical Background	16
1.2.1 - Modal Testing.....	16
1.2.2 - Reciprocity: A Brief History & its Applications	17
1.2.3 - Circuit Analysis	18
Kirchhoff’s Laws.....	18
Tellegen’s Theorem.....	19
Equivalent Circuits	19
Two-Port Analysis	20
1.2.4 - The Round-Trip Identity.....	22
1.2.5 - Electro-Dynamic Shakers & Transduction.....	23
Transduction & Equivalent Circuits.....	23
General Explanation of Electro-Dynamic Shakers	24
Shakers as an Electro-Dynamic Transducer	24
1.2.6 - Section Summary.....	25
1.3 - Existing Scientific Theory & Background	26
1.3.1 - Vibration Measurement Equipment & Procedures.....	26
Sensors and Monitoring	26

1.3.2 - Modal Testing.....	29
General Principles & Practices.....	29
Applications of Modal Testing.....	29
Signal Processing & Analysis	29
Limitations of Modal Testing.....	34
The Round-Trip Identity.....	35
Geometry and Definitions.....	35
1.3.3 - Circuit Analogies	37
Mechanical Systems.....	37
Acoustic Systems	40
1.3.4 - Electric Motors	42
General Principles.....	42
DC Motors.....	43
Brushless DC Motors	44
AC Motors	46
Other Notable Motor Types	47
Motor Selection for Electro-Mechanical Tests	47
1.4 - Part 1 Summary & Conclusions	48
PART 2: DEVELOPMENT OF EXISTING THEORY & EXPERIMENTAL VERIFICATION	50
Part 2 Outline	50
2.1 - Verification of The Published Round-Trip Identity	51
2.1.1 - dBFA Setup.....	51
Input and Output Settings	52
Measurement Parameter Settings	52
Display Settings.....	52
Trigger Threshold	52
2.1.2 - Measurement Procedure.....	52
Results Matrix Structure:.....	53
2.1.3 - Results	54
Validation of Reciprocity.....	54
Round-Trip Validation	55

2.4.4 - Conclusions	56
2.2 - Network Theorems Applied to the Round-Trip Identity	58
2.2.1 - Kirchhoff's Laws / Firestone's Laws & Tellegen's Theorem	58
2.2.2 - Equivalent Circuits & Two-Port Analysis	58
2.3 - Applying Transfer Matrix Analysis to the Round-Trip Identity	61
2.4 - Development of The Electro-Mechanical Round-Trip Identity	63
2.4.1 - Defining the System.....	63
2.4.2 - Transfer Matrices & Circuit Analogies	64
2.4.3 - Units-Based Validation of the Electro-Mechanical Round-Trip Identity.....	66
2.5 - Applying the Round-Trip Identity with Electrodynamical Shaker Properties: Initial 'Forwards-Path' Measurement.....	67
2.5.1 - Aims	67
2.5.2 - Methodology.....	67
2.5.3 - Results.....	69
Conclusions and Further Work.....	71
2.6 - Applying the Round-Trip Identity with Electrodynamical Shaker Properties: Reverse-Path Measurement.....	72
2.6.1 - The Reverse-Path Round Trip Identity:.....	73
2.6.2 - Results.....	74
2.7 - The Electro-Mechanical Round Trip Identity Applied to a Simply Supported Beam: Two-Shaker Setup.....	78
2.7.1 - Experimental Design & Setup	78
2.7.2 - Results.....	80
2.7.3 - Back Electromotive force and Associated Measurement Difficulties	82
2.7.4 - Changing the Electro-Mechanical Circuit Analogy	83
2.8 - Two-Shaker Experiment with the Revised Circuit Analogy Applied to a Simply Supported Beam	85
2.8.1 - Experimental Setup	85
2.8.2 - Results.....	86
2.8.3 - Conclusions	88
2.9 - Applying the Electro-Mechanical Round-Trip Identity to MDOF Systems	89
2.9.1 - Introduction to Multi-Degree-of-Freedom Analysis	89

2.9.2 - Experimental Changes.....	89
2.9.3 - Matrix Rank, Over-Determination & Regularisation	90
2.9.4 – Applying the Electro-Mechanical Round-Trip Identity to a Simple Beam with a Multi-Point Interface	91
2.10 - Part 2 Summary & Conclusions	95
2.10.1 - Summary	95
Development of the Electro-Mechanical Round-Trip Identity	95
Single-DOF Experimental Validation	95
Changing the Electro-Mechanical Circuit Analogy	96
Final SDOF Verification	96
2.10.2 - Conclusions.....	96
Theoretical Validity of the Electro-Mechanical Round-Trip Identity	96
Experimental Findings & Practical Considerations.....	97
Recommendations for Use & Limitations of the Electro-Mechanical Round-Trip Identity.....	98
PART 3: PLANS FOR FURTHER EXPERIMENTATION.....	101
Part 3 Outline	101
3.1 - Applying the Electro-Mechanical Round-Trip Identity to a Plate with a Multi-Point Interface ...	102
3.1.1 - Experimental Design.....	102
3.1.2 - Identifying Potential Challenges	103
3.2 - Applying the Electro-Mechanical Round-Trip Identity to a Simple DC Motor with a Multi-Point Interface	104
3.2.1 - Motor Selection	104
3.2.2 - Experimental Design.....	104
3.2.3 - Identifying Potential Challenges	105
3.3 – Applying the Electro-Mechanical Round-Trip Identity to More Complex Motor Designs	107
3.3.1 - Brushless DC Motors	107
3.3.2 - AC Induction Motors	108
AC Motor Input Signal.....	108
AC Motor Structure	108
3.3.3 - Stepper Motors	110
3.4 – Part 3: Summary, Conclusions & Further Work	111
3.4.1 - Summary & Conclusions	111

3.4.2 - Suggestions for Further Investigation	111
PART 4: APPENDICES.....	113
Appendix A: Glossary of Commonly Used Terms.....	114
Appendix B: Identifying the Optimal Method for Measuring Electrical Current	119
Introduction	119
Sensor Setup.....	122
Current Path & Connections.....	123
Powering the Sensor.....	124
Signal Determination & Interpretation	124
Conclusions	125
Appendix C: References.....	126

iii - Symbols, Values & Constants

This section provides a list of parameters, values and symbols that will occur frequently during this document. Definitions of these can be found at Appendix A.

Table ii.1: Commonly Used Symbols & Parameters

Symbol	Parameter	SI Unit
a	Acceleration	Metres per second squared, ms^{-2}
y	Admittance	Siemens, S
C_M	Compliance	Metres per Newton, mN^{-1}
I	Current	Amperes, A
ρ	Density	Kilograms per cubic metre, kgm^{-3}
x	Displacement	Metres, m
F	Force (Generalised)	Newtons, N
f	Frequency	Hertz, Hz
ω	Frequency (Angular)	Radians per second, $rad \cdot s^{-1}$
Z	Impedance (Generalised)	Mixed
L	Inductance	Henries, H
l	Length	Metres, m
M	Mass	Kilogram, kg
Y	Mobility (Generalised)	Mixed
P	Power (Generalised)	Watts, W
R	Resistance (Electrical)	Ohms, Ω
p	Sound pressure	Pascals, Pa
k	Stiffness	Newtons per metre, Nm^{-1}
τ	Torque	Newton Metres, Nm
u	Velocity (Generalised)	Metres per second, ms^{-1}
α	Velocity (Angular)	Radians per second, $rad \cdot s^{-1}$
v	Voltage	Volts, V
j	Unit imaginary number, $\sqrt{-1}$	None
X_E	Reactance (Electrical)	Ohms, Ω

Table ii.2: Subscripts & Accents

Symbol	Name	Unit	Explanation / Qualifiers
A	Acoustic quantity	Various	Subscripts indicate respective domain
E	Electrical quantity	Various	
M	Mechanical quantity	Various	
$[x \dots x]$	Vector / matrix	None	Square brackets indicate vectors / matrices
\int	Integral	Various	Numerous variables may be integrated
$\frac{dy}{dx}$	Derivative	Various	Numerous variables may be differentiated
$ _ $	Magnitude	None	Straight brackets indicate magnitude
$_$	Vector	None	Straight single bar indicates a vector quantity

iv - List of Tables & Figures

Table iii.3: List of Tables

Table Number	Title	Page Number
1.3.1	Equivalent Parameters for the Mobility and Impedance Analogies (adapted from Beranek, 1996)	37
1.3.2	Electrical, Mechanical and Acoustical Analogies (adapted from Beranek, 1996)	39
2.1.1	Experimental Apparatus – Verification Experiment	50
2.1.2	Measurement Parameters for Verification Experiment	51
2.5.1	Forwards-Path Measurement Channel Allocation	68
2.7.1	Two-Shaker Experiment Channel Allocation	78
2.9.1	MDOF Experiment Analyser Channel Allocation	92
2.9.2	Multi-Point Interface Results Matrix	93
B.1	Relevant LEM HX 05-P Current Sensor Specifications	121

Table iii.4: List of Figures

Figure Number	Title	Page Number
1.2.1	Example of Reciprocity in Terms of Inputs and Outputs of a System or Function	16
1.2.2	Kirchhoff's Law Summaries	18
1.2.3	Two-Port Network Diagram	20
1.3.1	FRFs in the Time & Frequency Domains	31
1.3.2	Types of Frequency Response Function	32
1.3.3	(A) Round-Trip Geometry (B) Round-Trip Paths, where portions of the Round-Trip path are numbered	35
1.3.4	Fundamental Motor Components and Structure	42
1.3.5	Phases and Driving Signals for a Three-Phase BLDC Motor	44
1.3.6	Component interactions in a Three-phase BLDC motor	44
1.3.7	Three-Phase AC Supply Signals	45
2.1.1	Measurement Positions on a Simple Beam	50
2.1.2	Example Coherence Plot for Excitation of a Simply Supported Beam	52
2.1.3	Reciprocity Validation with H_1 Data	53
2.1.4	H_1 vs. H_2 Response Comparison	54
2.1.5	Reconstructed Accelerance Responses at c_1 (A) and c_2 (B) using The Round-Trip Identity	55
2.2.1	Equivalent Circuit for a Simple Modal Testing Setup	58
2.3.1	Transfer Matrix System Diagram	60
2.4.1	Electro-Mechanical Transfer Matrix System Representation	63
2.5.1	Schematic Round-Trip Representation (Forwards-Path)	66
2.5.2	Diagram of 'Forwards-Path' Measurement Setup	67
2.5.3	Comparison of Measured and Reconstructed Values of A_{cc} (Forwards-Path)	69
2.6.1	Visual Representation of Forwards (A) and Reverse (B) Round-Trip Paths	71

2.6.2	Reverse-Path Experimental Setup	72
2.6.3	Comparison Between Forwards-Path and Reverse-Path Accelerance Response FRFs	74
2.6.4	Reciprocity Checks for A_{ab} vs. A_{ba} (A) and A_{ac} vs. A_{ca} (B)	76
2.7.1	Two-Shaker Experimental Setup Diagram	78
2.7.2	Two-Shaker Measured vs. Reconstructed Accelerance Responses at c (Forwards & Reverse)	79
2.7.3	Two-Shaker Measured vs. Reconstructed Phase Responses at c (Forwards & Reverse)	80
2.8.1	Revised Two-Shaker Setup for the Simple Beam Experiment, using the Impedance-Mobility Analogy	84
2.8.2	Two-Shaker Forwards-Path Accelerance Responses for a Simple Beam	85
2.8.3	Two-Shaker Reverse-Path Accelerance Responses for a Simple Beam (Excitation Comparison)	86
2.9.1	Multi-Point Interface Block Region Diagram	91
2.9.2	Proposed Experimental Setup for the MDOF Experiment Applied to a Simply Supported Beam	92
3.1.1	Proposed Experimental Design for the Analysis of a Plate with a Multi-Point Interface	102
3.2.1	Single-Phase DC Motor Experimental Setup	103
3.3.1	BLDC Motor Feedback Loop & Signal Paths	106
3.3.2	Three-Phase AC Supply signals	108
3.3.3	Squared AC Power Phases and Summations	109
B.1	Diagrammatic Representation of Common-Mode Signals	118
B.2	Electro-Mechanical Round Trip Comparison – Measured vs. Current Clamp Responses (Reverse-Path)	119
B.3	Current Sensor Structure & Pin Assignments	122
B.4	Current Sensor Position Diagram	123
B.5	Linear Interpolation Over Sensor Measurement Range	124

v - Acknowledgements

I have enjoyed the challenges presented by conducting original research - whilst my studies have been largely self-motivated, there are a number of people without whom they would have been significantly more challenging.

Firstly, I would like to thank Prof. Andy Moorhouse, who has provided invaluable guidance and insight into the workings of The Round-Trip Identity and supported me throughout this process. I would also like to thank Dr. Josh Meggitt for always being willing to answer my persistent questions and help with the setup of my practical work! I am grateful for Kevin Wiene's input to the design of my experiments, which helped overcome several significant challenges.

My studies would not have been possible without the support of my parents, whose generosity has been invaluable - especially so over the last few years. Thank you for allowing me to be able to freely pursue my ambitions and further my knowledge.

I am indebted to my girlfriend, Claire for her constant support throughout my studies. Thank you for all that you have done to keep me motivated, and for inspiring me to apply myself in the same way that you continue to in your own work. Your expertise in reviewing scientific documents has also been incredibly helpful in polishing this document!

Given the current state of the world, the last few months have been incredibly different to any expectations I might have had. This has led being in the company of several people pretty much non-stop. I'd like to thank my ~~long-standing~~ long-suffering flatmate, Chris, and significantly more recent flatmate, Charlotte, for putting up with my weird sleeping patterns and unrelenting puns! Thank you to both of you, and also to Claire, for keeping me fed over the final push to finish my thesis. You've saved me from countless late-night bowls of cereal.

Finally, I would like to thank Neil Purslow, for helping me to discover the field of acoustics and setting me on the path that I am now on. I'm delighted to have found a topic that fascinates me to this extent and am excited to see where my career takes me from here.

PART 1: RESEARCH CONTEXT, EXISTING WORKS & THEORY

Part 1 Outline

The initial part of this thesis aims to provide the reader with a solid understanding of topics that underpin The Round-Trip Identity, modal testing and electrical network theorems. This will be achieved through a thorough discussion of relevant literature and a detailed scientific background.

Part 1: Contents

SECTION	TITLE
1.1	Introduction & Research Context
1.1.1	Research Context
1.1.2	Thesis Aims & Objectives
1.1.3	Thesis Outline
1.2	Review of Practical & Theoretical Background
1.2.1	Modal Testing
1.2.2	Reciprocity: A Brief History & Its Applications
1.2.3	Circuit Analysis
1.2.4	The Round-Trip Identity
1.2.5	Electro-Dynamic Shakers & Transduction
1.2.6	Section Summary
1.3	Existing Scientific Theory & Background
1.3.1	Vibration Measurement Equipment & Procedures
1.3.2	Modal Testing
1.3.3	Circuit Analogies
1.3.4	Electric Motors
1.4	Part 1 Summary & Conclusions

1.1 - Introduction & Research Context

1.1.1 - Research Context

Accurately quantifying the vibration of an object is the subject of a significant amount of research. This may be necessary for reasons ranging from reducing annoyance caused by noise and vibration from products, through to managing vibration levels to prevent failure of components in critical applications such as aerospace or automotive industries.

Whilst modern computer modelling solutions can be applied to complex systems, experimental testing remains a fundamental part of analysis of vibrating structures. Experimental data can be fed into numerical models in order to calibrate them, inform their design and improve the extent to which they reflect real-world scenarios.

Experimental modal tests are an established practice in determining the modal properties of a test structure. This process needs to be carefully considered in order to obtain measurements that are representative of the test object, but this often leads to practical difficulties, challenges and limitations. As a result, any method that presents more options for obtaining high-quality, representative data is of significant value. One such method is The Round-Trip Identity.

The Round-Trip Identity allows reconstruction of the vibratory properties of an object at a remote position on the object. It may not be possible to apply excitation at this position for practical reasons but understanding how the structure behaves at that point may be of particular interest.

The Round-Trip Identity was originally intended to be applied to mechanical problems. Subsequent work has suggested that the identity could be expanded to problems in additional domains, opening up the potential for numerous new applications.

1.1.2 - Thesis Aims & Objectives

- To experimentally verify the Round-Trip Identity for a simple mechanical system
- To propose modifications to the Round-Trip Identity that allow it to be implemented using both mechanical and electrical parameters
- To experimentally verify the proposed modifications with a series of increasingly complex tests, starting with a simply supported beam
- To evaluate the effectiveness of the identity and the ease of its application
- To detail the design of a series of experiments to apply the identity to multi-degree-of-freedom systems
- To provide guidance and suggestions for the successful implementation of the identity, and detail potential future experiments and further work

1.1.3 - Thesis Outline

This body of work provides a thorough overview of the literature and theory underpinning experimental modal analysis methods and electrical network theorems, with a particular focus on the application of network theorems to the modal analysis of hybrid mechanical and electrical systems.

The foundational theory that the work is based on is The Round-Trip Identity developed at The University of Salford by Professor Andy Moorhouse and Dr Andy Elliott. This theory allows reconstruction of frequency response functions at remote locations on a test structure, without the need to excite the structure at that position. Initially the identity contained solely mechanical parameters, but subsequent work by Moorhouse & Elliott extended this to include an airborne excitation. This led to interest in potential new applications of the identity, including the potential for electrical applications.

This work aims to develop a new form of The Round-Trip identity that includes electrical parameters in addition to mechanical ones. Many mechanical devices that are subjected to modal testing are powered electrically, so this would result in the identity being applicable to a wider range of problems.

An initial experiment was conducted to verify the Round-Trip Identity. The existing identity was then developed by applying principles from network theorems and equivalent circuit theory. Following this, a series of original experiments was designed to validate the newly devised Electro-Mechanical Round-Trip Identity, concluding with recommendations for the design of future experiments, the practicality of implementing the identity and considerations for its use.

1.2 – Review of Practical & Theoretical Background

This section provides a summary of some of the main established foundational theories and bodies of research that underpin this study. It covers details required for the novel theoretical development and practical experimentation contained in parts 2 and 3 of this thesis. Whilst authors in the field of acoustics have considered some of these topics in combination with each other, it appears that connecting all of these topics and theories and applying them to an external system is novel. It is divided into the following key areas:

- Modal Testing
- Reciprocity
- Equivalent Circuit Theorem and Other Network Theories (Kirchhoff's laws, Tellegen's Theorem and Two-Port analysis)
- The Round-Trip Identity
- Transduction (with specific reference to electro-dynamic shakers)

A more technically detailed explanation of many of the topics included in this review can be found in Section 1.3.

1.2.1 - Modal Testing

The modern era of modal testing is considered by Brown & Allemang to have started in the mid 1960s. Whilst the equipment was available prior to this, this was the first point in time where equipment and sensors were commercially available, and the accompanying theory was sufficiently developed. The Fast Fourier Transform was first implemented in 1965, and the first real-time analyser was developed in 1967 (Brown & Allemang, 2007).

Halvorsen & Brown later published an impulse method for structural frequency response testing in 1977, outlining the benefits and limitations of testing using impulsive excitations (Halvorsen & Brown, 1977). The first application of multiple input, multiple output (MIMO) testing was in 1979. Modern developments in computer processing power and speeds have enabled rapid testing of complex systems, with impressive functionality in terms of data processing, visualisation and analysis.

A thorough overview of modal testing practices and underpinning theory is provided in Modal Testing by Ewins. This comprehensive resource covers all fundamental aspects of modal testing and analysis.

Generally, performing a modal test is comprised of several main processes, categorised by Ewins (2000) as:

- The theoretical nature of the vibrating structure
- Accurate measurement of this vibration, using the most appropriate means based on current guidance, standards and best practice
- Thorough, robust and appropriate data analysis methods
- A relevant, realistic modelling method that considers the limitations of the obtained data and desired outputs

The end result of modal analysis is a set of modal parameters that describe a system in terms of its resonances, mode shapes and damping. These can be fed into numerical models and simulations.

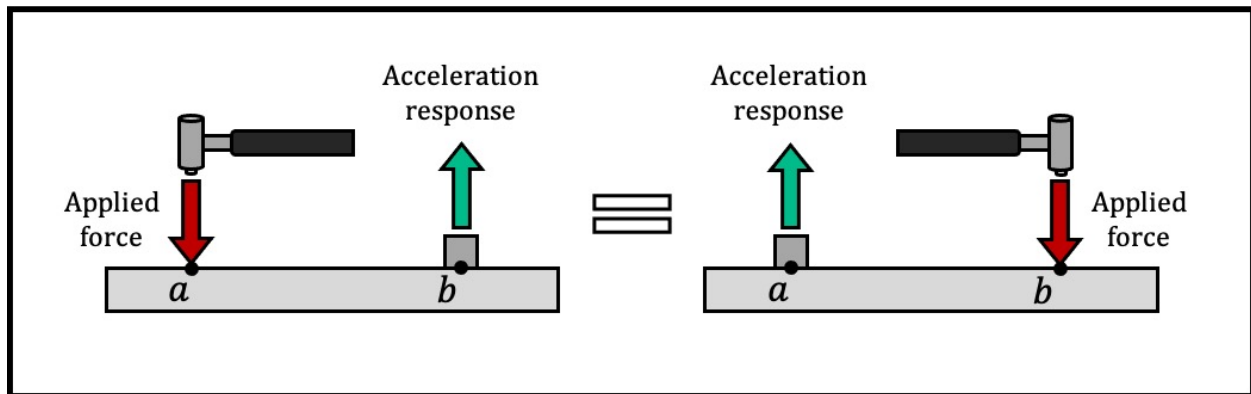
Ewins notes that these stages are often considered individually, but that the process is most effective when consideration is given to the connections between them. For example, it is important to consider how data will be measured when considering the analysis methods and subsequent modelling process that will be applied. Similarly, a fundamental misunderstanding of vibratory phenomena could result in inappropriate measurement practices or poor experimental design choices.

A more thorough and technically detailed explanation of modal testing is provided at Section 1.3.2 of this thesis.

1.2.2 - Reciprocity: A Brief History & its Applications

The principle of reciprocity is applicable to a diverse range of problems involving linear systems. It states that if a unit load or excitation is applied at a point a in a system, and the response at another point b is measured as Y_{ab} , the same load or excitation applied to point b would result in an identical response being measured at point a , Y_{ba} . This means that the response of the system is independent of the direction of the transfer path through it, that is that $Y_{ab} = Y_{ba}$. An example of this is shown in Figure 1.2.1, with the excitation of a beam using an impact hammer, and measurement of an acceleration response using an accelerometer. As stated, the resulting transfer function describing the response of the beam is independent of the direction of the transfer path being considered:

Figure 1.2.1: Example of Reciprocity in Terms of Inputs and Outputs of a System or Function



Reciprocity can be applied to numerous fields, dating back to work as early as the 19th Century. Its influence is explored thoroughly by Potton (2004). Some of the most notable contributions include:

- Optical reciprocity – originating from work by Helmholtz in 1866, through his extension of Green’s theorem. Green’s theorem is named after Green due to the influence of his divergence theorem (Green, 1828), but was first proven by Riemann in his 1851 inaugural dissertation (Riemann, 1851).
- Acoustic reciprocity – attributable to Volume II of Rayleigh’s Treatise of Sound (Rayleigh, 1878), based upon Helmholtz’s work.

- Electromagnetic reciprocity – originating from Lorentz’s work on electromagnetic reciprocity in 1896. This resulted in the development of two-port analysis, initially applied to electrical networks.

Reciprocity in the context of modal analysis is largely attributed to the work of Maxwell and Betti and referred to as The Maxwell-Betti Reciprocal Work Theorem, first published in 1872. The theorem is expressed as with the previous relationships, but more specifically in terms of displacement observed by linearly elastic structure with a loading force applied to it.

Reciprocity has been an important principle underpinning many areas of physics. This principle is fundamental in modal testing and analysis. The implementation of The Round-Trip Identity also heavily relies on the principle of reciprocity.

1.2.3 - Circuit Analysis

Circuit analysis is an important skill for designing functioning electronic devices. Its importance is highlighted by the powerful tool that is equivalent circuit theory.

Use of equivalent circuits allows complex problems in a variety of domains to be solved by representing them as an equivalent to an electrical circuit. This is often far simpler than the alternative - solving multiple complex partial differential equations. As a result, an understanding of interactions between simple electronic circuit components and properties is invaluable due to its transferability to problems in acoustical, electrical, magnetic or other systems (or combinations thereof).

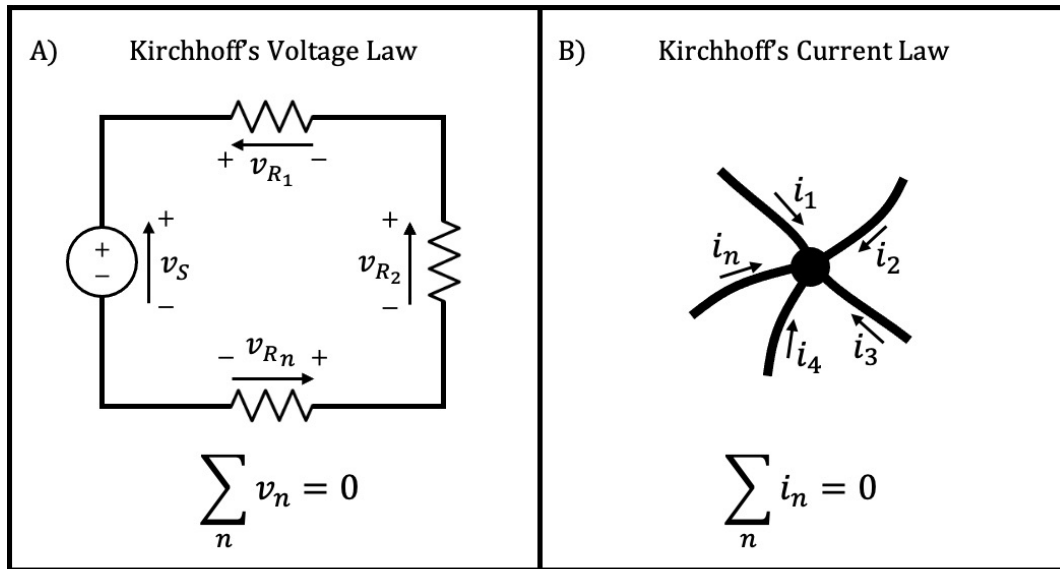
Kirchhoff’s Laws

Kirchhoff devised two laws that are fundamental in circuit analysis – one relating to voltage and the other to current. These describe how voltage and current behave in electrical networks and are based on Maxwell’s equations of electromagnetism.

Kirchhoff’s Voltage Law states that the sum of voltages around a circuit loop is equal to zero. A visual representation of this is shown in Figure 1.2.2.A.

Kirchhoff’s Current Law states that the sum of currents at a node is equal to zero. A visual representation of this is shown in Figure 1.2.2.B.

Figure 1.2.2: Kirchhoff's Law Summaries



Combined application of Kirchhoff's laws and Ohm's Law can enable determination of voltage, current and resistance values at any given point or across any given component in a circuit. These fundamental variables can be used to calculate many other related parameters. For these reasons, Kirchhoff's laws are indispensable in circuit and network analysis. They also form the foundation for several other useful network theorems.

Penfield, Spence & Duinker (1970); Ramachandran & Ramachandran (2001) and Quintela et al (2009) all concur that Kirchhoff's Laws are applicable to a network based on its topology, and not the specific properties in question. This means that Kirchhoff's Laws can be applied to many other types of system, not just electrical circuits.

Tellegen's Theorem

Tellegen's Theorem applies to all circuits that obey Kirchhoff's voltage and current laws. It states that a given instant in time, the sum of instantaneous power in a network (or branch of a network) is equal to zero. This is a logical extension of Kirchhoff's laws, given that electrical power is the product of voltage and current, which are the subjects of Kirchhoff's Laws.

Penfield, Spence & Duinker and Quintela et al. also explain that the theorem can be applied to many systems, irrespective of linearity, time variance, reciprocity or hysteresis (Penfield, Spence & Duinker, 1970 and Quintela et al, 2009). This is because Tellegen's Theorem can be derived solely from Kirchhoff's laws, which are valid for many other types of system and are a consequence of the topology of a network, irrespective of the nature of the variables in question.

Equivalent Circuits

Equivalent circuits elegantly relate electrical circuits to systems in other non-electrical domains. They are a powerful tool for analysing systems and arise from similarities between differential equations relating the different domains. These equations are similar in their form in terms of mechanical displacement and electrical charge.

Early work on electro-mechanical equivalent circuit analogies by Firestone summarises that every linear mechanical system can be reduced to a group of closed mechanical circuits, and that force and velocity relationships equivalent to Kirchhoff's voltage and current laws can be applied as a result. Firestone refers to the mechanical versions of Kirchhoff's laws as "force and velocity laws" (Firestone, 1933).

Additional likeness can be drawn by comparing impedances in both domains. In the electrical domain, electrical impedance is the ratio of voltage and current:

$$Z_E = \frac{V}{I} \quad (1.2.1)$$

Mechanical impedance is the measure of opposition to an applied force, given by the ratio of force and velocity:

$$Z_M = \frac{F}{v} \quad (1.2.2)$$

This likeness gives rise to one of two electro-mechanical analogies that can be considered – the impedance analogy – so named because it preserves the notion of impedance in the analogy between mechanical and electrical systems.

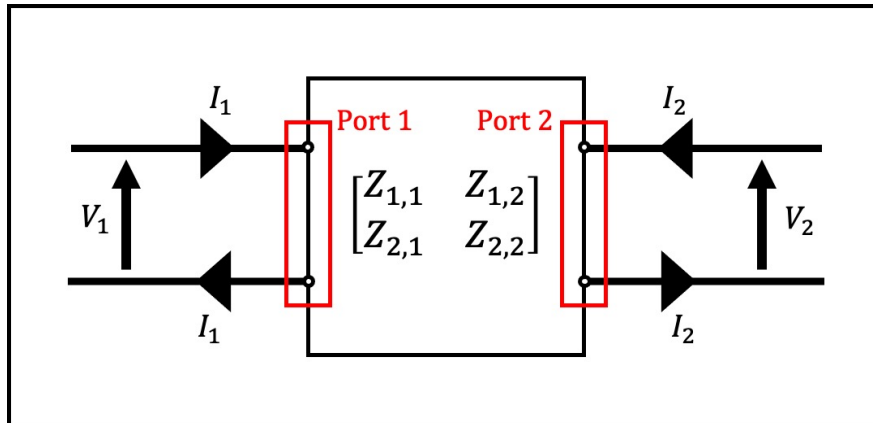
This is of interest to vibration measurement and modal analysis because many vibrating systems can be simplified as linear problems involving springs, resistances and masses. All of these fundamental mechanical elements have electrical circuit equivalents.

This brief explanation is sufficient to emphasise the value of equivalent circuits, as they allow many useful electrical network theorems to be applied to mechanical systems in a manner that can often simplify calculations. A more technical explanation of electro-mechanical equivalent circuits, component equivalencies and related calculations can be found at Section 1.3.3.

Two-Port Analysis

Two-port analysis is a valuable tool for modelling reciprocal systems. The term "port" refers to a pair of terminals at the periphery of an electrical network, where a signal can be applied to or exit the network. Two-port networks have two pairs of terminals, connected by a network of circuit elements. The properties of this network are arbitrary. The network connecting the ports can be considered as a "black box" type system, the contents of which are arbitrary, but with the combined effect of the network being given by a transfer function. This function applied to a signal at the input port gives the output signal at the opposing port. This is visually represented in Figure 1.2.3.

Figure 1.2.3: Two-Port Network Diagram



The current flowing into and out of each port and the potential difference across each set of terminals are sufficient to characterise the network with an impedance matrix (or more generally a transfer matrix). Each element of this matrix relates the voltage of a port to the current at a port. This results in four potential combinations and thus four elements in the impedance matrix.

The elements are related as such:

- $Z_{1,1}$ is the quotient of voltage V_1 by the current I_1
- $Z_{1,2}$ is the quotient of voltage V_1 by the current I_2
- $Z_{2,1}$ is the quotient of voltage V_2 by the current I_1
- $Z_{2,2}$ is the quotient of voltage V_2 by the current I_2

The value of each element can be determined by holding the voltage and current values unrelated to the element at zero. If the network does not contain dependent sources (that is elements with properties that are reliant on other network elements), $Z_{1,2}$ and $Z_{2,1}$ will be similar to each other, i.e. reciprocal. This property of the impedance matrix will prove to be useful later in this work, when implementing the Round-Trip Identity.

The notion of the impedance matrix as a means of characterising a system extends beyond electrical network analysis. This can be achieved through pairing equivalent circuit theory with two-port analysis. Many types of problems in differing domains (or hybrid systems) make use of transfer matrices, especially those considering wave propagation through stratified media.

An interesting application of two-port analysis and transfer matrices is the calibration of measurement microphones according to BS 61094-2:2009. This standard applies two-port analysis to the context of a system with mechanical, electrical and acoustical aspects.

The standard details an equivalent circuit that is derived from the microphone calibration setup. This circuit is suitable for two-port analysis, which allows determination of an impedance matrix and two-port equations in terms of the pressure sensitivities of the microphones (BSI, 2009).

A reciprocal microphone is defined by the standard as being linear, passive and having open circuit reverse and forward transfer impedances that are equal in magnitude.

The standard details a method for performing calibrations with either three microphones (two being reciprocal), or two microphones (one of which is reciprocal) with an auxiliary sound source.

BS 61094-2:2009 outlines the stages of calibration by reciprocity as follows:

- For two microphones, determine the product of pressure sensitivities of the coupled microphones, based on their acoustic and electrical transfer impedances.
- Present the two microphones to the same external source so that they experience an identical sound pressure level. The ratio of the output voltages is then equivalent to the ratio of pressure sensitivities.
- When the pressure sensitivity ratio is known, each individual sensitivity can be determined from the product and the ratio of the two sensitivities.
- For three microphones, connect them together via a coupler, sequentially in pairs. Using one microphone as a source and the other as a receiver will allow determination of the electrical transfer impedance for each pair. The acoustic transfer impedance can be determined from the properties of the microphone.
- These transfer impedances can then be used to determine the product of the pressure sensitivities for each combination of microphones. The sensitivity of each of the 3 individual microphones can be determined from the three pair-wise sensitivity products.

The definitions and methods contained in this standard provide an insight into the importance of boundary conditions when defining impedance matrices and defining a system. The definitions for electric transfer impedance and acoustic transfer impedance refer to a blocked microphone diaphragm and unloaded electrical terminals respectively. Without these conditions being met, measurements will be invalid. This will be considered when defining boundary conditions in original experiments conducted as part of this study

BS 61094-2:2009 (BSI, 2009) also features equivalent circuits that represent the system. It derives two-port equations from them in order to allow calculation of pressure sensitivities of the two microphones.

1.2.4 - The Round-Trip Identity

The Round-Trip identity is a useful tool for conducting modal analysis of 'difficult' structures. In practice, a machine, assembly or structure may need to be tested during operation or positioned in the scenario that it will be used or installed in (referred to as in-situ testing) to obtain useful data. A problem that can arise as a result is that suitable excitation regions are inaccessible. Excitation at these points using a force hammer or electro-dynamic shaker is therefore not viable. Positions may also not be suitable for mounting of sensing equipment such as accelerometers.

Given the identification of this practical difficulty, a method for determining the vibratory properties at a remote position is clearly desirable. The round-trip theory was devised to address this by Moorhouse & Elliott in 2013, following on from their previous work on measurement of structural dynamic

properties *in situ* (Moorhouse, Elliott & Evans, 2009 and Moorhouse, Evans & Elliott, 2011). The difficulties provided by certain test methods requiring free suspension of a test structure were noted, and it was argued that even if this was achievable, it would not necessarily yield transferrable or representative results in other contexts.

It is pertinent to explain the term “*Green’s Function*” at this point, as it will be necessary in order to explain the development of the Round-Trip Theory. Green’s Functions are a mathematical tool used to solve normal or partial linear differential equations. They have underpinned discoveries and developments in a wide range of fields throughout physics and engineering since their inception by Green in the 1830s. The field of primary concern to this body of work is structural dynamics.

Moorhouse & Elliott’s first work on the round-trip identity aimed to reconstruct Green’s Functions from experimental data at passive locations, where there is no directly applied external force.

The paper identifies that despite its focus being on structural problems, there is no reason why the identity could not be applied to any linear, time invariant (LTI) system. This led to subsequent work which extended the identity into the acoustical domain, namely with an airborne excitation method applied using a calibrated volume velocity source (Elliott & Moorhouse, 2017).

The work experimentally validated the round-trip identity with an airborne excitation method. This inclusion of acoustical parameters (volume velocity and sound pressure) expands potential applications of the round-trip theory to an entirely new set of problems. As originally stated in Moorhouse & Elliott’s 2013 paper, there is no reason why the identity cannot be applied to any LTI system (Moorhouse & Elliott, 2013). A logical extension to working in mechanical and acoustical domains is to consider electrical applications. This work has identified a clear connection between the mechanical domain and the electrical domain – in the forms of two-port and equivalent circuit analysis. It therefore seems that these theories could be combined to extend the Round-Trip Identity to allow characterisation of remote points in hybrid electro-mechanical systems. Perhaps the most obvious electro-mechanical device that this could be applied to is the electric motor – a device that can be found in countless different machines across industry and society.

Following this conclusion, further discussion of transduction between these two domains is particularly relevant, as an understanding of this will help inform experimental design in order to validate any novel theories.

1.2.5 - Electro-Dynamic Shakers & Transduction

Transduction & Equivalent Circuits

Transduction is defined as the conversion between two different types of energy. This change in energy will always obey the principle of conservation of energy, where energy cannot be created or destroyed, only transferred. This transfer is not always 100% efficient, so some losses may occur, for example thermal radiation from operation of electrical devices.

Transduction is performed in many systems by components categorised as sensors or actuators. Sensors respond to a stimulus and actuators provide control over devices or systems. Examples of

sensors include microphones, accelerometers and Hall effect sensors. Examples of actuators include motors and loudspeakers and electro-dynamic shakers.

General Explanation of Electro-Dynamic Shakers

An electro-dynamic shaker is a device not unlike a loudspeaker that takes an electrical signal and outputs a reciprocating motion. The properties of the input electrical signal determine those of the vibration outputted by the shaker. Shakers have become an important tool in modal analysis due to the high quality, clean responses they can give due to their high signal-to-noise ratio. A more detailed technical explanation of shakers can be found at Section 1.3.1.

Shakers as an Electro-Dynamic Transducer

Shakers are of particular interest to this work, having been identified as a valuable tool for modal analysis and also a transducer between the mechanical and electrical domains. Understanding the nature of this transduction will help identify appropriate criteria for shaker and electric motor use contribute to maximal quality of results in these cases and allow development of theories that connect the mechanical and electrical domains.

Most existing work on shaker properties focusses on building a model of the shaker itself, in order to better understand its effects and limitations during modal testing (Smallwood, 1996; Della Flora & Gründling, 2008). Significant investigations were made by Smallwood in 1996-1997 (Smallwood, 1996 & 1997). Smallwood's work aims to achieve two objectives:

- To be able to “run force-controlled vibration tests without the need to measure force”.
- To develop a virtual testing environment where the “testability of a test item could be checked before the test was conducted” (Smallwood, 1997)

Smallwood's work places significant focus on determining the two unknown variables (out of force, voltage, acceleration and current). This is suggested as being to either determine voltage and current requirements for testing with a given shaker, or to quantify the maximum achievable force or acceleration in the reverse case. Smallwood notes that it may be desirable to set force limits when testing, and the method would allow this without direct measurement of this force.

This differs from the approach of this study, which aims to characterise properties of an external system and not the internal properties of the shaker, as is the case with Smallwood's research. It should be noted that this aim is not possible without building on an understanding of the internal properties of the shaker.

A shaker consists, much like a loudspeaker, of a moving coil positioned in a magnetic field. A table structure is connected to this via the shaker armature, with the device under test mounted to it. Passing a current through the coil causes a force in the axial direction, resulting in the motion of the shaker armature and table.

Magnetic flux density (i.e. the strength of a magnetic field) is typically constant and homogenous in the air gap between the shaker coil and the body, except at low frequencies with large amplitude displacements (Della Flora & Gründling, 2008). This means that the force generated by the shaker is proportional to the current in its coils. This suggests that the behaviour of a shaker should satisfy the

conditions required for equivalent circuit or two-port analysis – that is in terms of linearity and time invariance.

1.2.6 - Section Summary

This section has summarised the contributions of some key bodies of work in fields ranging from modal analysis and principles that underpin it. This is most notably in relation to the principle of reciprocity, and how it underpins experimental modal analysis, and across many other scientific and mathematical fields.

The relevance of several key network theorems was discussed (Kirchhoff's Laws, Tellegen's Theorem and Two-Port Analysis), with an emphasis on considering these beyond the scope of electrical problems and circuit analysis. These tools are valuable in the analysis of other types of system or network, including those that can be considered as hybrids spanning two or more interfacing domains.

An overview of transduction was provided, focussing mainly on the context of electro-dynamic shakers. These are of particular interest to this work as they are a commonly used excitation method in experimental modal analysis. It was identified that work relating to electro-dynamic shakers is primarily concerned with characterising the properties of the shaker itself and does not extend in scope to analysis of the system connected to the shaker.

The Round-Trip Identity is the theory that underpins the entirety of this research, and an overview of its background, context, applications and scope for modifications and resulting applications was provided. This theory was originally developed by Moorhouse & Elliott in 2013, who have subsequently published work relating to applying the identity with an airborne excitation in 2017.

Following this review of some relevant bodies of research, this work will continue with a more robust and detailed background on important topics that provide a foundation for the development of the Electro-Mechanical Round-Trip Identity.

1.3 - Existing Scientific Theory & Background

The purpose of this section is to provide a thorough explanation of the aspects of science that underpin the development of the Electro-Mechanical Round-Trip Identity. Consequentially this draws on a range of topics relating to mechanical and electrical systems, in addition to signal processing methods that are involved with the analysis of such systems. A summary of electric motors is provided, with a focus on their structure, operation and comparative benefits. This will be drawn on in Part 3, where the Electro-Mechanical Round–Trip Identity will be applied to a range of different motors.

This section is structured as follows:

1.3.1 - Vibration Measurement Equipment & Procedures

1.3.2 – Modal Testing

1.3.3 – Circuit Analogies

1.3.4 – Electric Motors

1.3.1 - Vibration Measurement Equipment & Procedures

Sensors and Monitoring

Sensors are essential in measuring noise and vibration-related parameters. Commonly used sensors in vibro-acoustics include accelerometers, force transducers and measurement microphones. This study will also be concerned with electrical parameters and their measurement. This section outlines the fundamentals of how and when each type of sensor should be used, and how basic electrical parameters can be measured or calculated from measurements.

- Accelerometers are used to measure acceleration where they are mounted on a test structure. They convert an acceleration value into a corresponding voltage level. They consist of a small block that is mounted rigidly to the test structure, typically with a strong adhesive. Accelerometers need to be considered as being coupled to the test structure, so a rigid connection is necessary. Different models of accelerometers can either measure acceleration in one axis or in three axes (referred to as being tri-axial).
- Force transducers are used to measure the force applied to a structure. They convert a force into a corresponding voltage level. A force hammer is essentially a hammer fitted with an integrated force transducer in its tip. An impedance head is an alternative to a force transducer that combines the functions of force transducers and accelerometers, allowing simultaneous measurement of acceleration.
- Microphones convert a pressure incident to their diaphragm into a proportional voltage level of corresponding magnitude. They are used for airborne pressure-based acoustic measurements. There are many different types of acoustic measurement that can be made with a microphone. BSI and ISO guidance documents should be referred to where standards exist for a given measurement procedure.

Sensors have varying sensitivities, so an appropriate sensor should be chosen accordingly. They are typically connected to an analyser via a cable. The signal is interpreted and processed by the analyser and can be viewed and processed via a connected computer.

Force Hammers

Force hammers are used to excite a structure impulsively and allow measurement of the force used to excite the structure. This makes them common tools in modal analysis of structures. Consistent experimental technique is important when using a force hammer, and good coherence between successive hammer hits should be monitored during measurement. Handheld hammers are typically used in industry, despite mechanically triggered hammers potentially seeming advantageous in terms of repeatability and consistency. This is because it is often necessary to excite test structures in hard to reach positions or at awkward angles, making a handheld hammer a more convenient option due to its versatility.

Electrodynamic Shakers

Electrodynamic shakers are a commonly used tool in experimental modal analysis. Shakers apply a continuous (or sometimes intermittent) source of vibration to a test structure. The amplitude of this vibration is determined by the amplitude of signal sent to the shaker. Different types of signal (including different types of noise, various pulses and sweeps) can be used, depending on the requirements of the test. Shakers are used to excite a structure for a period of time, over which the response of the test structure at response points is averaged. Properly conducted shaker measurements can yield very clean frequency response functions. There are many factors to consider when using a shaker in order to ensure a high-quality measurement – this section aims to outline the most significant factors.

- Use of stingers and sensors
 - If the test structure is directly connected to the shaker, the dynamic properties of the shaker will be imparted on the test structure. Stingers are connected between the test structure and the shaker plate to prevent this. An idealised stinger will constrain vibration into a single axis, decoupling the test structure from the shaker to the greatest extent possible. This is because a stinger has a high axial stiffness and low lateral stiffness.
 - Stingers of varying lengths and thicknesses can be used. Increasing the length of a stinger will reduce its bending stiffness and can result in measured FRFs being corrupted by the resonances of the stinger, causing additional peaks. If a stinger is too short, it will impose the dynamic effects of the shaker on the test structure. This results in shifting modal frequencies and creating new modes. If a stinger is too thick, it will not effectively constrain the direction of transmitted vibration. A stinger that is too thin will be too fragile for use in testing.
- Stinger materials
 - It is important that a stinger is in good condition and is not bent or damaged in any other way, as this can result in distortion of the measured FRFs.

- Improper stinger alignment will result in transmission of side loads, resulting in distortion of mode shapes and low quality FRFs.
- Alignment and positioning
 - A trunion is a frame that supports the body of a shaker and can be used to position a shaker at an angle. Cloutier et al. state that this can be particularly important when exciting structures with horizontal and vertical modes that are highly uncoupled (Cloutier et al, 2019).
 - If the shaker is attached at a point on a structure that is insufficiently rigid and is overly compliant, force dropout can occur with the shaker, most notably at resonant frequencies of the structure.
- Common excitation types
 - Shakers can be driven with a variety of different types of signal depending on the application required. Some of the most common excitation types are random noise (white, or other filtered spectra), burst random noise or swept sine signals.
 - Random noise is commonly used due to its simplicity and ease of implementation. It requires windowing in order to be implemented, and this results in some spectral leakage. Random noise also requires many averages to be taken in order to avoid non-linearity effects (Avitable, 2017).
 - Signals such as a swept sine offer a higher signal-to-noise ratio to other commonly used options.

1.3.2 - Modal Testing

General Principles & Practices

Modal testing is performed on structures to determine and characterise their dynamic behaviour and predict or describe their vibratory response, allowing us to understand and therefore control and mitigate excessive vibration. Modern technology has led to rapid advances in computer modelling solutions, but these methods are not perfect and often can benefit from experimental measurements as inputs or to validate models. An understanding of different types of modal testing and their related processes and applications is a valuable skill in engineering today.

The process of modal testing and analysis consists of two main stages. The first stage is to perform experimental modal analysis, consisting of modal testing and the subsequent formation of frequency response functions that describe the system. This is followed by modal parameter estimation, where FRFs are analysed in order to extract resonant frequencies, mode shapes, damping-related parameters and mode shapes. This is achieved through curve fitting of FRFs. Modal parameters are considered as the outputs of the modal analysis process, which can then be fed into numerical models.

Applications of Modal Testing

A common use for experimental modal analysis is to inform design or calibration of a numerical model or simulation, such as finite element analysis. Data obtained during modal tests can be fed into computer modelling systems. Carefully considered processes of this nature can allow verification of models, if they are able to show convergence with real-world data and behaviour of real systems. Careful calibration and fine-tuning of such systems can allow them to reflect and predict real-world scenarios or phenomena far more effectively. These hybrid experimental and numerically modelled systems can be very powerful, cost effective and time-efficient when considering complex vibratory problems or designs. Modal testing can also be performed for verification purposes on physical prototypes to check conformity with design specifications and tolerances.

Dynamic Substructuring (DSS) is another area of interest in relation to modal analysis. It is the process of dividing a product or object up into component parts, performing modal analysis individually on these parts, thus defining frequency response functions that characterise them, then combining them to assess the behaviour of the combined assembly. This makes it simpler to then determine the effect of subsequent modifications to a potentially complex assembly on the component level if changes are made to its design. The respective contributions of each component can also be evaluated and compared to inform further design decisions.

Meggitt explains that problems are considered as an “assembly frequency response function” which consists of a series of “sub-component FRFs”. In order to form a virtual acoustic prototype of a system, the active and passive properties of the sub-components must be independently characterised, along with the passive properties of the wider system (Meggitt, 2017).

Signal Processing & Analysis

There are a number of ways in which signals can be processed in order to derive useful information from them. This in terms of individual signals or be in the form of comparisons between signals. In the field of modal analysis, the aim is to gain an understanding of the mechanical properties of a system,

often in terms of relationships between inputs and outputs to the system. This section will outline some of the fundamental types of signal that can be derived from experimental measurements, explaining their calculations, relationships and applications. Many of these are applied in order to process analyse experimental data later in this thesis.

A signal analyser initially will record a time domain signal when recording data. The sampling frequency determines the rate at which samples are taken to represent the signal. The Fourier Transform can then be applied to the time domain signal, converting to the frequency domain. This domain is the primary one of interest in modal analysis, although time domain visualisation and monitoring can be useful to ensure quality measurements (when determining the impulsivity of a force hammer hit for example). This instantaneous frequency data (or with its resolution determined by the sampling frequency at least) is referred to as the instantaneous spectrum. This signal can then be processed to give the following fundamental parameters:

Autospectrum

The autospectrum is the time-averaged version of the instantaneous Fourier spectrum, based on the squared amplitude of the original signal. This is shown in Equation 1.3.1, where the autospectrum is $\bar{G}(f)$ and E is the averaging operator applied to the frequency domain signal $A(f)$.

$$\bar{G}(f) = E\{|A(f)|^2\} \quad (1.3.1)$$

Cross-Spectrum

The cross-spectrum is a directional function (requiring a specified direction as part of its definition) that is calculated from the complex instantaneous spectra of two different input signals. The amplitude of the cross-spectrum is equal to the product of the two signal amplitudes, and the phase is given by the phase difference between the two signals. This is shown in Equation 1.3.2 for the cross spectrum ($\bar{S}(f)$), considered from signal A to signal B in terms of its direction ($\bar{S}_{AB}(f)$).

$$\bar{S}_{AB}(f) = E\{A^*(f) \cdot B(f)\} \quad (1.3.2)$$

The cross spectrum of two signals and their respective autospectra are required to calculate a frequency response function connecting the two signals. It is preferable to refer to frequency response functions if the two signals being considered are an input and output to a system. This is fairly typical, in that the cross-spectrum is more commonly used as a precursor in the calculation of other functions than in its own right. Another example of this is the cross-correlation function, which also can be calculated from the cross-spectrum.

Coherence Functions

The coherence function is a method for measuring linear dependence between two signals. This makes it an important tool for checking the validity of or consistency between measured signals. It can also be used to calculate other parameters including signal-to-noise ratio and coherent output power.

It is given by Equation 1.3.3, where $\gamma^2(f)$ is the coherence function and $G_{AA}(f)$, $G_{AB}(f)$ and $G_{BB}(f)$ have their previous definitions.

$$\gamma^2(f) = \frac{|G_{AB}(f)|^2}{G_{AA}(f) \cdot G_{BB}(f)} \quad (1.3.3)$$

The value obtained from Equation 1.3.3 is an index between 0 and 1, with 1 meaning that the two signals are linearly related and 0 that they are entirely uncorrelated. The coherence function can also be obtained from the ratio of the H_1 and H_2 forms of frequency response functions (these functions are in the following section).

On a practical level, the coherence function can be applied to successive force hammer impacts in a modal test, in order to determine the repeatability of the excitations, a number of which are typically averaged. Ewins notes that this averaging improves statistical reliability and can help to remove unwanted random noise from measured signals (Ewins, 2000).

Frequency Response Functions

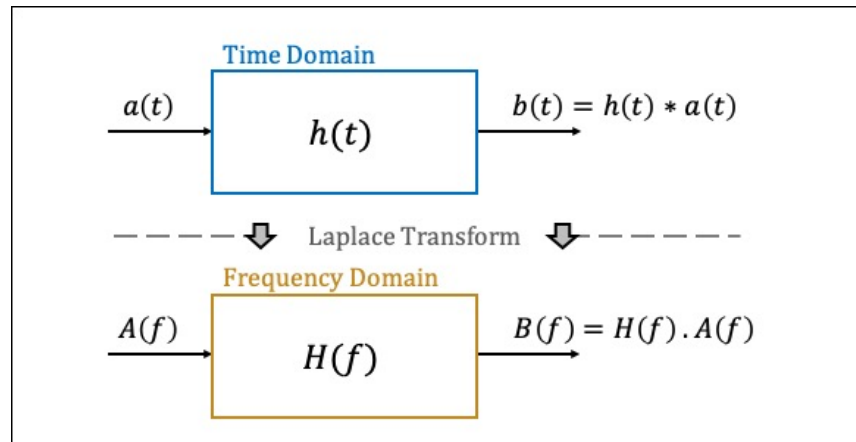
Frequency response functions (FRFs) are invaluable in the characterisation of systems and networks. They can be measured for a variety of systems, including acoustical, mechanical and electrical or combined systems comprising of multiple domains. They can be used to determine resonances of a structure or assembly (shown by peaks in a response), damping properties (indicated by the width of the resonance peaks) or to determine mode shapes (when multiple FRFs are considered in combination with respect to a common reference point on a structure).

FRFs are the ratio of the output to input for a system, describing the frequency domain relationship between the output and the input. This is shown in Equation 1.3.4, where $B(f)$ is the output, $A(f)$ is the input and $H(f)$ is the resulting FRF:

$$H(f) = \frac{B(f)}{A(f)} \quad (1.3.4)$$

Frequency Analysis by Randall (Randall, 1987) provides a more in-depth overview of their derivation and relationship with time domain signals. To summarise, the Laplace Transform can be used to convert an impulse response in the time domain to a frequency response. The Inverse Laplace Transform can be used to convert in the opposite direction. The Fourier Transform is more commonly used for this conversion in engineering applications. This is because it is easier to implement and sufficient for use in stable systems. A different form of the Fourier Transform must be applied to digital signals. This is referred to as the Discrete Fourier Transform (DFT). There are several different implementations of this – processing performed in this study will use the Fast Fourier Transform (FFT).

Figure 1.3.1: FRFs in the Time & Frequency Domains



Multiplying $A(f)$ and $B(f)$ in Equation 1.3.4 by the complex conjugate of $A(f)$ gives a more commonly used form of FRF, called H_1 . This form is advantageous as it minimises error with a noisy output signal. The H_2 parameter is given by multiplying $A(f)$ and $B(f)$ in Equation 1.3.4 by the complex conjugate of $B(f)$. This form minimises error when noise is present on the input signal. This is noted to be of particular use by Randall, who recognises that the input signal may be contaminated with noise when exciting lightly damped structures with noise signals using an electro-dynamic shaker. The input force spectrum is likely to be low at resonances of the structure, which can cause a noisy signal (Randall, 1987).

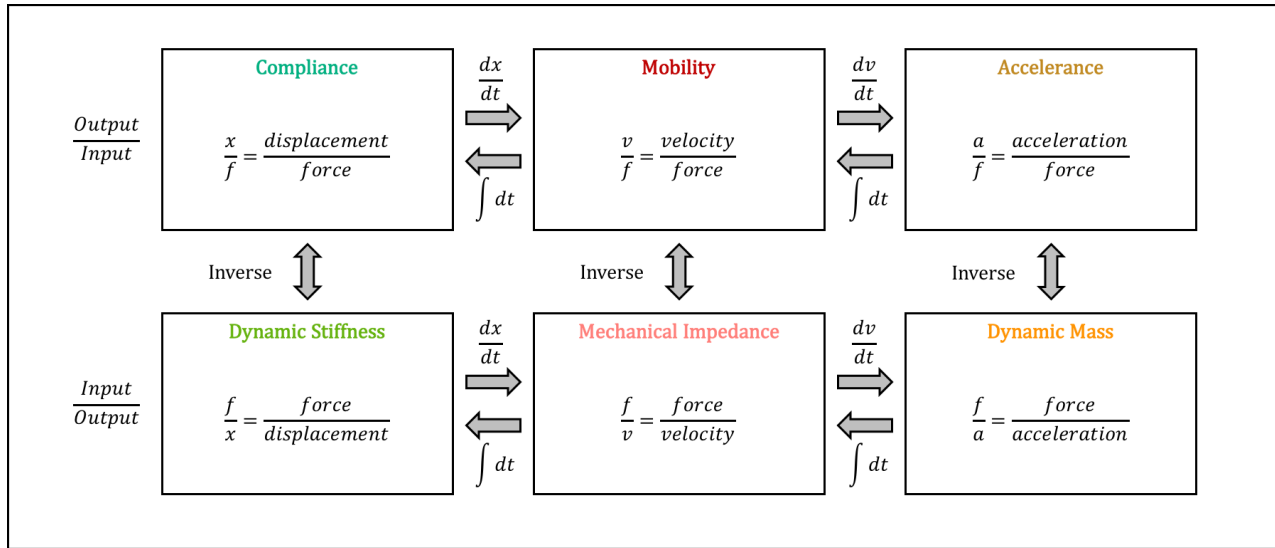
A frequency response function is sufficient to completely characterise a system that is linear and time-invariant (often referred to as LTI or 'ideal' systems). FRFs are complex quantities, containing both magnitude and phase information. The magnitude component is the ratio of output to input, while the phase component indicates the phase difference between output and input.

Types of FRF

As a ratio of output and input parameters, FRFs can take a number of forms. Commonly, accelerometers and force transducers (or both combined as an impedance head) are used to conduct modal tests. This means that the most direct FRF to measure is accelerance, as it is directly obtained from the measured parameters. An accelerance value can then easily be converted into other forms as desired. Conversion between FRFs can be achieved by taking the inverse, integrating or differentiating. As this is performed in the frequency domain, integration and differentiation become equivalent to dividing or multiplying by $j\omega$ respectively, where ω is the angular frequency in radians per second ($\omega = 2\pi f$) and $j = \sqrt{-1}$.

Figure 1.3.2 summarises common FRF types and how to convert between them.

Figure 1.3.2: Types of Frequency Response Function



Accelerance

Accelerance is the ratio of acceleration to force. Peaks of an accelerance response correspond to the natural frequency of the test object.

It can be integrated with respect to time to give mobility, or the inverse of it can be taken to give dynamic mass.

Mobility

Mobility is the ratio of velocity and force. It is a commonly used FRF as many physical mechanisms are proportional to velocity, such as sound radiation from a surface, which is clearly of interest for acoustical design problems. Therefore, reducing mobility at a given point will reduce the amplitude of sound radiation from that point.

Compliance

Compliance is the displacement of an object when a force is applied to it, given by the ratio of displacement to force. This can also be obtained by integrating mobility, double integrating accelerance or inverting dynamic stiffness FRFs.

Dynamic Stiffness

This parameter is intuitively the inverse of compliance, being defined as the extent to which a structure resists deformation when a force is applied to it. It can also be obtained by integrating mechanical impedance or double integrating dynamic mass with respect to time. Dynamic stiffness is important in the study of elastomeric materials, and design of resilient mountings for vibration isolation. Analysis of dynamic stiffness is performed to determine isolator placement or to set stiffness targets for mounting locations.

Mechanical Impedance

Impedance is defined as the opposition provided by a structure to motion or energy flow. More specifically, it is the complex form that combines resistance and the equivalent imaginary quantity of

reactance. In the mechanical domain this is the extent to which a structure resists motion when a unit force is applied to it. It is given by the ratio of force and velocity.

It can be obtained by taking the inverse of mobility, integrating the dynamic mass, or differentiating the dynamic stiffness, both with respect to time. Notches in a mechanical impedance FRF correspond to the natural frequencies of the structure.

Mechanical impedance is a useful parameter in the field of structural dynamics. An example application is obtaining operational forces applied to a structure, using a laser to measure velocity of a test structure mounted on a vibrating plate excited by a known force. Overlaying mechanical impedance FRFs of two structures will determine their combined dynamic behaviour. If their FRFs show amplitude separation, then the two structures will not dynamically interact. If they coalesce then the components will interact.

Dynamic Mass

Dynamic Mass is the inverse of accelerance. As a result, notches in a dynamic mass response correspond to the natural frequency. For a SDOF system, the asymptotic region succeeding the natural frequency equals the mass of the system.

Limitations of Modal Testing

Modal testing is an important tool for analysis of structural dynamics, but it is important to be mindful of its limitations, especially when relying on the results of modal analysis to calibrate a numerical model.

In terms of factors that can contribute to a lack of precision, a detailed breakdown is provided by Ashory, who divides sources of error and imprecision into three main categories (Ashory, 1999):

Experimental data acquisition errors

This includes mechanical errors attributable to the mass-loading effect of transducers, interactions between the shaker and structure, effects from the structural supports, measurement noise and non-linearity of the test structure.

Signal processing errors

Signal processing errors are often consequences of implementing the discrete Fourier Transform, which is integral for frequency domain signal analysis – these include spectral leakage (a consequence of signals being non-periodic within the designated sampling window), in addition to aliasing effects and averaging errors. It should also be ensured that the frequency range of interest is sampled sufficiently regularly as to not introduce bias errors at low frequencies (Marudachalam, 1992). All of these effects can introduce shifting of spectra and add random noise and error to results.

Modal analysis errors

The estimation of modal parameters from FRFs involves curve fitting. Introducing some error through this process is avoidable, as with any data fitting operation. Marudachalam notes that whilst curve fitting of FRFs can reduce the presence of noise, it will not solve any bias error issues present in the dataset (Marudachalam, 1992).

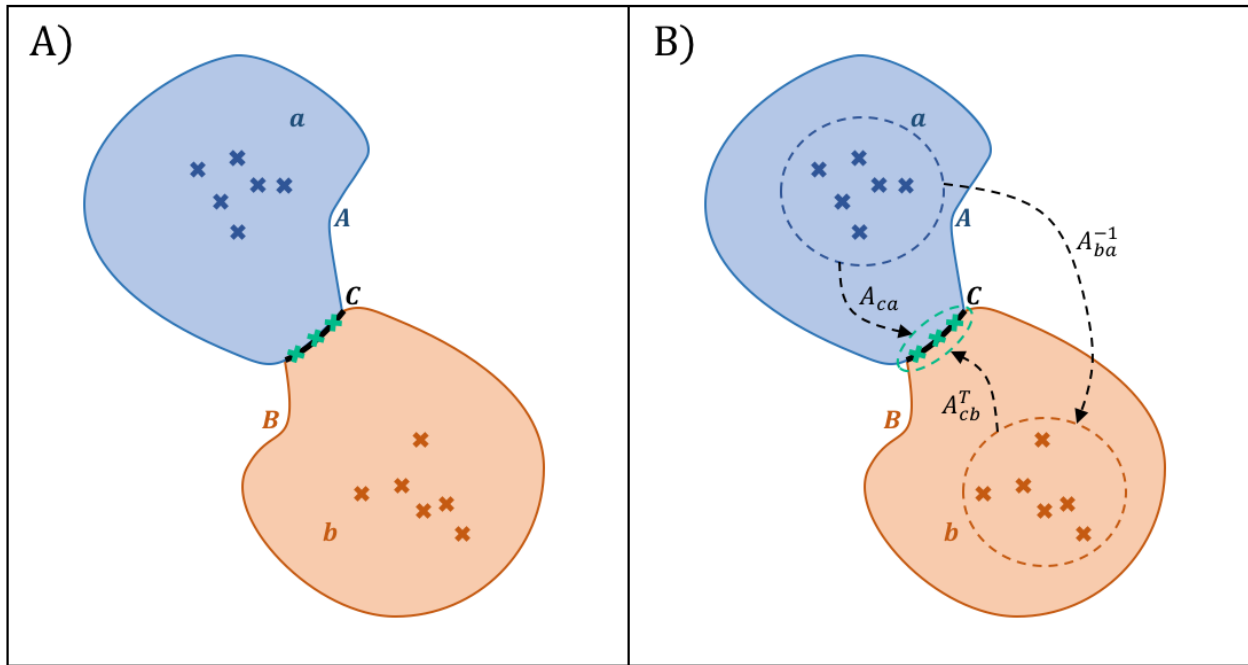
The Round-Trip Identity

Sometimes it is not practical or possible to excite a structure at the position of interest. This might be because of the need for a device or product to be fully assembled or in operation during testing, preventing access to internal points. Some structures are difficult to excite with sufficient amounts of energy to perform modal analysis (this may damage the structure, or it may simply be far too large or massive to excite with a sufficient amount of energy to obtain meaningful data). In such cases, a method for determining vibratory response due to a 'remote' (virtual) excitation is particularly useful. Such a method was first published by Moorhouse & Elliott (Moorhouse & Elliott, 2013), referred to as the round-trip identity. The original form of the identity is primarily concerned with mechanical parameters, i.e. the acceleration (and subsequently derivable parameters) induced by an applied force. Subsequent work extended the identity to measurement of point impedances with an airborne excitation method (Moorhouse & Elliott, 2017). This subsequent work suggests that the identity has potential further applications and that modified forms might be applicable to similar problems requiring remote excitation, hence this research project. This section will explain the original round-trip identity. The novel extensions to the identity developed during this project are outlined in Sections 2.2 – 2.4 of this thesis.

Geometry and Definitions

Consider a linear, time invariant (LTI) system, comprised of two subsystems, A and B , which are connected at an interface, C (shown in Figure 1.3.3). Points a and b are positioned arbitrarily within their respective subsystems.

Figure 1.3.3: (A) Round-Trip Geometry (B) Round-Trip Paths



FRF matrices can be formed between the sets of points. These will be referred to with the notation A_{mn} , where m and n are the response and excitation positions respectively. Moorhouse & Elliott's original paper uses mobility matrices, but the identity can be applied to any other form of FRF as desired. This work will primarily use accelerance FRFs, with the identity expressed in terms of accelerance matrices.

For discrete interfaces, the identity states that:

$$A_{cc} = A_{ca} A_{ba}^{-1} A_{cb}^T \quad (1.3.5)$$

The matrices include indices corresponding to each portion of the 'round-trip' path – that being from c to a , a to b and b to c . These portions of the Round-Trip path are indicated in Figure 1.3.3(B). A reversed path version of the identity also exists – this will be detailed later in Part 2 of this thesis. It should be noted that none of these matrices require excitation at the interface C , allowing determination of a frequency response function at a remote position. None of the matrices require measured responses at points in the A region, so at these points the structure need only be excited, without necessarily measuring a response and the applied force.

Practically, the FRFs can be obtained by mounting accelerometers on the test structure at b and c points (a detailed explanation of good practice relating to accelerometer mountings and other experimental considerations can be found at Section 1.3.1), then exciting the structure with an impact hammer or electro-dynamic shaker as follows:

- Excite at a points, and simultaneously measure responses at b and c points.
- Excite at b points and simultaneously measure responses at b and c points.

- In the experiments reported later in this thesis, a third step is added for validation, namely excitation at c points. Normally this step, which requires excitation at c , is assumed not possible.

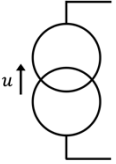
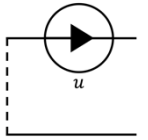
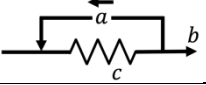
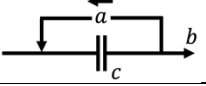
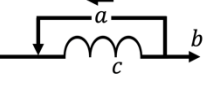
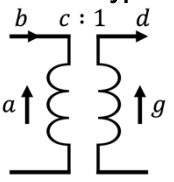
1.3.3 - Circuit Analogies

Many systems can be visualised and expressed using equivalent circuit analogies. In these analogies, an 'equivalent' circuit can be formed that corresponds to a non-electrical system (or one that is a combination of both domains, and others such as magnetic). Differing analogies can be considered, some being more efficient in certain scenarios than others, depending on the system of interest. Representing a system as an equivalent circuit is advantageous for many reasons. They often greatly simplify calculations and application of circuit analysis theorems to them can help reduce complex looking problems to simpler ones.

Mechanical Systems

The two analogies for mechanical systems are the mobility and impedance analogies. The equivalent parameters in each of these is outlined in Table 1.3.1, adapted from Beranek (1996). It should be noted that element analogies are valid where the product of the a and b variables gives units of power in that domain. The a variables will be referred to as "through variables" and b variables as "across variables" in this study, due to their connection to the topology of the circuit. Some literature sources alternatively feature the terms "flow" and "drop" variables to describe a and b variables respectively.

Table 1.3.1: Equivalent Parameters for the Mobility and Impedance Analogies (adapted from Beranek, 1996)

Variable / Circuit Element	Electrical	Mechanical Analogy	
		Mobility type	Impedance type
Across variable	Voltage, v	Velocity, u	Force, F
Through variable	Current, i	Force, F	Velocity, u
Constant-drop generator 	Voltage supply	Velocity source	Force source
Constant-flow generator 	Current supply	Force source	Velocity source
Resistance-type element 	Resistor, R_E	$\frac{1}{R_M}$	Mechanical resistance, R_M
Capacitance-type element 	Capacitor, C_E	Mass, M_M	Compliance, C_M
Inductance-type element 	Inductor, L	Compliance, C_M	Mass, M_M
Transformation-type element 	Transformer-type Relationships: $a = cg$ $cb = d$ $\frac{a}{b} = c^2 \frac{g}{d}$		

The impedance analogy states that voltage is equivalent to force and current to velocity. This preserves the analogy between electrical and mechanical impedance but will not preserve the topology of a mechanical system. This means that a component considered to be in series in one domain will be in parallel in the other.

The mobility analogy states the reverse - that is, that voltage is equivalent to velocity and current is equivalent to force. The advantage of this is that it preserves the topology or structure of a mechanical

system, so series components will remain series in the analogy (the same is true for parallel components). The disadvantage is that the analogy between electrical and mechanical impedance is not preserved. Mechanical impedance is represented as an electrical admittance and a mechanical resistance is represented as an electrical conductance in the electrical equivalent circuit.

Additional Considerations

Beranek outlines some considerations that should be given to the application of equivalent circuit theory, and conditions that must apply to the quantities being equated. Discussing these is relevant as some of these aspects will need to be considered when developing and implementing the Electro-Mechanical Round-Trip Identity.

For a mechanical component to be fully analogous to an electrical one, it must have a 'drop' (velocity or force, depending on the analogy) between its terminals, and have a 'flow' variable (again, determined by the analogy) acting through it.

Part of what makes the analogy between mechanical and electrical components compelling is that there are numerous parameters that can be equated. Power and impedance are quantities that are important in the analysis of systems in both domains.

Mechanical power can be defined as work done per unit time. This equation can be manipulated to show that mechanical power can be expressed as the product of force and velocity. This is shown in Equation 1.3.6:

$$P_M = \frac{Work}{t} = \frac{F \cos(\theta)x}{t} = F \cos(\theta) v \quad (1.3.6)$$

This is analogous to electrical power, which can be expressed as the product of voltage and current. Therefore power in both domains can be expressed as the product of a drop, or across variable, and a flow, or through variable.

Mechanical impedance is defined as the ratio of applied force to velocity at a given position. Electrical impedance is typically characterised by its real and imaginary components – resistance and reactance respectively. Resistance is equated to voltage and current by Ohm's Law, which states that voltage is equal to the product of current and resistance.

As previously stated, the impedance analogy maintains consistency between mechanical and electrical impedance.

The two analogies can be described as mathematical 'duals' of each other. Duality can be observed between two systems that mirror one another in their characteristics. A simple example case of a dual analogy is that a straight line can be defined by connecting two points and a point can be described by the intersection of two straight lines.

The following relationships can be observed between the mobility and impedance analogies:

- Elements in series in one analogy correspond to those in parallel in the other.

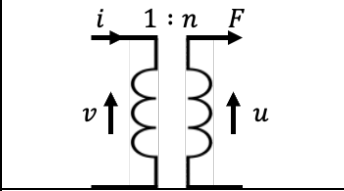
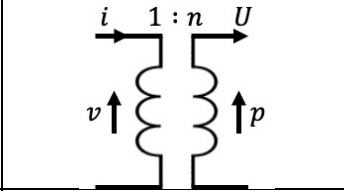
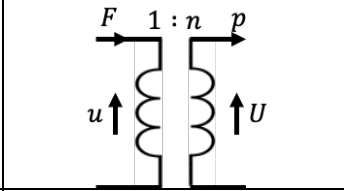
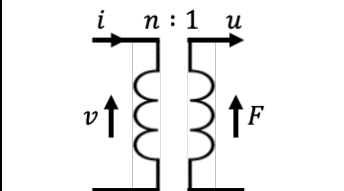
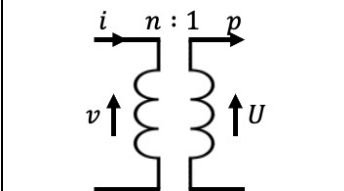
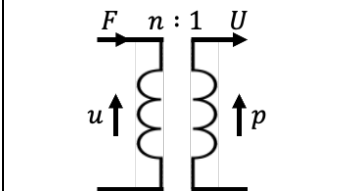
- Resistance-type elements become responsiveness elements, capacitance elements become inductive, and inductive elements become capacitive.
- The sum of the voltage drops across elements in a mesh of one analogy correspond to the sum of currents at a branch point of the other analogy. That is, that ‘flows’ in one analogy become ‘drops’ in the other.

Conceptually these aspects are clearly analogous to the line and point example used earlier.

Acoustic Systems

Beranek not only details equivalencies between mechanical and electrical systems, but also acoustical ones. For acoustical systems, some fundamental equivalencies are shown in Table 1.3.2, adapted from Beranek’s summary of the topic (Beranek, 1996):

Table 1.3.2: Electrical, Mechanical and Acoustic Analogies (adapted from Beranek, 1996)

Variable / Circuit Element	Electrical	Mechanical		Acoustic	
		Mobility-type	Impedance-type	Mobility-type	Impedance-type
Across variable	Voltage, v	Velocity, u	Force, F	Pressure, p	Volume velocity, U
Through variable	Current, i	Force, F	Velocity, u	Volume velocity, U	Pressure, p
Resistance-type element	Resistor	$1/R_M$	Mechanical Resistance, R_M	$r_A = \frac{1}{R_A}$	Acoustic resistance, R_A
Capacitance-type element	Capacitance, C_E	Mass, M_M	Mechanical compliance, C_M	Acoustic Inertance, M_A	Acoustic compliance, C_A
Inductance-type element	Inductance, L_E	Compliance, C_M	Mass, M_M	Compliance, C_A	Acoustic Inertance, M_A
Impedance-type element	Electrical impedance, Z_E	Mobility, Y_M	Mechanical impedance, Z_M	Acoustic Admittance, Y_A	Acoustic impedance, Z_A
Analogy		Electro-Mechanical	Electro-Acoustic	Mechano-Acoustic	
Mobility-type					
Impedance-Type					

Detailed discussion of acoustical equivalent circuits is beyond the scope of this work, which is primarily concerned with mechanical and electrical circuits. Further work could modify the Round-Trip Identity to apply to more complex, multi-domain problems, and in such cases, acoustical equivalent circuits may well be relevant. The design of electroacoustic devices such as microphones and loudspeakers considers mechanical, electrical and acoustical domains, so is potential for applications in this sector.

Alternate forms of the identity would allow determination of a range of variables in different types of system, for example reconstructing a remote volume velocity or acoustic impedance response in a hybrid system based on a combination of mechanical, electrical and acoustical parameters.

1.3.4 - Electric Motors

This section provides a summary of the design, operation and relative benefits for different types of electric motor. This is drawn upon in Part 3 of this thesis, where the Electro-Mechanical Round-Trip Identity is applied to electric motors

General Principles

Motor Applications

Electric motors are used to transduce an electrical signal into a mechanical torque. This is invaluable within many products, devices and machines across a wide range of industries and applications, from consumer products and manufacturing, to automotive and the built environment.

Due to their prevalence in society, it is desirable to understand the workings and behaviour of electric motors. This section will identify different types of motors and outline how they work and their respective benefits or drawbacks.

The move towards electric vehicles and advancements in motor technologies have resulted in far more powerful, compact and efficient motors, which can sometimes operate at very high rotation speeds. This progress is noted by Kim, stating that a modern 100 horsepower motor can be roughly the same size as a 7.5 horsepower motor used in 1987 (Kim, 2017). It is important to design to manage noise and vibration alongside these changes in motor properties and increase in power, and modern brushless designs are a significant improvement over more antiquated brushed systems.

The vibratory and acoustic character of a motor operating at a very high rotation speed will be significantly different to a lower speed motor and will present different design challenges as a result.

An understanding of different types of motors, their design and typical use cases is important when considering adapting The Round-Trip Identity to include electrical parameters, as analysis of electric motors would be a useful application of the Electro-Mechanical Round-Trip Identity.

General Terminology

It is relevant to explain some of the key terms that are used when characterising motors in terms of their design and mechanical performance:

- A rotating magnetic field (RMF) is the fluctuating magnetic field that is generated by the coils of a motor and results in its motion.
- The RMF rotates at the synchronous speed, N_s , which is proportional to the AC power supply frequency in an AC motor or the input voltage level in a DC motor.
- Slip is the difference between the rotational speed of the spindle (N_R) and the synchronous speed of the RMF. It is calculated using Equation 1.3.7:

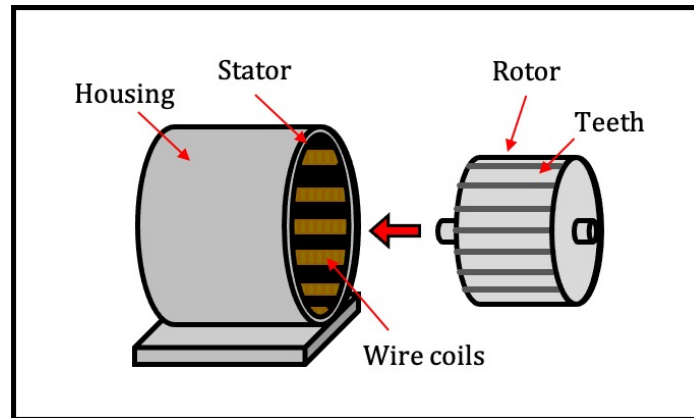
$$Slip = \frac{N_s - N_R}{N_s} \quad (1.3.7)$$

Structure

A motor consists of a static housing (referred to as the stator) and a piece that freely rotates within or around the stator (referred to as the rotor). Either the rotor or the stator will contain a ring of wire coils

or permanent magnets. If the rotor contains wire coils, the stator will contain permanent magnets and vice versa. These components are shown in Figure 1.3.4:

Figure 1.3.4: Fundamental Motor Components and Structure



When an electric current is applied to the wire coils, a magnetic field is generated. This field interacts with the permanent magnets on the opposing piece, generating a torque and causing the motor to move. The sequential excitation of pole pairs results in sustained motion of the rotor due to the changing magnetic field.

The types of power signal and the layout of coils and magnetic poles will vary based on the type of motor. Motors can be powered by AC or DC sources, but most modern brushless DC motors (BLDC) are actually digitally controlled AC motors, controlled with a stepped series of periodic signals, but powered with a DC supply.

The sequential excitation of sets of wire coils in a repeating pattern causes the rotor to continue to move. The number of steps or 'phases' before this pattern repeats is commonly referred to when characterising motors.

Generally, a higher number of phases will result in smoother motion of the rotor (and smoother generation of torque), but a more complex signal (or set of signals governed by a control device) will be needed to be used to power the motor. Lower numbers of phases also can require additional starting mechanisms, as they cannot independently generate the initial torque required to start rotation.

DC Motors

Variations & Operation

An important distinction between DC and AC motors is that DC motors achieve their motion through the interaction between two stationary magnetic fields, and AC motors achieve this through interaction between two rotating magnetic fields.

Traditionally DC motors featured wire commutator brushes on the rotor that physically bridge the connection between the rotor and the stator. These are spring loaded to ensure good contact between the two surfaces.

Developments in technology have resulted in brushless DC motors becoming increasingly common, due to their improved durability, reliability, efficiency and generally lower noise levels for a given power output when compared to brushed designs. Brushes degrade over time and this can result in sparking, making brushed DC motors not as suitable for critical, long-lifetime applications.

The simplest form of DC motor is a single-phase DC motor. This is powered by a DC current passing through the main coil generating a stationary magnetic field. Two stationary magnetic fields are generated – one in the rotor and an opposing one in the stator. As a result of this, the motor cannot start itself, and requires an auxiliary coil, connected via a capacitor in series, to generate its initial torque. This capacitor provides a phase shift (and delay) of 90° to the signal passing through it. Once this torque has been generated, the interaction between the two stationary magnetic fields can continue to sustain the motion of the rotor at a constant speed.

An advantage of DC motors is that they are simple to control in terms of speed and torque, as the input voltage is proportional to rotor speed and the current to the torque. This would make them simpler when considering which electrical parameters should be monitored and measured in relation to the Electro-Mechanical Round-Trip Identity. This will be discussed in more detail in Section 3.2.

Brushless DC Motors

It is worth considering Brushless DC (BLDC) motors separately to DC motors. The operation of BLDC motors is significantly different to true DC ones. Brushed DC motors have mechanical commutation (switching between phases), whereas BLDCs feature digital commutation, controlled by a combination of microprocessors and sensors.

BLDC Motors are multi-phase motors that make use of a digital speed controller (DSC) to send pulsed voltage signals to sequential sets of coils. Typically, the rotor is a permanent magnet, and the stator is the electromagnet. A DSC typically takes the form of an integrated circuit or microprocessor mounted on a printed circuit board (PCB). The DSC receives a feedback signal from Hall Effect sensors mounted adjacent to the stator windings in order to monitor position and rotational speed.

For a 3-phase design, when coil A is excited, the opposite polarity poles of rotor and stator are attracted together, causing a small rotational movement to align them. As the two near, the next coil is energised, causing another small rotational movement towards the excited coil. This repeats for the third coil and then the cycle starts again, but with the opposite polarity (A → -C → B → -A → C → -B being an entire cycle).

Figure 1.3.5 shows how the pulses outputted by the DSC control the currents applied to the coils.

Figure 1.3.5 –Phases and Driving Signals for a Three-Phase BLDC Motor

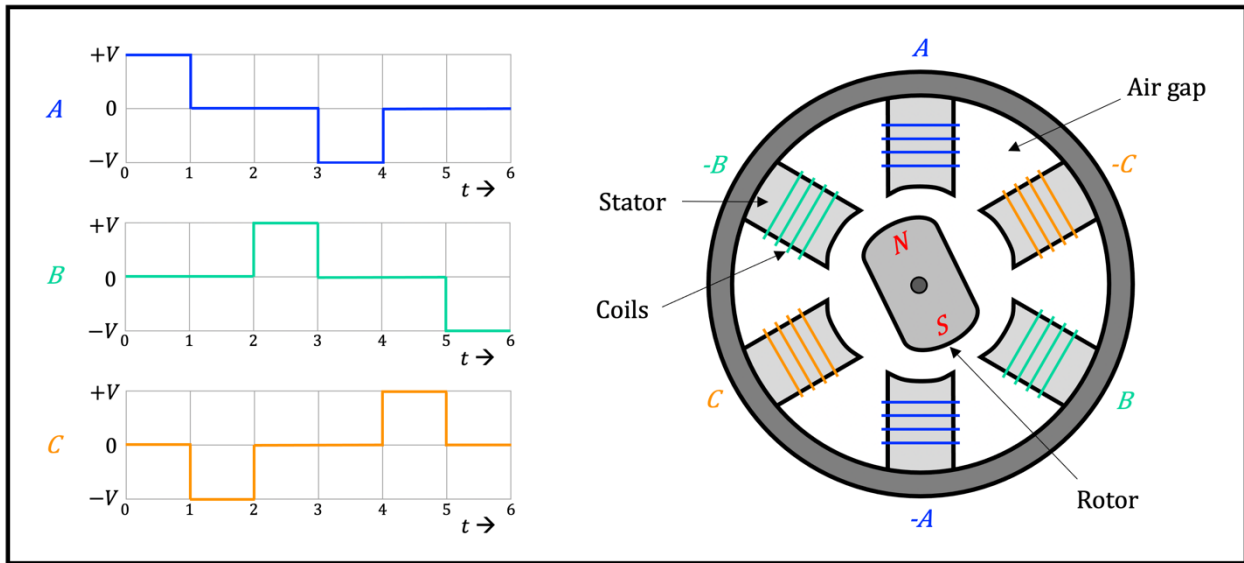
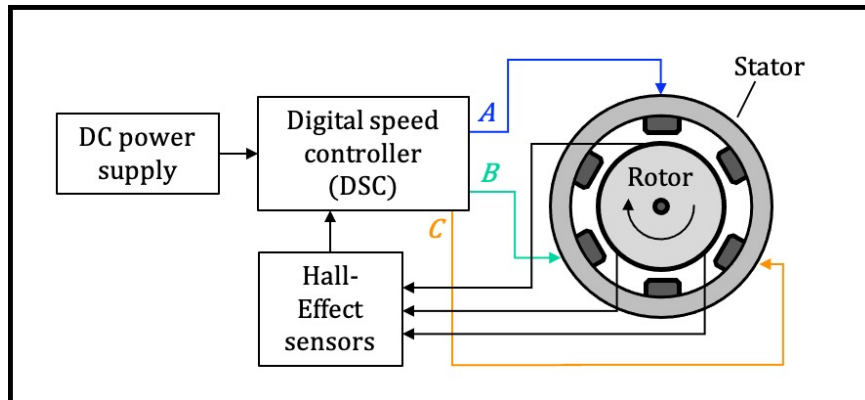


Figure 1.3.5 shows the simplest pattern required to operate the motor, where only one set of coils is active at a time. In this case, the power efficiency of the motor will be low, so in practice it is better to use a multi-stepped pattern to generate larger and smoother torque. This can be achieved by wiring a free end of adjacent coils together and slightly overlapping successive pulses.

The interactions between components of a 3-phase BLDC motor are shown in Figure 1.3.6.

Figure 1.3.6: Component interactions in a Three-phase BLDC motor



Sensors are also required to monitor the instantaneous position and speed of the rotor. Hall Effect sensors are typically used, which are electrically isolated from the motor, but pick up the induced changing magnetic fields generated in each coil or set of coils. This creates a feedback loop to the DSC, which can respond rapidly to changes in signal from the sensor.

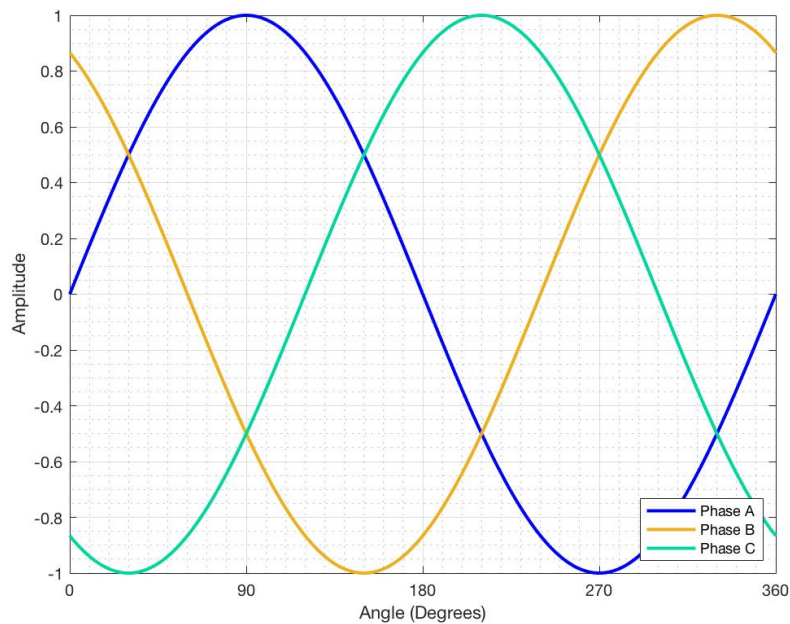
AC Motors

Variations & Operation

AC motors are powered by AC signals. Their rotational speed is controlled by varying the frequency of the AC input using an adjustable frequency drive control. This AC signal generates two rotating magnetic fields. These fields rotate at the same speed, so the phase angle between the two will remain the same, yielding a constant force and constant motion of the rotor.

Simple AC motors often have 3 phases, and are powered by 3-phase AC supplies, consisting of 3 sinusoidal AC signals that have a phase difference of 120° . This is shown in Figure 1.3.7.

Figure 1.3.7 – Three-Phase AC Supply Signals



AC motors are not inherently self-starting, but the ‘squirrel cage’ modification seen in many designs allows this, referring to the shorting of the end of the rotor bars resembling the geometry of a cage.

The two main types of AC motor are synchronous and induction (or asynchronous). The main difference before these is the method of generating the magnetic field on the rotor (this is the same on the stator).

A synchronous AC motor will always rotate at the synchronous speed (N_s) of the stator magnetic field, so changing the frequency of the AC supply will directly control the rotational speed. In an asynchronous design, however, there will always be a slight difference between the synchronous speed and the rotor speed – this is slip, as defined previously in Equation 1.3.7. The rotor speed will always be slightly lower than the synchronous speed in an asynchronous motor.

AC motors are very efficient and require significantly less maintenance compared to other designs, making them appropriate for critical and long-life applications. They are the motor of choice in many electric vehicles, as their power efficiency at a wide range of rotational speeds means only a single

transmission is required. AC designs are typically only available starting at power levels in the order of several kilowatts (Kim, 2017).

Other Notable Motor Types

Stepper Motors

Stepper motors feature very accurate control over the instantaneous rotor angular position without the need for a closed feedback loop. The rotor and stator have differing numbers of electromagnet teeth. As a result, only one group of rotor teeth aligns with the stator teeth at any one time. The geometry of this means that a DC input pulse results in rotor rotation of a known angle. The greater the number of teeth, the smaller the angle of rotation will be, and the higher the precision of the motor.

A significant advantage of stepper motors is that they are able to generate full torque whilst stationary and change direction rapidly.

Stepper motors are often used in computer-controlled tools in manufacturing, and in other high-precision applications, such as in consumer electronics and medical devices. They would be selected over a BLDC or AC induction motor in scenarios where a motor is required to repeatedly stop, start and change direction, whereas BLDC and AC motors are more suited to scenarios involving continuous motion.

Motor Selection for Electro-Mechanical Tests

A single-phase DC motor is the simplest type of motor, so initial work will focus on the analysis of this design. The electrical signals involved in controlling this type of motor are significantly less complex than any types of motor that feature speed controllers or digital switching.

The most relevant motor type to contemporary, real-world applications would be a modern AC or BLDC motor, but the analysis of such a device presents a significantly greater number of challenges. This is both in terms of the complexity of the input signal (or set of signals) that controls the motor and the design of the device itself. There may be difficulties in terms of where to break-in to the device to make voltage and current measurements. This may be in the form of physical and practical constraints, but also in terms of selecting appropriate measurement positions that satisfy the boundary conditions of the Electro-Mechanical Round-Trip Identity. This is discussed in-depth in Part 3 of this thesis.

Given that BLDC motors often feature several Hall-Effect sensors (adjacent to the stator windings) as part of their feedback loops, it may be possible to take readings from these built-in sensors and combine them somehow to give meaningful current responses. Alternatively, measurement of current could be taken from the DSC, at the point where the motor feeds back to it.

1.4 - Part 1 Summary & Conclusions

Part 1 of this thesis has provided an overview of important works of literature and scientific principles that underpin experimental modal analysis and electrical network theorems. This work aims to combine elements from both of these fields in order to devise a modified form of the Round-Trip Identity that can be applied to hybrid electrical and mechanical systems. Such systems are commonplace in society, as many devices that would typically be subject to modal analysis vibrate as a consequence of moving parts that are driven by electricity.

In order to provide a thorough explanation of the Round-Trip Identity, it was first relevant to detail the foundational concepts and technologies that underpin experimental modal analysis and vibration testing. Principles such as reciprocity, measurement techniques and signal processing methods required for modal analysis were discussed.

The Round-Trip Identity, as first published by Moorhouse and Elliott in 2013, was identified as being concerned solely with mechanical parameters (Moorhouse & Elliott, 2013). Subsequent work by Moorhouse and Elliott found that the identity could be applied with airborne excitation methods (Elliott & Moorhouse, 2017), opening up a whole new range of potential applications and uses for the identity. The rationale behind this study was to further increase this range of applications, primarily into the electrical domain.

A summary of several foundational network theorems was provided. This included the following theorems:

- Kirchhoff's Laws
- Tellegen's Theorem
- Equivalent Circuits
- Two-port analysis
- Equivalent circuit theory

It was identified that whilst many of these theorems are typically applied to electrical networks, they can in fact be applied to a wide range of types of system. This can be in a range of domains, including mechanical, acoustic, magnetic, or hybrid systems involving multiple domains. Combining these theorems can greatly simplify the analysis of potentially complex systems. An understanding of the limitations of these theorems and in which contexts they are valid is important to ensure systems are characterised in the correct way.

Electro-mechanical circuit analogies and two-port analysis were topics of particular focus, as these theories will be applied to The Round-Trip Identity in Part 2 of this thesis in order to formulate the Electro-Mechanical Round-Trip Identity.

A summary of different types of motors was provided, detailing their structures, how they are powered and the advantages, disadvantages and applications of each design. These details are important when considering how the Electro-Mechanical Round-Trip Identity can be applied to electric motors, in particular the physical structure of motors and the signals used in powering them or in positional sensing and feedback loops.

Part 2 of this thesis will apply the scientific theory covered by this section to the Round-Trip Identity. This will consist of proposed modifications to the identity to include electrical parameters. This theory will then be validated with a series of increasingly complex experiments, in order to determine the practicality and validity of the modified form of the identity.

Following each experiment, results will be evaluated, and modifications will be made in order to improve the quality of the results in subsequent iterations.

PART 2: DEVELOPMENT OF EXISTING THEORY & EXPERIMENTAL VERIFICATION

Part 2 Outline

Part 2 of this thesis builds on the foundation laid by existing work and previously established theory. Novel modifications to The Round-Trip Identity are developed through the application of electrical network theorems to the identity. These modifications are then experimentally verified through a series of original experiments. Iterative changes are made following each experiment in order to validate the application of the Electro-Mechanical Round-Trip Identity to more complex scenarios, and in order to determine the optimal implementation of the identity in different scenarios.

Part 2: Contents

SECTION	TITLE
2.1	Verification of the Published Round-Trip Identity
2.2	Network Theorems Applied to the Round-Trip Identity
2.3	Applying Transfer Matrix Analysis to the Round-Trip Identity
2.4	Development of the Electro-Mechanical Round-Trip Identity
2.5	Applying the Round-Trip Identity with Electrodynamic Shaker Properties: Initial 'Forwards-Path' Measurement
2.6	Applying the Round-Trip Identity with Electrodynamic Shaker Properties: 'Reverse-Path' Measurement
2.7	The Vibro-Electric Round Trip Identity Applied to a Simple Beam: Two Shaker Setup
2.8	Two-Shaker Experiment with the Revised Circuit Analogy Applied to a Simply Supported Beam
2.9	Applying the Electro-Mechanical Round-Trip Identity to MDOF Systems
2.10	Part 2 Conclusions & Summary

2.1 - Verification of The Published Round-Trip Identity

The first stage of experimental work conducted as part of this study was an initial verification of The Round-Trip Identity, as published in the Moorhouse & Elliott's 2013 paper (Moorhouse & Elliott, 2013). A simple modal testing setup was devised, with a freely supported, 120mm steel beam being selected as the test object. The test object was considered as a simple beam, which is defined in structural dynamics as being symmetric about its shear centre, homogeneous, and that its cross-section is small compared to its length (Strømmen, 2014).

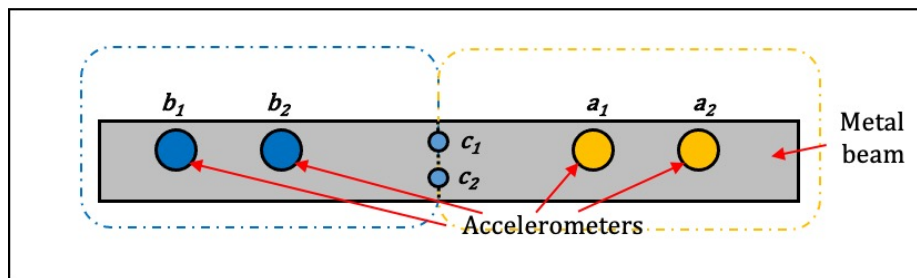
The equipment used in the experiment is shown in Table 2.1.1.

Table 2.1.1: Experimental Apparatus- Verification Experiment

Item	Quantity	Notes
Accelerometer	4	Cleaned of any glue from previous uses. Connected to channels 2-5 on the analyser
Laptop	1	Running dBFA suite
Analyser	1	Connected to laptop via network cable into 'previous' port
Impact hammer	1	Connected to channel 1 on the analyser
Superglue	1	To rigidly adhere accelerometers to beam
Metal beam	1	Test object
Cables	4	To connect accelerometers to the analyser

The beam was marked with 6 positions, as indicated in Figure 2.1.1. These marked the locations of impact positions for the force hammer. The c points were considered as being in the plane of the boundary between the A and B regions, in accordance with the specified geometry in the Round-Trip theory.

Figure 2.1.1: Measurement Positions on a Simple Beam



The accelerometers were positioned on the underside of the beam, at positions b_1 , b_2 , c_1 and c_2 . Accelerometers were not necessary at a_1 and a_2 due to the Round-Trip Identity not requiring responses at these positions. The accelerometers were mounted underneath the beam so that the impact hammer did not physically strike them. This meant it was important to ensure the correct orientation of the accelerometers, so as not to give values with negative magnitude.

2.1.1.1 - dBFA Setup

dBFA's "Transient / Impact Testing" mode was selected. This section will explain the program and hardware settings.

Input and Output Settings

Five channels were set up on the analyser. Channel 1 was assigned to the impact hammer and channels 2–5 as the four accelerometers.

Measurement Parameter Settings

Table 2.1.2 shows the parameters that were recorded by the analyser. These parameters are explained in more detail in Section 1.3.2.

Table 2.1.2: Measurement Parameters for Verification Experiment

Measurement Parameter		Details
Coherences		A function that indicates the similarity between two signals
Frequency response functions (FRFs)	H_1	An FRF or transfer function, weighted to reduce noise from the output
	H_2	An FRF or transfer function, weighted to reduce noise from the input
Autocorrelation		A measure of the similarity between a signal and a delayed copy of itself, indicative of temporal variance
Cross-Correlation		A measure of the similarity between two signals

Display Settings

The measurement bandwidth was set to 5kHz. The longest available FFT length was selected. The impact hammer was selected as the reference channel for the calculation of FRFs.

Trigger Threshold

A trigger threshold was assigned to the impact hammer to determine when a measurement should start upon an impact. The inputted trigger value was indicated as a red line on the on-screen meter, to check the trigger was set to an appropriate value. 5% was set as the trigger threshold value and a pre-delay of 10ms was set to prevent the start of the impulse preceding the recording of data. This was as, if a recorded excitation deviated from being impulsive with respect to time, distortions could result when applying the Discrete Fourier Transform to the signal.

2.1.2 - Measurement Procedure

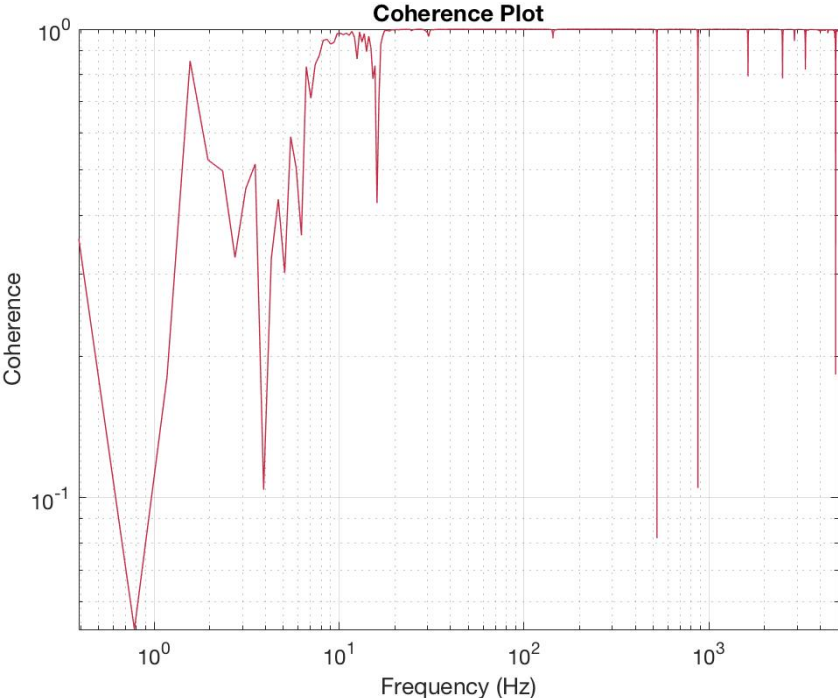
The impact hammer was used to excite the beam at each of the six response points. Measurement at each position consisted of four impact hammer hits, which were averaged then stored in the dBFa measurement software. The process of averaging was previously identified as helping to reduce random noise contamination on resulting frequency response functions.

Coherence function plots were displayed on the measurement software to indicate if successive impacts were sufficiently consistent. Nodal positions in FRF responses were particularly sensitive to small changes in position, resulting in significant notches in measured coherence functions when the beam was struck in slightly different locations between hits.

Coherence was comparatively poor at low frequencies, but this is a consequence of excitation with a relatively small hammer head. A larger force hammer or a force hammer with a softer tip would be required to achieve improved coherence at low frequencies. An example plot of a coherence function

is shown in Figure 2.1.2, where a set of four excitations were applied at the interface point c_1 and compared with each other.

Figure 2.1.2: Example Coherence Plot for Excitation of a Simply-Supported Beam at c_1



The example coherence plot shows that coherence was poor at very low frequencies (below 10Hz). Good coherence was obtained between 20Hz and 500Hz, but above 500Hz, intermittent sudden sharp minima in coherence occurred. This can be caused by a force hammer impact that is not perfectly impulsive or where subsequent impacts occurred in slightly different positions prior to averaging. The margin for error with double hits is significantly lower with lightly damped structures. The effects of hammer usage were minimised in subsequent experiments from improved technique following further practice using the force hammer. Subsequent experiments also compare responses obtained when exciting the beam with an electro-dynamic shaker.

Results Matrix Structure:

In all cases, the measurement matrices were three-dimensional with the Z-axis corresponding to frequency. The frequency axis has been omitted in the two-dimensional representations that follow to improve clarity. The structure of the H_1 matrix is shown in Equation 2.1.1, where A_{cc}^M is the measured accelerance at the interface, C :

$$A = \begin{bmatrix} A_{cc}^M & A_{ca} & A_{cb} \\ A_{bc} & A_{ba} & A_{bb} \end{bmatrix} \tag{2.1.1}$$

This expands to the matrix shown in Equation 2.1.2:

$$A = \begin{bmatrix} A_{c1c1} & A_{c1c2} & A_{c1a1} & A_{c1a2} & A_{c1b1} & A_{c1b2} \\ A_{c2c1} & A_{c2c2} & A_{c2a1} & A_{c2a2} & A_{c2b1} & A_{c2b2} \\ A_{b1c1} & A_{b1c2} & A_{b1a1} & A_{b1a2} & A_{b1b1} & A_{b1b2} \\ A_{b2c1} & A_{b2c2} & A_{b2a1} & A_{b2a2} & A_{b2b1} & A_{b2b2} \end{bmatrix} \quad (2.1.2)$$

The Round-Trip Identity was then implemented on the accelerance matrix. The identity allowed calculation of a matrix containing reconstructed values of accelerance at the boundary, c (A_{cc}^R). Equation 2.1.3 shows the Round-Trip Identity, where each variable is a $2 \times 2 \times Z$ matrix, where Z is an array of frequency values:

$$A_{cc}^R = A_{cc}^M = A_{ca} A_{ba}^{-1} A_{cb}^T \quad (2.1.3)$$

The structure of the generated A_{cc}^R matrix is shown in Equation 2.1.4:

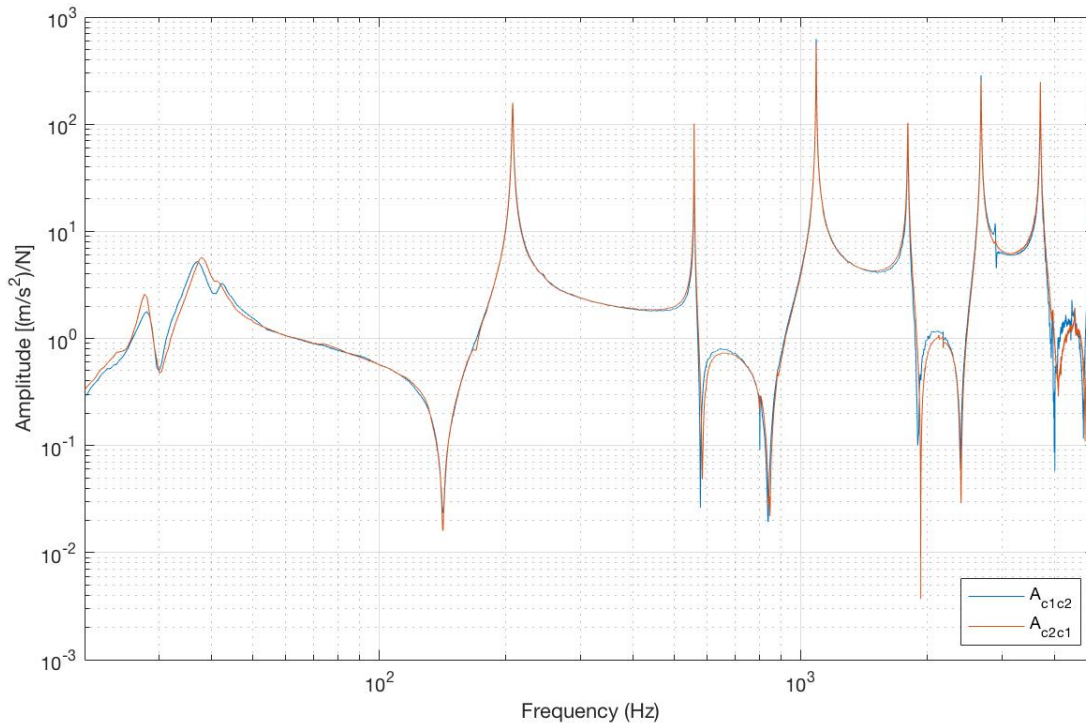
$$A_{cc}^R = \begin{bmatrix} A_{c1c1}^R & A_{c1c2}^R \\ A_{c2c1}^R & A_{c2c2}^R \end{bmatrix} \quad (2.1.4)$$

2.1.3 - Results

Validation of Reciprocity

Elements of the H_1 matrix were plotted against each other to check their reciprocity. Figure 2.1.3 shows the responses of two reciprocal transfer functions at the interface points. The two responses are generally very similar, except for several regions exhibiting low levels of noise. This level of similarity shows that this system behaves reciprocally. This is a requirement for implementing The Round-Trip Identity.

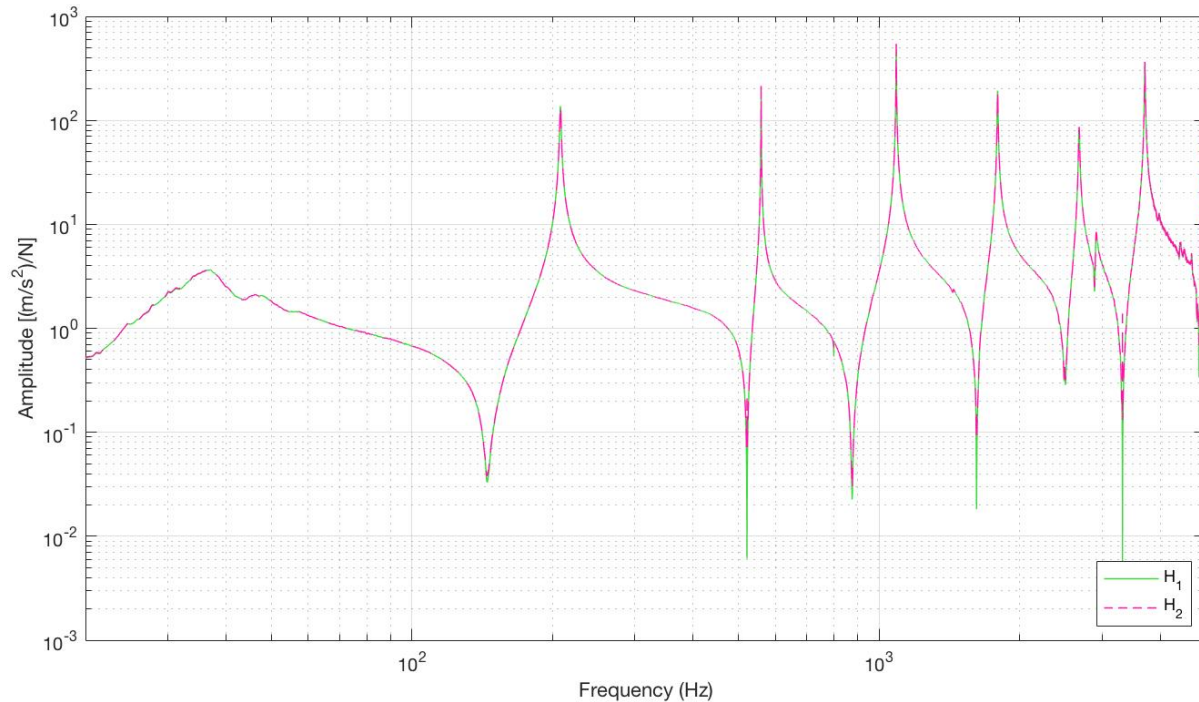
Figure 2.1.3: Reciprocity Check (Using H_1)



Comparison of H_1 and H_2

H_1 and H_2 are two different forms of FRF, weighted to minimise noise on the output or input channels respectively. A comparison of the two functions is shown in Figure 2.1.4. There is minimal observable difference between the H_1 and H_2 functions in this case so, for the rest of this experiment, H_1 was used when implementing the Round-Trip Identity.

Figure 2.1.4: H_1 vs. H_2 Response Comparison at c_1

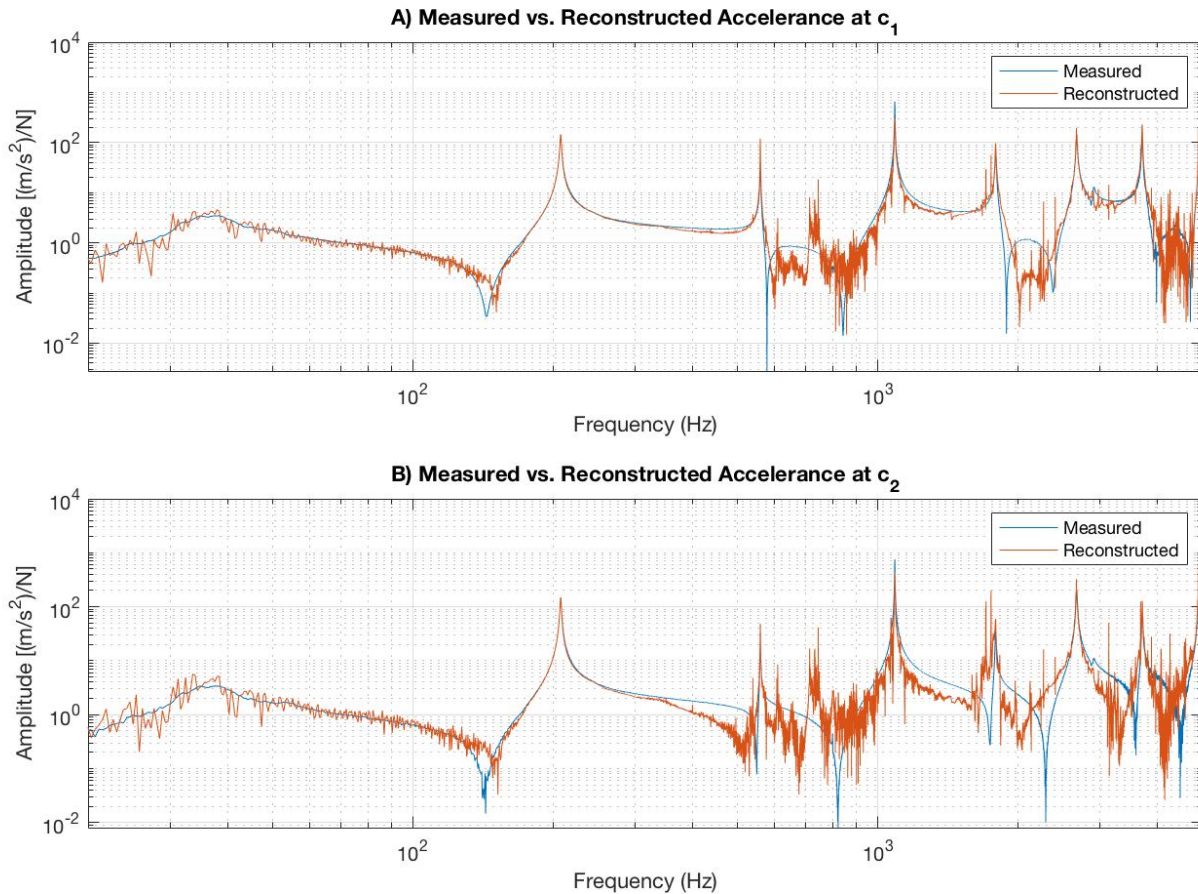


Round-Trip Validation

The Round-Trip Identity was applied to reconstruct the acceleration at two points on the interface, C . This was implemented in accordance with the Results Matrix Structure section.

The reconstructed acceleration FRF at the point c_1 on the interface C is shown in Figure 2.1.5(A). The reconstructed acceleration FRF at the point c_2 on the interface C is shown in Figure 2.1.5(B). Both are compared against the measured acceleration FRFs when exciting at the corresponding position at the interface C , A_{cc}^M .

Figures 2.1.5.A and 2.1.5.B – Reconstructed Accelerance Responses at c_1 (A) and c_2 (B) using The Round-Trip Identity



The reconstructed responses show a good level of agreement at low and mid frequencies up to around 600Hz. Above this frequency there is significant noise, especially at anti-resonance frequencies and positions of low amplitude. Despite this, several of the most significant peaks show good agreement. The fit of the c_1 response is significantly better than the c_2 response at higher frequencies.

2.4.4 - Conclusions

The results of the experiment have shown that the Round-Trip Identity presented by Moorhouse & Elliott (Moorhouse & Elliott, 2013) can be used to reconstruct the response to excitation at a passive location on a test structure. This can be in terms of many different forms of FRF, such as accelerance, mobility, or dynamic impedance. This experiment used accelerometers to measure acceleration and recreated the accelerance of the simply supported beam at a defined point.

A significant limiting factor of the quality of reconstructions was the experimental technique of using the force hammer. An impact that was not a perfect Dirac delta impulse resulted in inaccuracies in reconstructed frequency response functions. A hammer impact that was not a perfect Dirac delta would result in a band-limited response. This could also account for some of the noise seen on the reconstructed responses at the upper end of this frequency band, where measurements may consist of noise and minimal signal.

Insufficient signal-to-noise ratio and lack of repeatability in the hammer impacts could both reduce coherence and degrade the results. Subsequent iterations of the experiment focus on improved technique and repeatability of impacts with the force hammer in order to improve the accuracy of the results.

Another potential reason for noise on the reconstructions is that they were obtained by the inversion of a 2×2 matrix, which is an operation known to amplify measurement noise. Adding more B points to the beam would help to over-determine the system and reduce the effects of this when finding the inverse (or pseudoinverse) of a matrix.

An electro-dynamic shaker was used as an alternative excitation method in subsequent experiments. These experiments attempt to use a combination of mechanical parameters (as in this experiment) and electrical parameters of the shaker to reconstruct acceleration responses. The following section explains the theory behind the modifications to the Round-Trip Identity that will allow the inclusion of electrical parameters.

2.2 - Network Theorems Applied to the Round-Trip Identity

2.2.1 - Kirchhoff's Laws / Firestone's Laws & Tellegen's Theorem

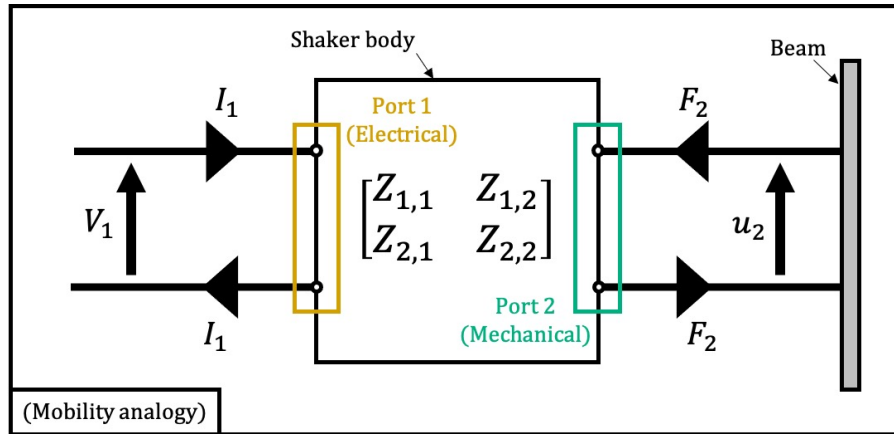
As explained in Section 1.2.3, Kirchhoff's Voltage and Current Laws can be applied to many systems, not just electrical ones. This is also true for Tellegen's Theorem, as this can solely be derived from Kirchhoff's Laws. Whilst these laws are not directly applied in this context, they underpin the application of other theories detailed in this section. Ramachandran & Ramachandran state the application of Tellegen's Theorem to a network is not determined by linearity, time invariance or reciprocity. It is also not dependent on the circuit components, but instead based on the topology or structure of the network (Ramachandran & Ramachandran, 2001).

2.2.2 - Equivalent Circuits & Two-Port Analysis

Combined application of equivalent circuit theory followed by two-port analysis of the resulting circuit could be a useful method for characterising a system with both electrical and mechanical aspects. This was identified as being an established method for the calibration of measurement microphones in standard BS 61094-2:2009, where the interface was between electrical and acoustical domains (BSI, 2009).

If considering a simple modal testing setup with a single electro-dynamic shaker exciting a simply supported beam, the interface between the electrical and mechanical domains occurs inside the electro-dynamic shaker. The shaker can be modelled as a transformer according to equivalent circuit theory or considered as a two-port network. This equivalent circuit is shown in Figure 2.2.1, which uses the mobility analogy. If considering the impedance analogy, the positions of force and velocity would be swapped. The numerical indices remain consistent with Figure 1.2.3, for ease of forming and identifying elements in an impedance matrix. All variables are complex functions of frequency.

Figure 2.2.1: Equivalent Circuit for a Simple Modal Testing Setup



According to the mobility analogy, velocity is equivalent to voltage and force equivalent to current. Based on this, the elements of the impedance matrix can be defined:

- $Z_{1,1}$ is the quotient of voltage V_1 by the current I_1
- $Z_{1,2}$ is the quotient of voltage V_1 by the force F_2
- $Z_{2,1}$ is the quotient of velocity u_2 by the current I_1
- $Z_{2,2}$ is the quotient of velocity u_2 by the force F_2

This impedance matrix consists of one purely electrical element ($Z_{1,1}$), one purely mechanical element ($Z_{2,2}$), and two elements that comprise a mixture of mechanical and electrical terms ($Z_{1,2}$ and $Z_{2,1}$). If the network (and therefore the matrix) is reciprocal, then these two terms should in theory be identical, as explained in Section 1.2.2. It should be noted that the analogy considers velocity, but this work is concerned with measurement of acceleration. In the frequency domain, this conversion (from acceleration to velocity) can be performed by dividing by a factor of $j\omega$.

Smallwood's 1997 paper on electro-dynamic shaker characterisation details an impedance matrix that represents a shaker. The two-port model of a shaker is identified as valid as long as the system behaves linearly and that the force and acceleration can be described adequately by a single pair of variables Smallwood, (1997). The model breaks down when motion cannot sufficiently be described by a single acceleration and single force. This will become important when considering systems with multiple degrees of freedom later in this study.

Smallwood notes that electro-dynamic shakers are typically characterised based on their maximum capability in terms of mechanical parameters, such as displacement, force, and acceleration. This is normally considered with the shaker in an unloaded state (or sometimes with a specified added mass), which Smallwood argues is of limited use and transferability to real-world problems. It also makes assumptions about the rigidity of the test structure, assuming it to be perfectly rigid.

Smallwood emphasises that the shaker's capabilities are dependent on the specifications of the power amplifier it is connected to and that the two should be characterised as a unit. This is helpful in defining the extents of the systems being considered, especially in the electrical domain. Incorrect

consideration of the full extents of and boundaries between these 'sub-systems' could result in any derived identities being invalid. Whilst Smallwood's work is of direct interest to this project, one key difference to note is the focus on introspectively looking to identify properties of the shaker, whereas this work is attempting to use known properties of the shaker as a tool to analyse external systems. A similar approach was taken by Brown & Peres (2008), who identified a method for developing an impedance model of a shaker with a method that involves coupling two shakers that are positioned opposite to each other, with their stingers and impedance heads coupled together.

The electro-dynamic shaker can be considered as a two-port network that features one electrical port and one mechanical port. The application of equivalent circuit theory to the shaker and connected test object allows the system to be considered as a single continuous hybrid system, with mechanical and electrical extents. The Round-Trip Identity can be modified to be applied to this system, as both extents of it satisfy the condition of being linear, time-invariant and reciprocal.

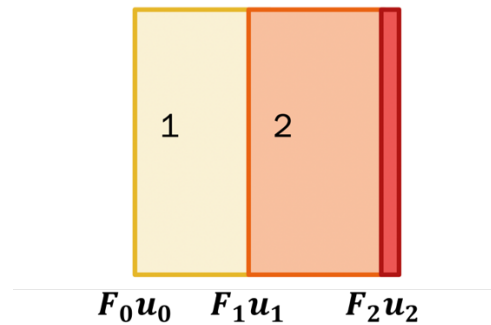
2.3 - Applying Transfer Matrix Analysis to the Round-Trip Identity

Transfer matrix analysis can be used to solve problems of wave propagation in stratified systems. It can be applied to systems that can be considered as a discrete series of subsystems, each only interacting with the subsystems adjacent to it (Campa & Camporeale, 2010).

The transfer matrix method is a powerful tool that can be applied to problems involving any type of wave, including quantum particles, acoustic, and elastic waves.

Consider a one-dimensional system comprised of two distinct, adjacent layers or material, with boundaries at either end of the structure and between each layer (shown in Figure 2.3.1).

Figure 2.3.1: Transfer Matrix System Diagram



The applied force and resultant velocity of the waves incident to the structure are F_0 and u_0 respectively. The force and velocity of the wave after it has propagated through region 1 are F_1 and u_1 respectively.

Using the transfer matrix method, F_1 and u_1 can be related to F_0 and u_0 by Equation 2.3.1:

$$\begin{bmatrix} F_1 \\ u_1 \end{bmatrix} = [1] \begin{bmatrix} F_0 \\ u_0 \end{bmatrix} \quad (2.3.1)$$

The matrix [1] is the transfer matrix that describes region 1 of the structure. Similarly, the relationship between the variables after they have passed from region 1 through region 2 (F_2 and u_2) can be expressed in with the variables F_1 and u_1 and [2], the transfer matrix for region 2. This is shown in Equation 2.3.2:

$$\begin{bmatrix} F_2 \\ u_2 \end{bmatrix} = [2] \begin{bmatrix} F_1 \\ u_1 \end{bmatrix} \quad (2.3.2)$$

This method is advantageous, as we can describe the combined properties of regions 1 and 2 (and thus the entirety of the system) in terms of the inputs and outputs to the system. Substituting the right-hand side of Equation 2.3.1 for the vector $\begin{bmatrix} F_1 \\ u_1 \end{bmatrix}$ gives Equation 2.3.3, which expresses F_2 and u_2 in terms of F_0 and u_0 :

$$\begin{bmatrix} F_2 \\ u_2 \end{bmatrix} = [2][1] \begin{bmatrix} F_0 \\ u_0 \end{bmatrix} \quad (2.3.3)$$

This theory thus far is limited in scope to the mechanical domain. This can be extended to include electrical variables, as a means for modifying the Round-Trip Identity.

2.4 - Development of The Electro-Mechanical Round-Trip Identity

This section sets out modifications that can be made to the Round-Trip Identity in order to include electrical parameters instead of solely mechanical ones. This has been identified as being a potentially useful modification given the abundance of products or machines comprising of hybrid mechanical and electrical systems or interfaces.

2.4.1 - Defining the System

When considering the case of an electro-dynamic shaker exciting a simply supported beam, it is apparent that transduction is present in the system in several forms. Whilst typical modal analysis is primarily rooted in the mechanical domain, the system itself comprises of a number of different domains:

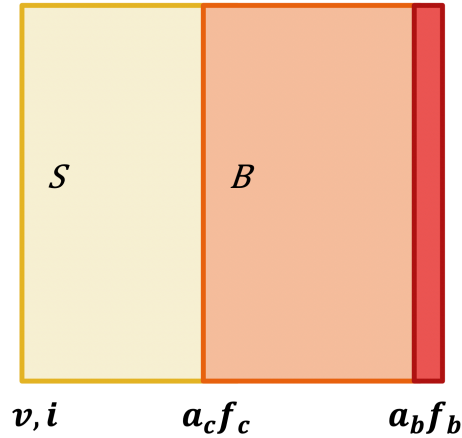
- Electricity is used to power the mechanical shaker. A power supply causes a potential difference across the terminals of the shaker.
- The AC voltage applied across the shaker terminals sets up a changing magnetic field in the wire coils contained in the shaker body.
- The changing magnetic field causes the shaker armature to oscillate, transducing the changing magnetic flux into an oscillating force applied to the armature. The armature is connected to the stinger, which, in turn, is rigidly coupled to the beam, resulting in mechanical excitation of the beam.

This transfer path technically comprises of three distinct domains: electrical, magnetic and mechanical. For simplicity in this initial investigation, the system is considered as a purely mechanical and electrical interface. However, it should be noted that there might consequentially be some factors that are overlooked due to magnetic effects. An electromagnetic interface will behave linearly until a point; increasing the current will normally result in a linearly proportional increase in magnetic flux, but eventually the iron core of the electromagnet will become saturated. This means any increase in applied current will not result in significant increase to magnetic flux, which will tend towards a maximum. Kim notes that most devices in normal operation run at the top end of this linear region (Kim, 2017), so considering the magnetic portion of the system to be linear is a valid assumption.

The shaker is considered as a two-port system, in terms of the system inputs and outputs being connected by a transfer function that describes the behaviour of the system as a whole. The behaviour of elements within this grouping are not characterised individually, only on a systemic level.

This description of the system can be related back to transfer matrix analysis. This system is shown in Figure 2.4.1.

Figure 2.4.1: Electro-Mechanical Transfer Matrix System Representation



This system appears similar to that performed in the explanation of transfer matrix analysis in the previous section, but the change of variables at position S from force and velocity to voltage and current should be noted. This work has previously detailed electro-mechanical analogies and circuits. This relation is underpinned by Firestone’s Force and Velocity laws (Firestone, 1933), which have been identified as modified forms of Kirchhoff’s voltage and current laws.

The S region corresponds to the shaker and the B section to the shaker armature, stinger, and beam. The corresponding transfer matrices describe the propagation effects over the transfer path through regions S and B .

The resulting transfer matrix equations (Equation 2.4.1) describe the relationship between electrical inputs to the shaker (in terms of voltage and current) and the outputted force and acceleration at the boundary between the shaker and the beam. It can be seen that the output vector is the product of the transfer matrix of the shaker, $[S]$, and the electrical input parameter vector:

$$[S] \begin{bmatrix} v \\ i \end{bmatrix} = \begin{bmatrix} a_c \\ f_c \end{bmatrix} \quad (2.4.1)$$

2.4.2 - Transfer Matrices & Circuit Analogies

As before, through substitution, the force and acceleration in the beam can be expressed in terms of the two transfer matrices and the input voltage and current (shown in Equation 2.4.2). The electro-mechanical analogy selected for this was the impedance analogy, which equates applied force with voltage and acceleration (via velocity) with current. This was chosen because of the logical relation between the variables when grouping them based on whether they act ‘through’ or ‘across’ a component.

$$[B] \begin{bmatrix} a_c \\ f_c \end{bmatrix} = [B][S] \begin{bmatrix} v \\ i \end{bmatrix} = \begin{bmatrix} a_b \\ f_b \end{bmatrix} \quad (2.4.2)$$

This form can be desirable as it allows us to consider a structure sequentially in terms of the transfer path (in this case shown from left to right in Equation 2.4.2).

The Round-Trip Identity cannot be implemented with Equation 2.4.2, as the a_c and f_c elements have been cancelled from the equations. These terms are required to reconstruct a mobility at the interface, C . This equation therefore needs to be reformulated. Instead of considering the problem in the sequence of wave propagation through the structure, elements can be grouped based on whether they can be considered as an input or output variable.

Acceleration can logically be considered as an output variable that occurs as a consequence of an applied force. Similarly, current can be considered as an output variable that occurs as a consequence of an applied voltage. These variables are positioned in the input and output vectors accordingly. This results in transfer matrix equations of the forms shown in Equation 2.4.3, where $[A]$ is the mechanical system transfer matrix and Z_E is the electrical system transfer matrix. Equation 2.4.3.A shows the mechanical matrix equation, while Equation 2.4.3.B shows the electrical matrix equation.

$$\begin{bmatrix} a_c \\ a_b \end{bmatrix} = [A] \begin{bmatrix} f_c \\ f_b \end{bmatrix} \quad (2.4.3.A)$$

$$\begin{bmatrix} i_c \\ i_b \end{bmatrix} = [Z_E] \begin{bmatrix} v_c \\ v_b \end{bmatrix} \quad (2.4.3.B)$$

Equations 2.4.3.A and 2.4.3.B only consider mechanical and electrical parameters respectively. Given that the purpose of this research is to incorporate electrical parameters into the calculations, these equations can be combined and modified to give Equation 2.4.4, where voltage and current are included as input and output variables respectively:

$$\begin{bmatrix} i \\ a_b \\ a_c \end{bmatrix} = \begin{bmatrix} A_{aa} & A_{ab} & A_{ac} \\ A_{ba} & A_{bb} & A_{bc} \\ A_{ca} & A_{cb} & A_{cc} \end{bmatrix} \begin{bmatrix} v \\ f_b \\ f_c \end{bmatrix} \quad (2.4.4)$$

This is in accordance with the impedance analogy identified in Section 1.3.3, based on Firestone's force and velocity laws. Equation 2.4.4 shows the expanded acceleration transfer matrix.

The addition of voltage and current terms mean that the measurement matrix is a 3x3 matrix instead of the 2x2 matrix used with the mechanical Round-Trip Identity. The remaining elements refer to hybrid electro-mechanical quantities. The elements of the mobility matrix are given by the following relationships, and are valid under the conditions specified in Matrix Equation 2.4.5:

Matrix Equation 2.4.5:

$$\begin{aligned} A_{aa} &= \left(\frac{i}{v} \right)_{f_b=f_c=0} & A_{ab} &= \left(\frac{i}{f_b} \right)_{f_c=0, v=0} & A_{ac} &= \left(\frac{i}{f_c} \right)_{f_b=v=0} \\ A_{ba} &= \left(\frac{a_b}{v} \right)_{f_b=f_c=0} & A_{bb} &= \left(\frac{a_b}{f_b} \right)_{f_c=0, v=0} & A_{bc} &= \left(\frac{a_b}{f_c} \right)_{f_b=v=0} \\ A_{ca} &= \left(\frac{a_c}{v} \right)_{f_b=f_c=0} & A_{cb} &= \left(\frac{a_c}{f_b} \right)_{f_c=0, v=0} & A_{cc} &= \left(\frac{a_c}{f_c} \right)_{f_b=v=0} \end{aligned}$$

The condition ' $f_n = 0$ ' means that no external forces could be applied at the corresponding position. These were defined as forces that were external to the entire system. The constraint ' $V = 0$ ' means

no external voltage could be applied to the entire system. These conditions do not apply to forces and voltages that are considered to be 'internal' to the system. It should be noted that terms in the same column have identical conditions, and that the first and third columns also have identical conditions. This means that the implementation of this method is not significantly more difficult compared to that of the mechanical Round-Trip Identity. The entire matrix must be determined in order to fully characterise the system, but following this, only three of the terms are required in order to implement the electro-mechanical Round-Trip Identity and reconstruct the response A_{cc} (four if including measurement of A_{cc} for verification purposes).

The measurement procedure required to obtain this transfer matrix is as follows:

- Determine values of A_{ca} and A_{ba} using a shaker attached to the beam with a stinger at the interface c .
- Determine A_{cb} by exciting the test structure at point b with a force hammer and measuring the response at points b and c .

The Round-Trip Identity can then be used to reconstruct a frequency response function (in this case an accelerance) at the interface point c , with an excitation also at point c . The Round-Trip Identity is shown in Equation 2.4.6:

$$A_{cc} = A_{ca} A_{ba}^{-1} A_{cb}^T \quad (2.4.6)$$

Values in the measurement matrix that are required to implement the Round-Trip Identity are highlighted in colour in Equations 2.4.4 to 2.4.6.

2.4.3 - Units-Based Validation of the Electro-Mechanical Round-Trip Identity

It can be shown that the units that result from applying this modified form of the Round-Trip Identity are consistent with the original form of the identity – that is in metres per second squared, per Newton ((m/s²)/N):

$$\left(\frac{a}{v}\right) \left(\frac{a}{v}\right)^{-1} \left(\frac{a}{f}\right) = \left(\frac{a}{f}\right) \quad (2.4.7)$$

The first two terms cancel to give the expected units of accelerance divided by force, (m/s²)/N. This agreement shows that the modifications to the original form of the round-trip identity are dimensionally consistent. Whilst this does not guarantee that the identity is valid, it is encouraging. Following this, the next step was to validate this extension of the identity experimentally. The next section details the design of a simple initial experiment designed to perform this function.

2.5 - Applying the Round-Trip Identity with Electrodynamic Shaker Properties: Initial 'Forwards-Path' Measurement

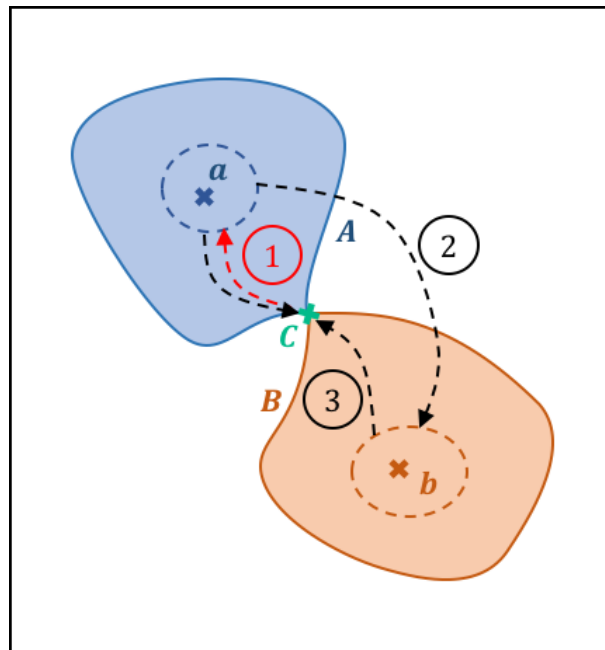
2.5.1 - Aims

The aim of the experiment was to identify if electrical quantities (in the form of voltage and current inputs to an electro-dynamic shaker) can be incorporated into the round-trip identity to reconstruct a remote point accelerance with a simple experimental setup.

2.5.2 - Methodology

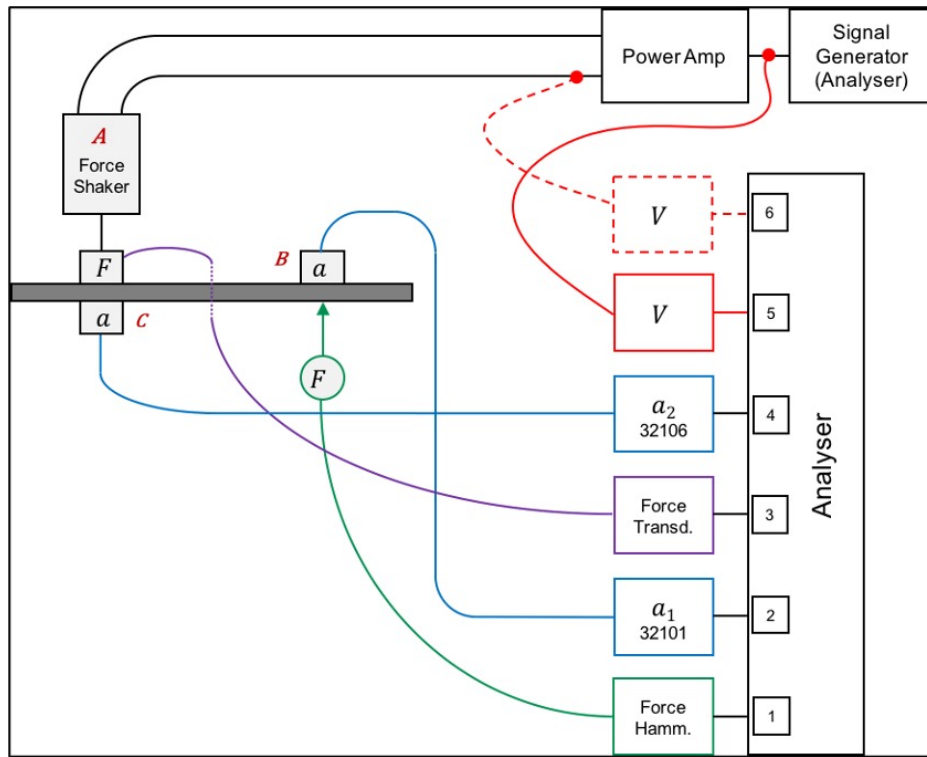
The forwards-path form of the Round-Trip Identity was chosen for this initial investigation (as previously expressed in Equation 2.4.6). This is the form of the identity detailed by Moorhouse and Elliott in their original paper on the identity (2013). Details of the geometry of the 'forwards-path' round-trip being considered are shown in Figure 2.5.1. The red arrow refers to the portion of the round-trip that is reversed during the implementation of the identity. Positions of points within each region are arbitrary.

Figure 2.5.1: Schematic Round-Trip Representation (Forwards-Path)



The experimental setup consisted of a 350mm long Perspex beam attached to a shaker via a stinger. This setup is shown in Figure 2.5.2.

Figure 2.5.2: Diagram of 'Forwards-Path' Measurement Setup



The positions of regions *A*, *B*, and the interface *C* are shown by their respective red letters. It should be noted that the position of the *B* region remains the same as with the previous verification of the mechanical Round-Trip Identity, but that the *A* region is different. Due to the modifications made to the Round-Trip Identity to incorporate electrical parameters, the *A* region is now considered as being measured at the terminals of the electrodynamic shaker. Consequentially, this means that the definition of the interface *C* connecting the two points has also changed. The region *C* is now considered as being an arbitrary point on the beam, in between the point where the stinger connects to the beam and the *B* region.

Other than the connection to the stinger, the beam was freely suspended with no net external forces acting on it. The stinger was mounted between the shaker and the beam to constrain the axis of vibration to a single direction. The voltage measured across the shaker terminals was used as a reference during the shaker measurements and the force hammer channel provided the reference when making force hammer measurements. The voltage was monitored by feeding it back into an analyser input channel. It was not necessary to measure current for the forward path measurements. Channel allocation and measurement details on the analyser were assigned as shown in Table 2.5.1.

Table 2.5.1: Forwards-Path Measurement Channel Allocation

Channel No.	Description	Units	Sensitivity
1	Force Hammer	N	0.01041
2	Accelerometer C	m/s^2	0.009596
3	Force Transducer	V	0.00335
4	Accelerometer B	m/s^2	0.009641
5	Voltage across Analyser	V	1
6	Voltage across Amplifier	V	1
7	Voltage across Resistor (Reference only)	V	1

Channel 7 was originally included when current was also being measured, by measuring the voltage drop across a known resistor. Given current measurement was not required for the forwards path measurement, this was omitted in this iteration of the experiment and will be included in subsequent iterations. The values of the voltage channels were all monitored in order to discern any differences between them. Readings from either channel 5 or 6 would be required to implement the forwards path identity. There was no observable difference between the two measurement positions with this simple setup, but both positions continued to be monitored moving forward with the experimental setup in case differences were to emerge in future. Channel 7 was not required for the forwards path measurement but was included at this stage to identify if responses were clean and noise-free for future development of experiments where current measurement would be necessary.

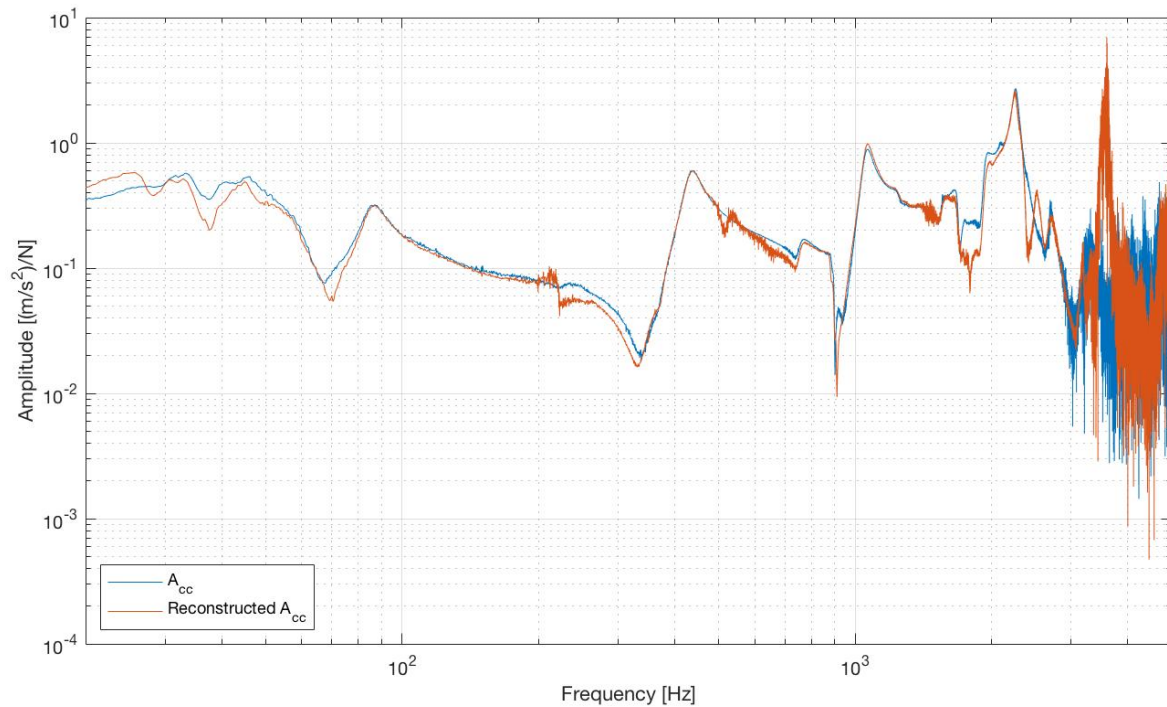
The beam was excited for 15 cycles during shaker measurement, then averaged over this period. This was deemed to be a sufficient number of averages to significantly reduce random errors. Verification of this was performed by performing a test measurement and identifying after what duration the changes to the on-screen FRF were minimal.

The force hammer measurement followed the shaker measurement. The beam was excited at point b and also at the interface, c for validation purposes (to enable calculation of A_{cc}). Four hammer hits were averaged at each position, in order to reduce random error. Monitoring of on-screen coherence functions during measurement allowed identification of double hits or inconsistent hammer impacts.

2.5.3 - Results

Results processing was performed in MatLab. The H_1 matrices for the hammer and shaker measurements were combined to create a single H_1 results matrix. Data that was not required in order to implement the Round-Trip Identity was removed from the matrix, condensing it in order to streamline the analysis and more easily identify any erroneous processing. This process resulted in a $3 \times 2 \times Z$ matrix. This processing was also performed with other measured parameters: autospectrum, cross-spectrum, and coherence functions. The positions of parameters required for implementation of the Round-Trip Identity were identified in the results matrix. These were loaded as variables and used to implement the Round-Trip Identity. The reconstructed value of A_{cc} was then compared against the directly measured value. This comparison is shown in Figure 2.5.3.

Figure 2.5.3: Comparison of Measured and Reconstructed Values of A_{cc} (Forwards-Path)



The two responses show generally good agreement between 80Hz and 3kHz. The frequency response over which the force hammer can obtain accurate results is dependent on both its dimensions and the type of tip used (a harder tip will allow slightly extended high frequency range), so these could have been limiting factors. Both responses became noisy above 3kHz and noisy regions could be found at 200Hz, 500Hz – 750Hz and 1.7kHz – 1.9kHz. Peaks showed very good agreement below 3kHz.

Reasons for a noisy response could include:

- Low signal-to-noise ratio when using the voltage as a reference. This was due to the voltage portion of the FRF, as examination of the voltage response showed regions of noise that were not present on the acceleration measurements.
- Inadequate technique using the force hammer. It was noted that any inconsistencies or double hits using the hammer would significantly impact the results due to the high internal damping of the Perspex beam. Time history responses were checked for adjacent transients indicating a double hit had occurred, but none were identified.

The quality of the response could be improved in subsequent repeats of the experiment by having multiple excitation points in the B region, which would over-determine the results matrix, improving the chance of solutions to matrix equations and improving the quality of reconstructed FRFs.

Better agreement between the measured and reconstructed responses could also be obtained by using a shorter stinger, as the available one was likely too long. The importance of an appropriate length of stinger is summarised by Cloutier et al. as follows:

“Generally, if the stinger is too short, the structure will have increased stiffness which can lead to shifts in mode frequencies and possibly additional modes. On the other hand, too long of a stinger can introduce additional peaks due to stinger resonances.” (Cloutier et al, 2019)

Another important factor is the condition of the stinger – a stinger that is bent or deformed, even if only very slightly, can result in distortion at certain modes. This could account for some of the distortion present on the reconstructed response as the stinger used was very slightly bowed.

Overall, the good agreement between the measured and reconstructed responses of A_{cc} shows that using electrical parameters in place of mechanical ones is a valid extension to the Round-Trip Identity.

Conclusions and Further Work

There was generally good agreement between the measured and reconstructed responses of A_{cc} . This means that the forwards-path Electro-Mechanical Round-Trip Identity is valid in practice, and that use of electrical parameters to reconstruct mechanical FRFs is possible. There is scope for improvement in the quality of the reconstructions, however. Experimental changes that may further improve the quality of the reconstructed response include:

- Using a shorter stinger to constrain the direction of vibration transmitted through the stinger more effectively.
- Improving hammer precision to help reduce noise on the results and extend the noise-free frequency range of the results.
- Adapting the experiment to improve the signal-to-noise ratio of electrical measurements. This could result in a significant reduction in noise present on the reconstruction. The low signal-to-noise ratio could have been introduced by the presence of the power amplifier in the signal chain, but this component is necessary in order to drive the shaker.

An alternate form of the Electro-Mechanical Round-Trip Identity can be derived by considering the reciprocal elements of the electro-mechanical measurement matrix and the reverse round-trip path. Following this experiment, the next step was to attempt to experimentally verify this ‘reverse-path’ form of the identity.

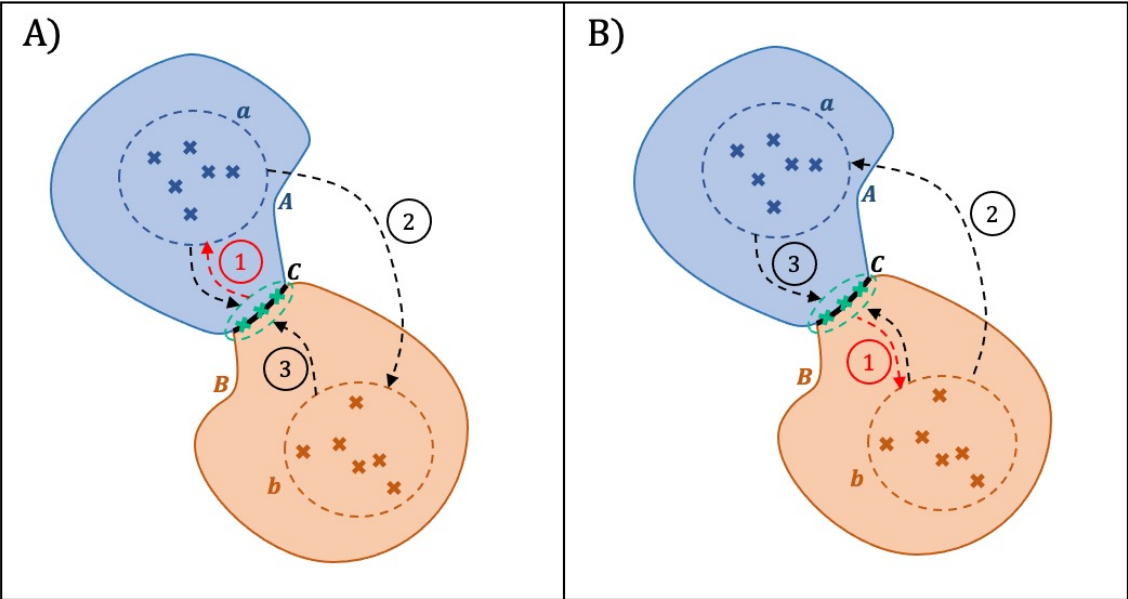
2.6 - Applying the Round-Trip Identity with Electrodynamic Shaker Properties: Reverse-Path Measurement

Following on from the forwards-path version of the experiment, the measurements were repeated, but with focus on the reverse-path measurement, exciting with an arbitrary force and achieving the reconstruction using the reciprocal elements in the matrix. This also consisted of a simultaneous repeat of the forwards-path measurement.

For the reciprocal measurements, current needed to be measured directly. This was obtained by measuring the voltage drop across a resistor of known value. This resistor needed to be capable of experiencing high power levels, as to prevent the resulting change in temperature and inaccuracy in the voltage measurement. As such, a high-power resistor was required. The value of the resistor used needed to be very low (in the order of several Ohms) to prevent it impeding the normal functioning of the shaker, which had an impedance of 3Ω at 500Hz . A 2.2Ω 100w resistor was deemed to meet these criteria.

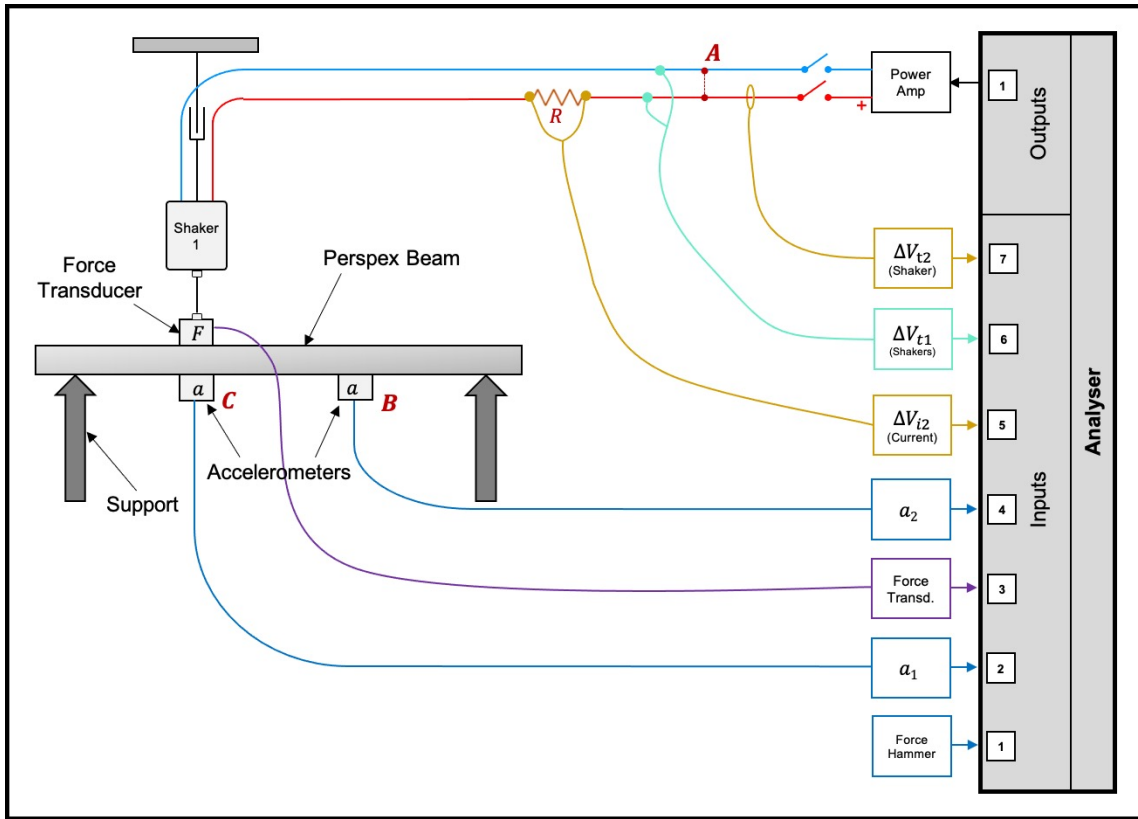
The reverse-path round-trip is the inverse of the original form of the identity, obtained by considering reciprocal elements of the electro-mechanical measurement matrix. The original form of the identity considered the three legs of the round-trip as being from c to b , b to a , and then a to c , with the first leg reversed. The inverse of this is therefore c to a , a to b , and then b to c , with the first leg also reversed. The forwards and reverse paths are represented in Figure 2.6.1, with 2.6.1.A showing the forwards path and 2.6.1.B showing the reverse path. Reversed legs of the round-trip are indicated by red arrows.

Figure 2.6.1: Visual Representation of Forwards (A) and Reverse (B) Round-Trip Paths



The setup for the reverse-path version of the experiment is shown in Figure 2.6.2 and is not significantly different to the forwards path setup, but in this case, channel 7 voltage readings were stored and used to calculate the current flowing into the electro-dynamic shaker.

Figure 2.6.2: Reverse-Path Experimental Setup



2.6.1 - The Reverse-Path Round Trip Identity:

In order to reconstruct the acceleration response at the interface *C* when considering the reverse-path, a modified form of the round-trip identity must be used. The original form of the identity is shown in Equation 2.6.1:

$$A_{cc} = A_{ca} A_{ba}^{-1} A_{cb}^T \quad (2.6.1)$$

This becomes the following expression for the reverse path measurement:

$$A_{cc,rev} = A_{cb} A_{ab}^{-1} A_{ca}^T \quad (2.6.2)$$

The elements of the acceleration matrix are the same as before, but the reverse method requires the use of different elements, based on the round-trip sequence being considered. The elements are highlighted in colour in Matrix Equation 2.6.3, to correspond to their position in the Round-Trip Identity.

Matrix Equation 2.6.3:

$$\begin{array}{lll}
 A_{aa} = \left(\frac{i}{v}\right)_{f_b=f_c=0} & A_{ab} = \left(\frac{i}{f_b}\right)_{f_c=0, v=0} & A_{ac} = \left(\frac{i}{f_c}\right)_{f_b=v=0} \\
 A_{ba} = \left(\frac{a_b}{v}\right)_{f_b=f_c=0} & A_{bb} = \left(\frac{a_b}{f_b}\right)_{f_c=0, v=0} & A_{bc} = \left(\frac{a_b}{f_c}\right)_{f_b=v=0} \\
 A_{ca} = \left(\frac{a_c}{v}\right)_{f_b=f_c=0} & A_{cb} = \left(\frac{a_c}{f_b}\right)_{f_c=0, v=0} & A_{cc} = \left(\frac{a_c}{f_c}\right)_{f_b=v=0}
 \end{array}$$

This is convenient because A_{ca} is recorded as part of the forwards path measurement. Only two additional parameters, A_{bc} and A_{ab} , need to be measured to reconstruct the accelerance response Y_{cc} using the reverse path identity. These are obtained by measuring the current flowing into the shaker at a and the acceleration at b , whilst exciting at c respectively. Measurement of current was not required when implementing the forwards-path form of the identity, if using the impedance analogy. The measurement of current was initially performed by measuring the voltage drop across a resistor and performing a subsequent Ohm's Law calculation to determine the current.

Calculation of the current was determined by calculating the voltage drop between positions V_1 and V_2 , measured immediately on either side of the resistor. The result was divided by the resistance value of the resistor, R (2.2Ω), in accordance with Ohm's Law. It was important to ensure the resistor temperature was kept as constant as possible, as this could cause inaccuracy in the Ohm's Law calculation. The resistor being used featured a heat sink in its design and was placed on a thermally conductive metal plate in order to dissipate as much heat as possible. A small increase in temperature of the device was noted, but this was not pronounced. The Ohm's Law calculation is shown in Equation 2.6.4:

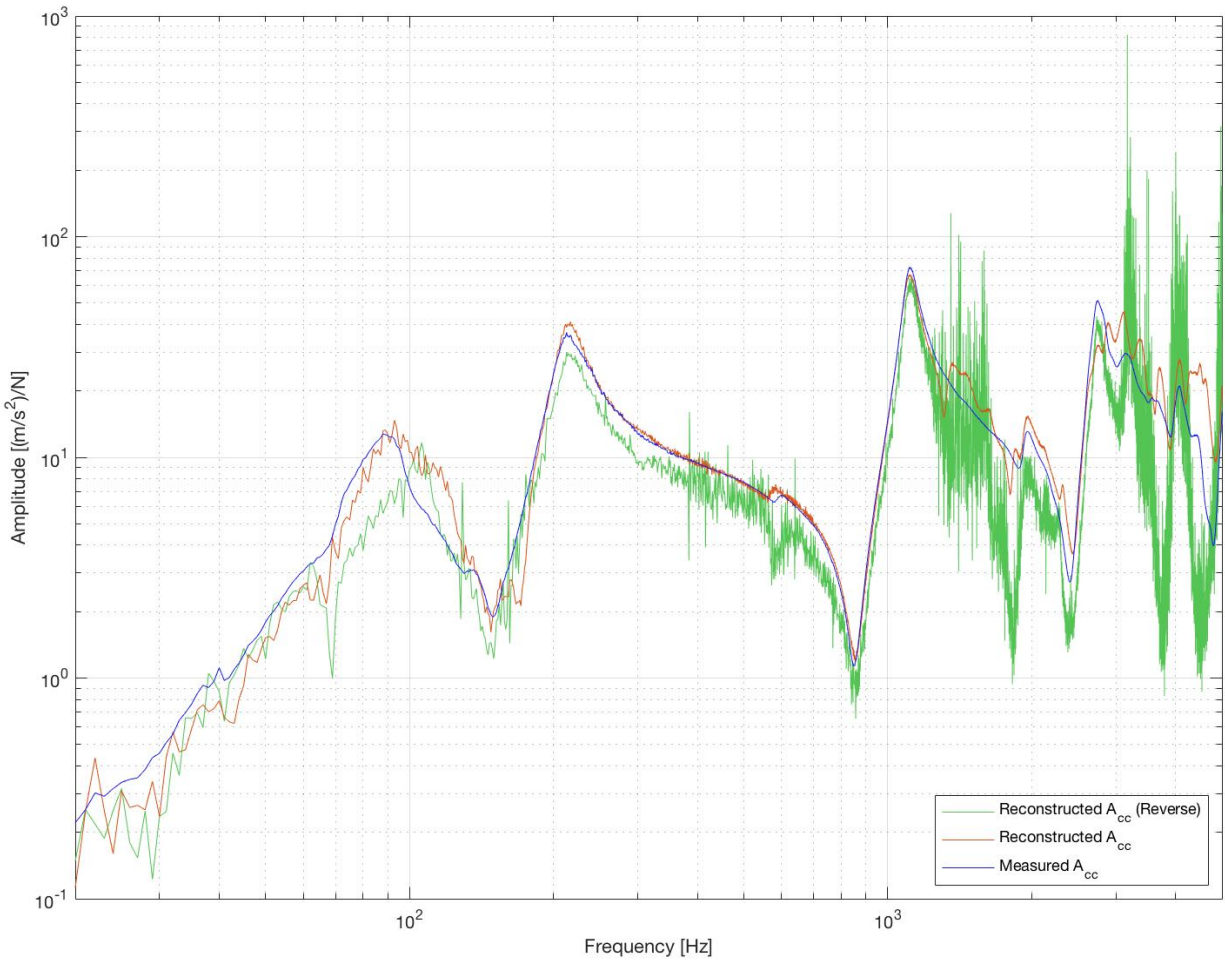
$$I = \frac{|V_1 - V_2|}{R} = \frac{|V_1 - V_2|}{2.2} \quad (2.6.4)$$

With the addition of the resistor to the setup, the a points were considered as between the power amp terminals and the resistor. This means that the shaker and the resistor were considered as being 'grouped' and that any functions describing the shaker's behaviour included the influence of the resistor as a part of this.

2.6.2 - Results

Figure 2.6.3 shows the comparison between the forwards-path and reverse-path accelerance response FRFs.

Figure 2.6.3 - Comparison Between Forwards-Path and Reverse-Path Accelerance Response FRFs.



Both reconstructed FRFs show reasonable agreement with the measured FRF in terms of their overall shape. There are regions that do not show good agreement – notably the peak around 100Hz and above 3kHz for both reconstructions. The forwards-path reconstruction is significantly higher quality than the reverse-path reconstruction, as the latter has significant levels of noise above 200Hz and becomes increasingly contaminated as frequency increases. Both reconstructed FRFs show significant notches in their responses below 100Hz, which are not present on the measured FRF.

The frequency alignment of peaks in the responses is generally good with the exception of the 100Hz peak. There is good agreement between 200Hz and 2kHz for the forwards-path FRF and between 200Hz and 1.1kHz for the reverse-path FRF.

The agreement in the magnitude of peaks in the responses is less strong than their frequency alignment. Exceptions to this are the anti-resonance at around 900Hz for the forwards path response and the peak at 1.1kHz for both reconstructions, which are very similar.

The reverse-path reconstructed response is significantly corrupted by noise across the frequency range of interest. This is most pronounced at higher frequencies but is still significant elsewhere. This

suggests that there was a fundamental issue associated with one or more of the measured FRFs that were used to implement the reverse-path identity.

The FRFs that were used for the reverse-path identity are A_{bc}^T , A_{ab}^{-1} , and A_{ca} . The first two of these three FRFs are unique to the reverse-path identity, but A_{ca} is present in both path forms, meaning it cannot be the source of noise as similar problems did not occur with the forwards-path reconstruction. The variables involved in the A_{bc}^T and A_{ab}^{-1} FRFs were inspected to identify the cause of noise. Equations 2.6.5.A and 2.6.5.B show how these FRFs were calculated:

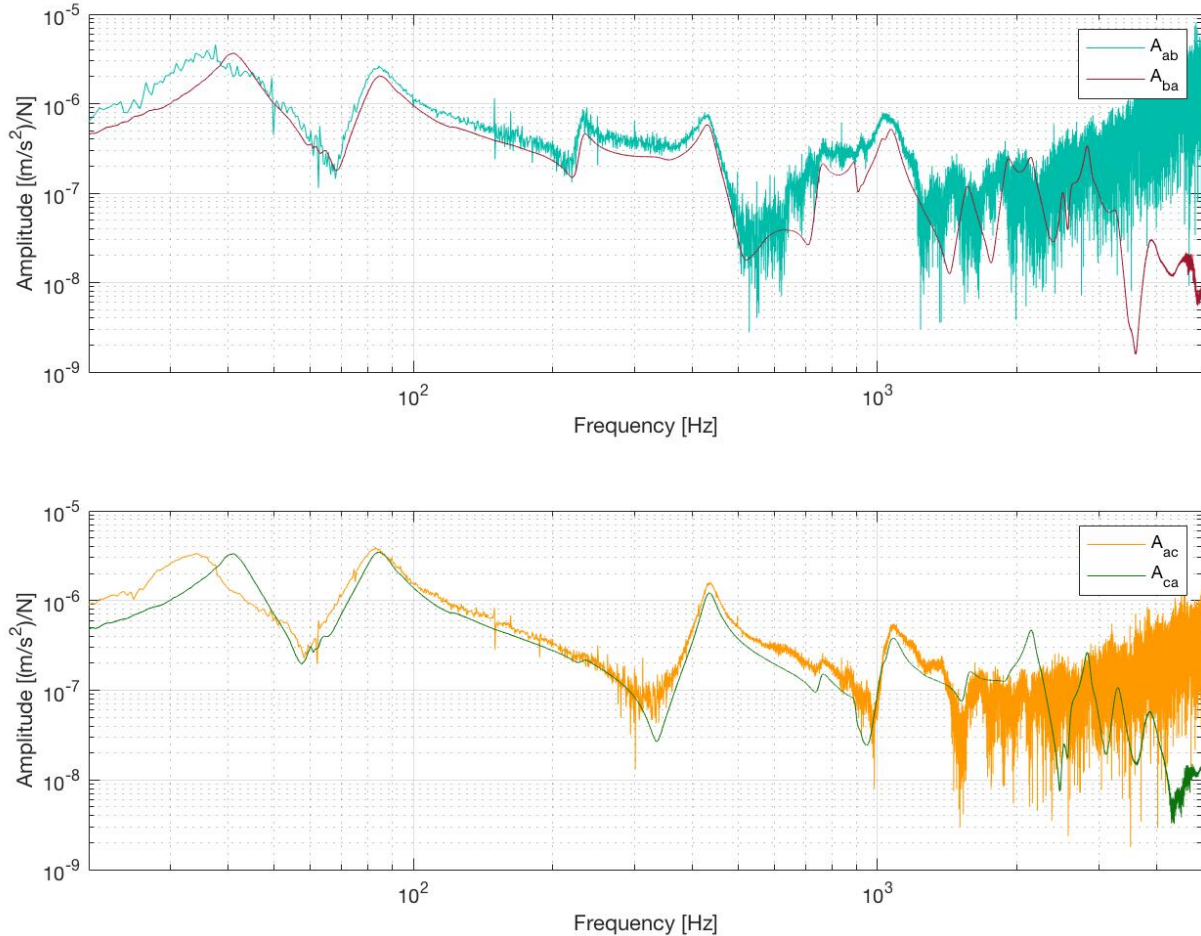
$$A_{bc} = \left(\frac{a_b}{f_c} \right)_{f_b=v=0} \quad (2.6.5.A)$$

$$A_{ab} = \left(\frac{i}{f_b} \right)_{f_c=0, v=0} \quad (2.6.5.B)$$

Equations 2.6.5.A and 2.6.5.B show that A_{bc}^T is a solely mechanical FRF, being the ratio of acceleration and force. A_{ab}^{-1} , however, is a hybrid electro-mechanical FRF, being the ratio of electrical current and mechanical force. Inspecting the two FRFs reveals that A_{ab}^{-1} is corrupted by noise and that A_{bc}^T is comparatively clean.

The element A_{ac} is in the same row as A_{ab}^{-1} in the measurement matrix and, being in the same row, is also the ratio of a current to another variable (in this case the applied force at the interface c). A_{ac} is also in the same column of the measurement matrix as A_{bc} , meaning that both are the quotient of a different variable by the force applied at the interface c . By inspecting the A_{ac} FRF, it can be confirmed that current is the variable causing the noise contamination as both A_{ab}^{-1} and A_{ac} FRFs show noise. These FRFs are shown in Figures 2.6.4.A and 2.6.4.B respectively, with the reciprocal elements in the measurement matrix included in each case. If the system is entirely reciprocal, FRFs that are between the same positions but measured in a different direction should be identical.

Figure 2.6.4: Reciprocity Checks for A_{ab} vs. A_{ba} (A) and A_{ac} vs. A_{ca} (B)



The cause of the noise shown in A_{ab}^{-1} and A_{ac} FRFs could be attributed to signal levels being very low when measuring current, as the shaker was not active during this portion of the measurement. It may indicate that use of a high-power resistor and Ohm's Law to measure current is not valid in this context, or that an alternative current measurement method with a higher bandwidth or signal-to-noise ratio could be required. Both responses are particularly noisy above 1kHz, suggesting that the bandwidth may be a limiting factor.

A potential solution to these problems could be provided by switching the excitation method to one that generates higher signal levels, changing the method for measuring current to one with a greater bandwidth, or modifying the identity to ensure measurement of current only occurs when the shaker is being actively driven. A combination of these solutions may prove most effective.

Following this experiment, the setup was modified to include an additional shaker to compare excitation methods and identify if use of a shaker could reduce noise on measured responses when measuring current.

The findings of this would then inform whether further modifications to the test rig, or the identity itself, were required.

2.7 - The Electro-Mechanical Round Trip Identity Applied to a Simply Supported Beam: Two-Shaker Setup

2.7.1 - Experimental Design & Setup

A variation of the previously used Perspex beam setup was devised in order to compare force hammer and shaker excitation methods. This was done to reduce the contamination of noise on the reverse-path reconstruction FRFs, which was identified as an area for improvement of the results obtained in Section 2.6.

The setup was similar to the previous iterations, but the force hammer was replaced with an additional shaker that was connected to the beam at the B region. This shaker was also connected using a stinger to constrain vibration to a single axis. Each shaker was powered independently and with a dedicated power amplifier.

Shakers can provide a very clean FRF over an extended frequency range when used correctly, so these changes could provide an improvement in the quality of the measured FRFs, especially at higher frequencies.

The experimental setup is shown in Figure 2.7.1. The analyser channel allocation is shown in Table 2.7.1.

Figure 2.7.1: Two-Shaker Experimental Setup Diagram

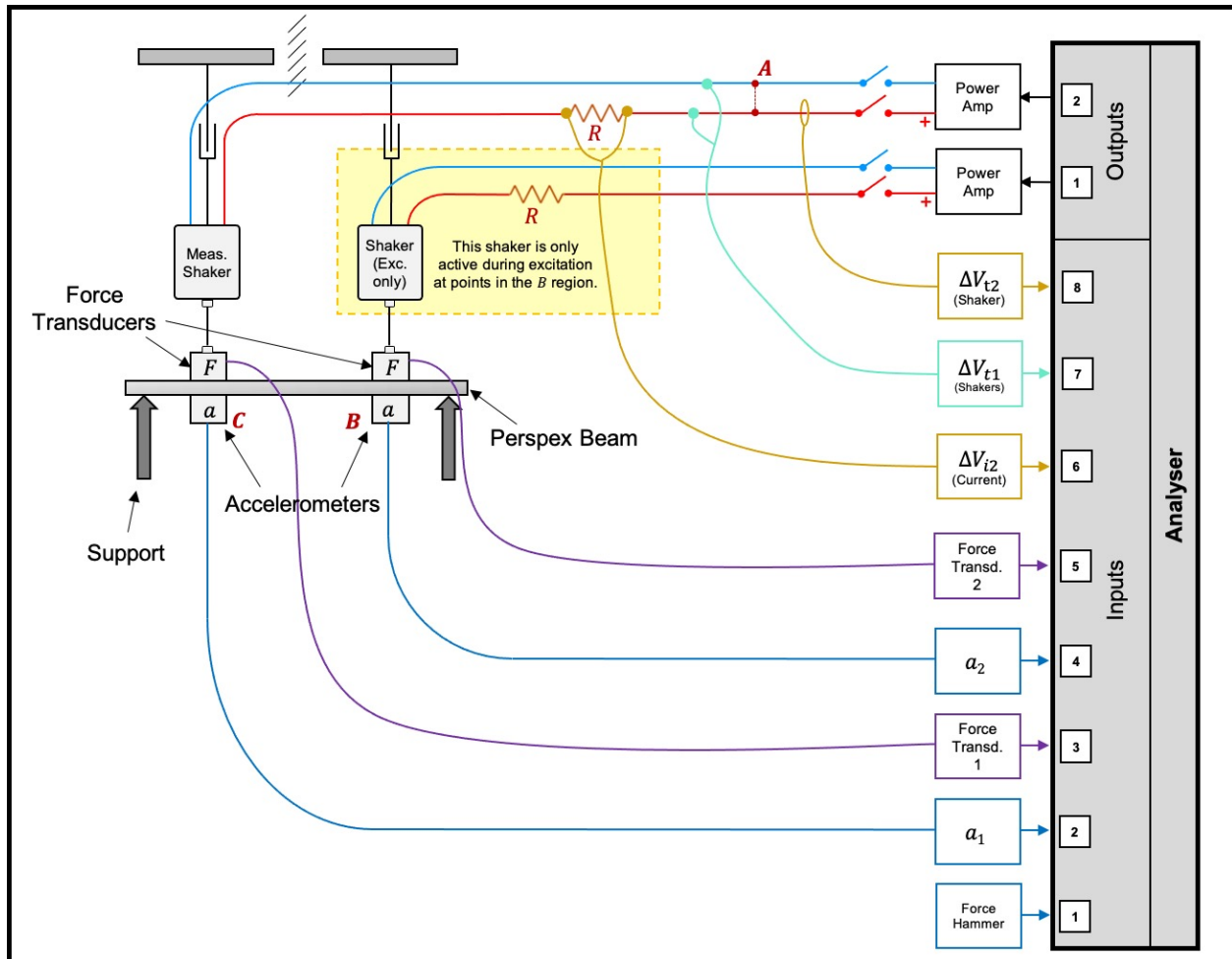


Table 2.7.1: Two-Shaker Experiment Channel Allocation

Channel No.	Description	Units	Sensitivity
1	Force Hammer	N	0.01041
2	Accelerometer C	m/s^2	0.009596
3	Force Transducer, C	N	0.00335
4	Accelerometer B	m/s^2	0.009641
5	Force Transducer, B	N	0.00357
6	Voltage across Resistor	V	1
7	Voltage across Amplifier	V	1
8	Voltage across Resistor (Reference only)	V	1

From this point the shaker connected at the interface, C will be referred to as the “measurement shaker”, and the shaker at B will be referred to as the “excitation shaker”, since it is only used for measurement of FRFs related to points in the B region.

Both shakers were fed an identical white noise output at separate times, with a signal level of +0.1 Volts outputted by the analyser. The excitation shaker was mechanically connected to the beam via the stinger for the duration of the experiment but was disconnected at its electrical terminals when

not exciting the beam. This was to satisfy the boundary conditions as identified in the electro-mechanical results matrix in Section 2.4.2.

Measurements were conducted as previously, but an additional shaker measurement was made using the excitation shaker at point *b*. The force hammer measurements were conducted to allow comparison of the two excitation methods. Sufficient measurements were made to allow both the forwards and reverse-path forms of the Round-Trip Identity to be implemented and evaluated.

2.7.2 - Results

Figure 2.7.2 shows the measured, forwards-path and reverse-path accelerance responses.

Figure 2.7.2: Two-Shaker Measured vs. Reconstructed Accelerance Responses at *c* (Forwards & Reverse)

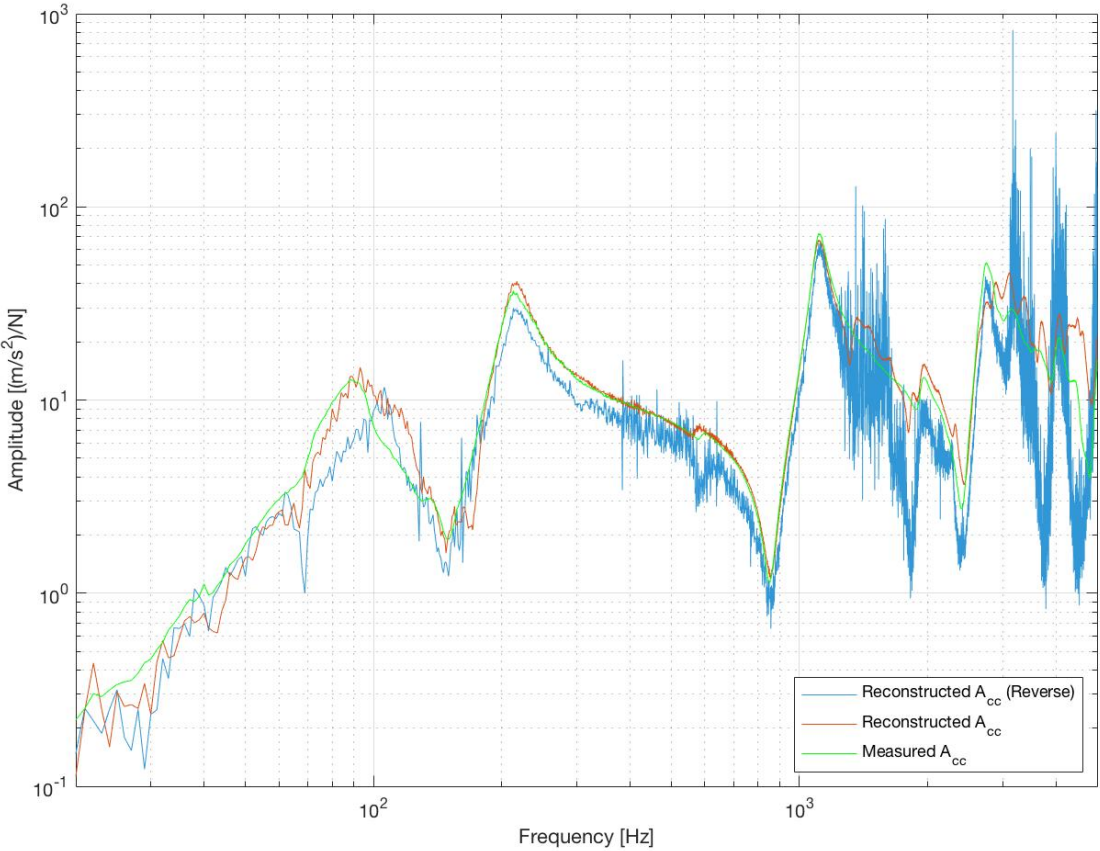
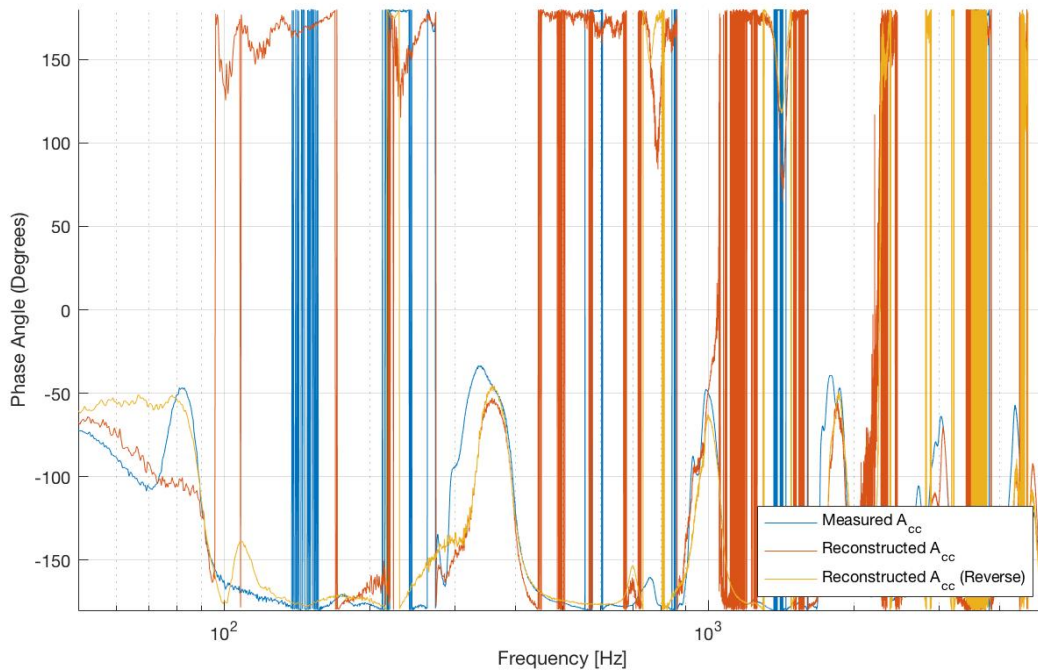


Figure 2.7.3 shows the measured and reconstructed phase responses that accompany the magnitude components shown in Figure 2.7.2. This is included in order to indicate that the phase responses do not contribute much useful information and that phase reconstructions were of good quality. As a result, phase responses will not be included alongside magnitude responses in the rest of this study unless they are of particular note.

Figure 2.7.3: Two-Shaker Measured vs. Reconstructed Phase Responses at c (Forwards & Reverse)



The reconstructed forwards-path accelerance response shows generally good agreement with the measured response. Regions of it are intermittently noisy, but not to an extent that causes significant deviation from the measured response, other than above 3kHz where this similarity starts to break down. Alignment of peaks in the forwards-path response is generally good, both in terms of frequency and amplitude.

The reverse-path response follows largely the same trend with respect to frequency as the measured and forwards-path responses but is contaminated by significant levels of noise that increase with frequency. Above 1kHz, the alignment with the measured response breaks down with little correlation and extreme noise contamination above 3kHz. The visible general trend in the data suggests that the reverse-path form of the identity is theoretically valid, but that there have been practical problems in terms of implementation and measurement. The reconstructed responses are a significant improvement over the initial reverse-path iteration of the experiment and are less noisy for the reverse-path FRF overall.

The causes of this can be narrowed down by looking at the parameters that constitute the reverse-path Round-Trip Identity but are not present in the forwards-path form. The quality of the forwards-path response indicates that there are minimal practical issues associated with the measurement of either A_{ca} , A_{ba} , or A_{cb} . A_{ca} is present in both identities, so is unlikely to be the cause of noise, leaving A_{bc} and A_{ab} as potential problem elements.

A_{bc} is a solely mechanical parameter, being the ratio of acceleration and force. A_{ab} is a hybrid electro-mechanical parameter, as the ratio of electrical current and force. Inspecting A_{ab} in MatLab shows

that the signal levels measured during the calculation of A_{ab} are very low. This is because this is essentially a measurement of the voltage in the circuit when the shaker is being driven in reverse by mechanical excitation. A voltage was measured from the circuit and Ohm's Law was applied to determine the corresponding current.

This voltage measurement can be considered as a measurement of a back or counter electromotive force, a phenomenon that arises as a consequence of fundamental laws of electromagnetism.

2.7.3 - Back Electromotive force and Associated Measurement Difficulties

“Back” or “counter” electromotive force (back EMF) is a voltage that is generated in the opposite direction to the flow of current in a circuit. It is caused by electromagnetic induction, specifically the motion of the armature with respect to the coils in an electro-magnetic device, which causes the generation of a voltage that acts in the opposite direction to (and in series with) the applied voltage that is used to power the device. This occurs in electric motors and moving coil devices.

Back EMF occurs as a consequence of Lenz's Law, which can be considered an electro-magnetic counterpart to Newton's Third Law. This states that when two bodies interact, they will exert a force that is equal in magnitude and opposite in direction upon each other. In the context of Newton's Law, this applies to mechanical forces, but Lenz's Law states that a change in a magnetic field will generate an electric field that opposes this change (Schmitt, 2002). Whilst Lenz's Law states this relationship qualitatively, Faraday was the first to express it quantitatively. Faraday's Law is shown in Equation 2.7.1, where N is the number of turns of wire on a solenoid, B is magnetic flux density of the magnetic field, in Teslas and A is the area of the coil in square metres:

$$V = -A \cdot N \frac{dB}{dt} \quad (2.7.1)$$

Consideration of back EMF is important in the context of this research, as with the impedance analogy, the measurement of A_{ab} is essentially a measurement of the back EMF induced due to the vibration of the beam moving the shaker table and generating a voltage and across its coils.

It can be seen from Faraday's Law that the induced back EMF increases with respect to the number of coils and the speed of the oscillation of the motor armature (equating to a higher rate of change of magnetic flux). Motors are designed with a back EMF constant in mind to allow them to draw sufficient current and generate the desired torque at a given speed.

The value of this will be extremely low under operational conditions, making the measurement of it difficult. These measurements were significantly impacted by the noise of the measurement system and having a low signal-to-noise ratio.

This means that with the impedance analogy, the reverse path is less practical to perform than the forwards one, which does not involve a variable that is as practically difficult to measure. Switching electro-mechanical analogies was identified as a potential method for minimising back EMF associated measurement difficulties. This is addressed in the following section.

Another option for improving the issues associated with measurement of current is to change the measurement method. A Hall-Effect sensor was implemented to measure current in experiments following this stage. Details of the design and implementation of this can be found at Appendix B.

2.7.4 - Changing the Electro-Mechanical Circuit Analogy

The two-shaker experiment demonstrated that it was difficult to measure voltage signal levels when implementing the reverse-path electro-mechanical Round-Trip Identity. This section will detail a change to the electro-mechanical Round-Trip Identity that presents improvements to both the forwards and reverse path measurements. This is in terms of ease of measurement and quality of reconstructed FRFs and is achieved through switching the electro-mechanical circuit analogy.

With the initial choice of the impedance analogy, force was equated to voltage, and velocity to current (with conversion from velocity to acceleration being performed by multiplying by a factor of $j\omega$). Swapping the positions of voltage and current in the analogy results in a measurement matrix with different elements, switching the analogy to the mobility form. In the revised matrix, current measurement is required for the forwards measurement and voltage for the reverse. This new matrix is more practical, as the measurement of current is only required when the measurement shaker is actively being driven. This means that current values are of a more easily measurable magnitude and are less likely to be corrupted by noise. Measuring the back EMF voltage for the reverse measurement path is also easier in practice, as the measurement chain is significantly more direct than when measuring current.

The revised matrix equation for the experiment, now using the mobility analogy, is shown in Equation 2.7.2. The switch in positions of voltage and current elements between Equations 2.4.4 and 2.7.2 should be noted:

$$\begin{bmatrix} v \\ a_b \\ a_c \end{bmatrix} = \begin{bmatrix} A_{aa} & A_{ab} & A_{ac} \\ \mathbf{A}_{ba} & A_{bb} & A_{bc} \\ \mathbf{A}_{ca} & \mathbf{A}_{cb} & \mathbf{A}_{cc} \end{bmatrix} \begin{bmatrix} i \\ f_b \\ f_c \end{bmatrix} \quad (2.7.2)$$

This yields the following measurement matrix:

$$\begin{aligned} A_{aa} &= \left(\frac{v}{i} \right)_{f_b=f_c=0} & \mathbf{A}_{ab} &= \left(\frac{v}{f_b} \right)_{f_c=i=0} & A_{ac} &= \left(\frac{v}{f_c} \right)_{f_b=i=0} \\ \mathbf{A}_{ba} &= \left(\frac{a_b}{i} \right)_{f_b=f_c=0} & A_{bb} &= \left(\frac{a_b}{f_b} \right)_{f_c=0, v=0} & \mathbf{A}_{bc} &= \left(\frac{a_b}{f_c} \right)_{f_b=i=0} \\ \mathbf{A}_{ca} &= \left(\frac{a_c}{i} \right)_{f_b=f_c=0} & \mathbf{A}_{cb} &= \left(\frac{a_c}{f_b} \right)_{f_c=0, v=0} & A_{cc} &= \left(\frac{a_c}{f_c} \right)_{f_b=i=0} \end{aligned}$$

Both forms of the electro-mechanical round trip identity are included below for reference. The positions of terms in the identities themselves are unchanged, but the variables used to calculate of some of these terms now differ (those in the left column and top row specifically, all of which include an excitation or response at a).

Equation 2.7.3 shows the Forwards-path form of the identity:

$$A_{cc} = A_{ca} A_{ba}^{-1} A_{cb}^T \quad (2.7.3)$$

Equation 2.7.4 shows the Reverse-path form of the identity:

$$A_{cc,rev} = A_{bc} A_{ab}^{-1} A_{ca}^T \quad (2.7.4)$$

These changes to the measurement matrix result in several changes to the measurement sequence, as follows:

- Perform the measurement shaker test to obtain A_{ca} (forwards-path and reverse-path) and A_{ba} (forwards-path). The reference channel should be the current (channel 7).
- Excite with the additional shaker at b points to obtain A_{cb} (forwards-path) and A_{ab} (reverse-path). The reference channel should be the force at B (channel 5). The measurement shaker circuit should be open during the measurement of A_{ab} in order to satisfy the boundary conditions shown in the measurement matrix.
- Use the impact hammer to obtain A_{bc} (for the reversed path) and A_{cc} (for verification). The reference channel is the force hammer (channel 1)

These changes were implemented in the experimental setup outlined in Section 2.8.

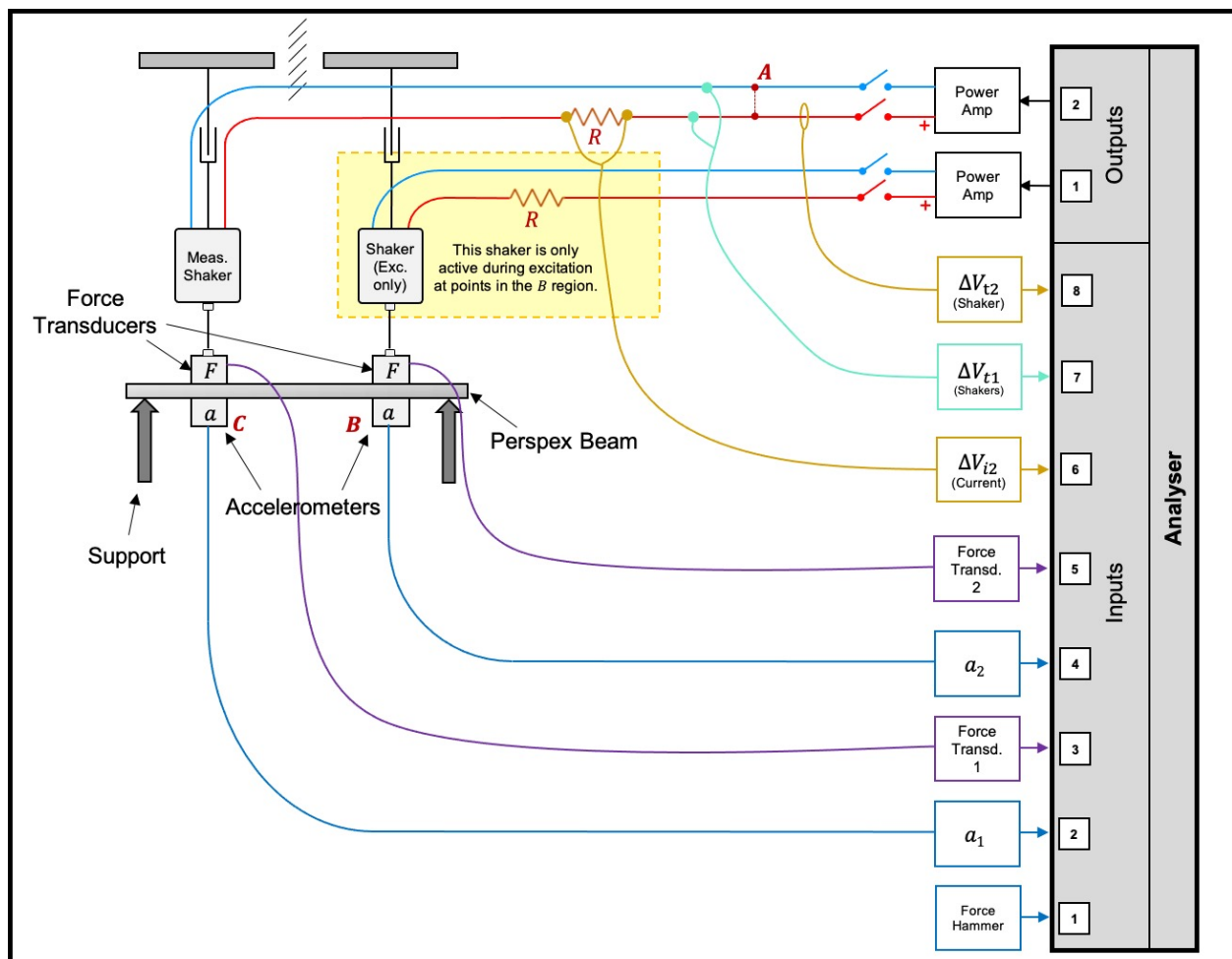
2.8 – Two-Shaker Experiment with the Revised Circuit Analogy Applied to a Simply Supported Beam

The two-shaker experiment was repeated with the revisions made due to the selection of circuit analogy. As before, the aim of this was to compare using an additional shaker for excitation with a force hammer. The quality of the forwards-path and reverse-path reconstructions were also compared.

2.8.1 - Experimental Setup

Figure 2.8.1 shows the revised setup for the experiment. This largely remains unchanged from the previous iteration. The voltage measurement position was moved to being made directly across the measurement shaker terminals, with a 2.2Ω high-power resistor acting as a buffer between it and the analyser. This was compared with measurements at several different positions and provided the voltage responses that were least contaminated with noise. A Hall-Effect current sensor was used in place of the resistor voltage-drop method. A thorough explanation of the design and implementation of this sensor can be found at Appendix B.

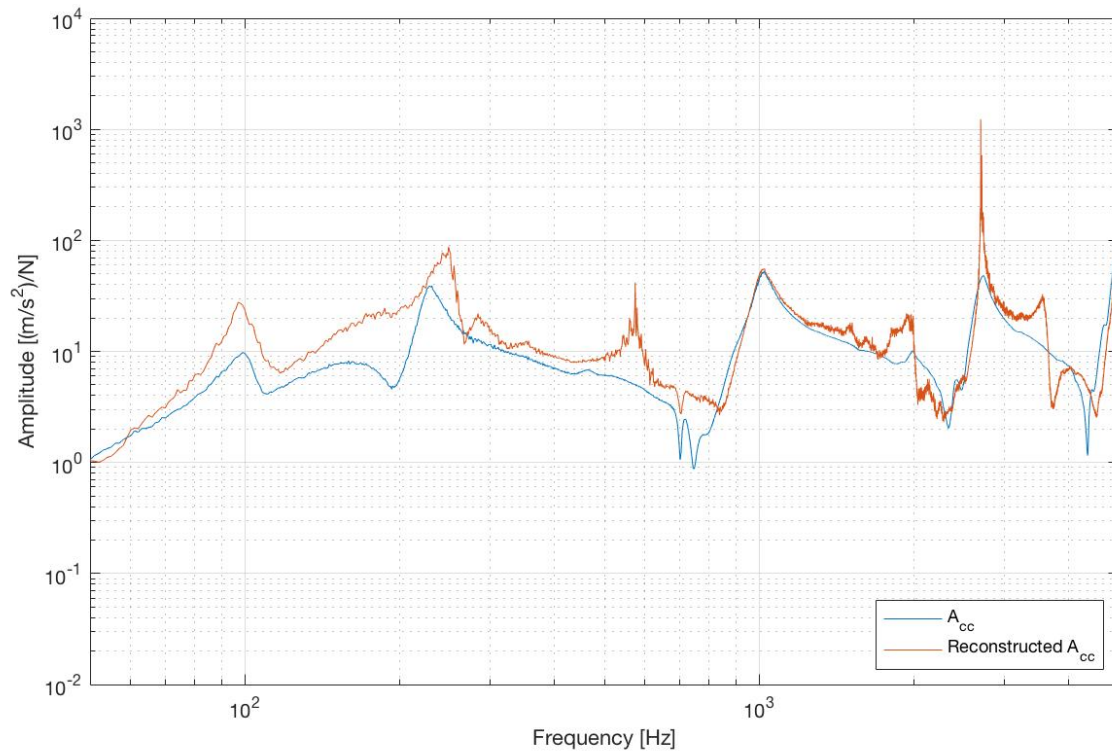
Figure 2.8.1: Revised Two-Shaker Setup for the Simple Beam Experiment, using the Mobility Analogy



2.8.2 - Results

Figure 2.8.2 shows the forwards-path responses at c , comparing the measured and reconstructed responses.

Figure 2.8.2: Two-Shaker Forwards-Path Accelerance Responses for a Simple Beam

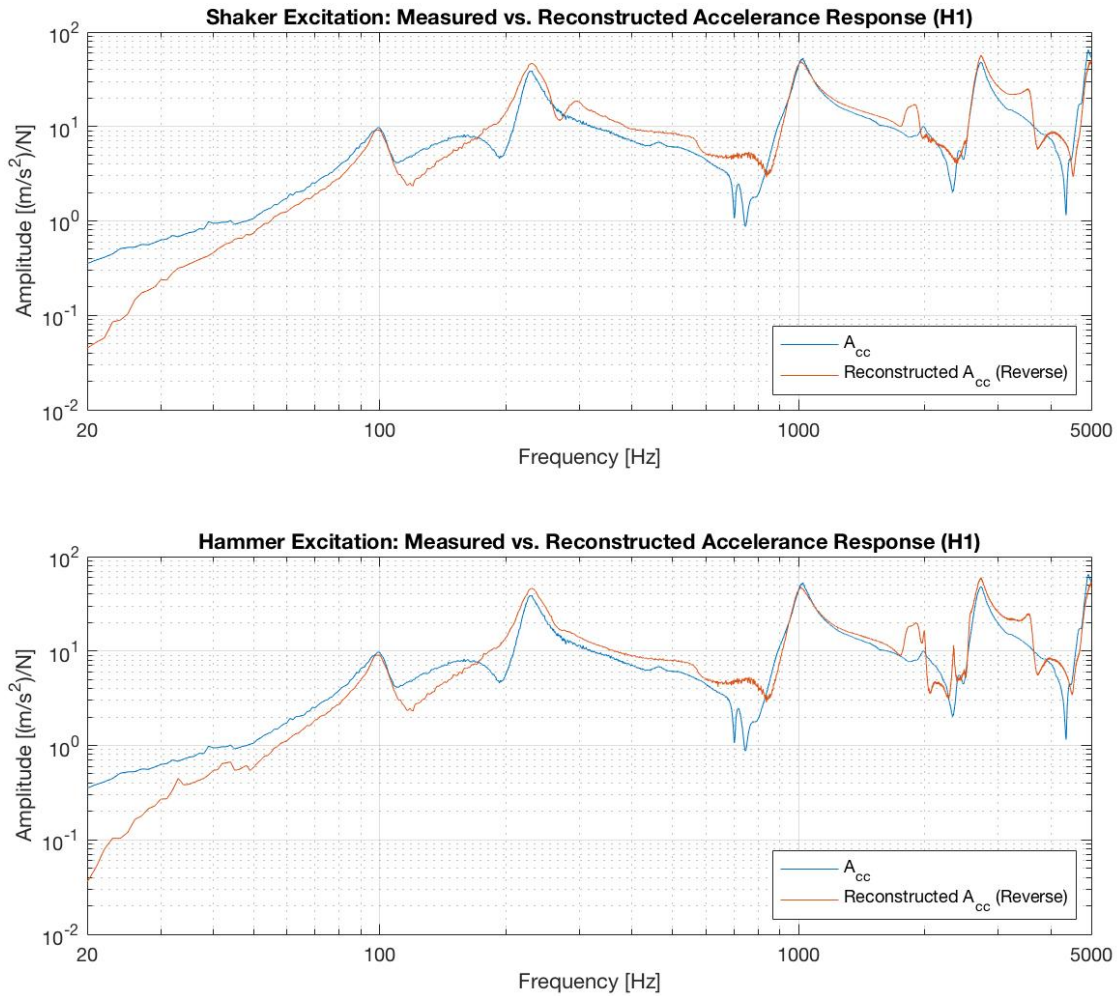


The forwards-path reconstruction using the mobility analogy shows significant improvements in levels of noise compared to previous experiments that used the impedance analogy. There is still scope for further reduction of noise, especially at points of low amplitude.

The agreement between measured and reconstructed responses is loose below 1kHz but improves slightly above this. There is general agreement in terms of the frequency alignment of peaks, but less correlation in terms of peak amplitude values, except for at 1kHz, where the region around the accelerance peak shows very good agreement.

Figure 2.8.3 shows the reverse-path responses, using the shaker and hammer respectively for excitation. Both are compared with the measured response at c .

Figure 2.8.3: Two-Shaker Reverse-Path Accelerance Responses for a Simple Beam (Excitation Comparison)



The reverse-path responses shown in Figure 2.8.3 are significantly less noisy than the forwards path response, only showing noisy regions at positions of low amplitude at frequencies above 600Hz. The reverse-path being less noisy than the forwards-path does not match the pattern seen previously with the impedance analogy. The reason for this could be that the electrical signal levels measured are much higher for the reverse-path than the forwards-path measurement, as the shaker is actively being driven during the reverse-path measurement. Previously, with the impedance analogy, this was the case during the forwards-path measurement. However, the portion of the measurement where the shaker is inactive still features significantly higher signal levels than with the impedance analogy, which encountered significant problems measuring very low back EMFs. This validates that the change in the circuit analogy was a substantial improvement, as the reduction in noise on responses is significant.

The measured and reconstructed responses show a reasonable level of agreement overall. There are still some regions that do not show a good level of agreement, notably below 100Hz and the positions of low amplitude from 100-200Hz, 700-800Hz, in addition to regions around 2kHz and 4kHz. The

shaker response shows a better fit than the hammer response at this 2kHz region. It is generally less noisy at positions of low amplitude and has a slightly smoother response, with fewer sudden notches than the hammer response.

The accelerance peaks are very similar for hammer and shaker responses, and both show good agreement with the measured response.

2.8.3 - Conclusions

The change from the impedance analogy to the mobility analogy significantly improved the quality of the reconstructed responses, most notably for the reverse-path identity.

The reverse-path mobility analogy method yielded sufficiently high-quality reconstructed responses that correlated well with the measured responses. This indicated that this form of the identity should be implemented in future experiments.

It should be noted that the forwards-path mobility form of the identity is likely to be more useful in practice as it does not require excitation at the interface C , unlike the reverse-path that requires excitation in each of the three regions.

The forwards-path mobility form of the identity requires excitations at a and b points and responses measured at b and c points. The reverse-path identity requires excitations and measurement of responses at each position. One of the benefits of the Round-Trip Identity is that it allows the reconstruction of FRFs at a remote position, without the need to measure at that position. This is not the case in this instance, which could be considered to make this form of the identity less useful.

The experimental work conducted to this point is sufficient to verify that the Electro-Mechanical Round-Trip Identity is valid for SDOF systems, but with the caveat that there is still some further optimisation required in order to improve the quality of results to the level of those for purely mechanical systems. As a result, this study goes on to investigate the application of the identity to more complex systems.

The experiments performed to this point have considered the interface C to comprise of a single point. Moorhouse & Elliott's original paper on The Round-Trip Identity (Moorhouse & Elliott, 2013) applies the identity to a range of interfaces, from single point to multi-point and continuous. Subsequent experimental designs in this study feature multi-point interfaces and multiple degrees of freedom.

2.9 - Applying the Electro-Mechanical Round-Trip Identity to MDOF Systems

To this point, this study has considered a simple, one-dimensional system in order to establish whether electro-mechanical extensions to the round-trip identity are valid. The next logical step is to apply this form of the identity to a more complex system with a greater number of degrees of freedom. This will better determine its feasibility for more complex, real-world problems. An example of a real-world scenario would be to use an electric motor as a test object, but an intermediate stage was included between this and the simple beam case. This was to minimise chance of errors due to significant simultaneous changes to the experimental setup.

An experiment was set up on a simply supported beam using two measurement shakers, but the work was unable to be completed due to COVID-19 forcing closure of university facilities. No data was obtained as a result. Despite this, details of the principles underpinning analysis of MDOF systems are included in this section. Part 3 of this thesis will outline further MDOF experiments that were planned to follow the validation of the identity in relation to SDOF systems.

2.9.1 - Introduction to Multi-Degree-of-Freedom Analysis

Ewins explains that MDOF tests and multi-point excitation methods are beneficial as they allow for excitation of structures, especially larger ones, in a way that more closely simulates their vibration during normal operation than with a single-point excitation (Ewins, 2000).

The proposed intermediate stage consists of a two-shaker setup (with one shaker for measurement and two for excitation only) and a multi-point interface connecting the two domains, a and b .

This more complex system requires a number of further considerations. When analysing a MDOF system, it must be ensured that there are sufficient receiver positions as to over-determine the system. For a system to be over-determined, it must have fewer unknowns than variables, otherwise there may not be solutions when solving matrix equations to form FRFs.

A plate will have a significantly higher number of modes than a simple beam. These can sometimes occur at the same frequency, referred to as repeated roots. Identification of a repeated root requires a sufficient number of sensors and excitation positions (Karakan, 2008).

2.9.2 - Experimental Changes

The decision was made to continue using the Perspex beam as a test object. The move to a metal beam (or other comparatively dense material) would provide additional challenges due to the significantly lower damping of the beam, resulting in sharper resonances and a higher dynamic range. This can result in the presence of noise at frequency regions of low amplitude and make it more difficult to obtain high-quality FRFs.

It was decided to change the test structure to a plate following the first MDOF beam experiment to minimise the iterative changes between experiments. A plate, according to Kirchhoff-Love theory, is assumed to be linearly elastic, homogeneous, and isotropic. It also has a thickness that is far smaller than its other dimensions.

There are difficulties associated with the modal analysis of plates that are not present for beams. These include potential for lower measurement coherence, the increased number of modes adding complexity, and the requirement of a larger excitation force that generates sufficient levels of vibration in the test structure to be measured successfully. Quantifying the vibration of plates is of particular importance as the flexural vibration that they exhibit couples readily with surrounding air. Manik notes that, as a result, this is typically the dominant noise-generating mechanism for airborne noise generated by machines (Manik, 2017).

Following successful implementation of the identity to a plate, the test object can be changed to a simple DC electric motor, then more complex motor variants. Sections 3.2 and 3.3 provide more details on this, for single-phase DC and more complex motors respectively.

This sequence minimises the number of changes between each step, with only one aspect of the setup changing each time.

2.9.3 - Matrix Rank, Over-Determination & Regularisation

The rank of a results matrix is an important consideration when designing modal analysis experiments and processing measured data. A matrix described as having ‘full-rank’ contains linearly independent columns and or rows. For a square matrix to be described as ‘full-rank’, its determinant must also be non-zero (Strang, 2006). If elements in a matrix are dependent on previous elements, the matrix is described as being ‘rank deficient’. Rank deficiency can magnify error and introduce noise to datasets. A rank-deficient system cannot be over-determined and attempting to solve the series of matrix equations that describe the system may not result in a unique solution as a consequence.

In the case of a simply supported beam, two degrees of freedom (one translational and one rotational) are being considered. This requires two accelerometers to completely describe the motion of the beam.

Use of further accelerometers does not provide new information, as the motion of the beam can be entirely described by the responses at the two accelerometers. This principle follows when considering a 6-DOF system; 3 correctly positioned accelerometers can completely describe the motion of this system in each co-ordinate axis, and the use of additional sensors does not necessarily add any independent new data. Large or complex systems may have significantly higher numbers of degrees of freedom and will require a greater number of sensors to characterise their behaviour as a result.

Despite this, it is often desirable to use more accelerometers than required to fully describe a system as it will ensure over-determination of the accelerance matrix. Thite & Thompson note that over-determination can reduce the sensitivity of matrix inversion methods to measurement errors. They note that in some cases however, over-determination does not help to “*reduce the magnification of errors*” (Thite & Thompson, 2003). In such cases, additional methods are required in order to reduce the impact of measurement errors. Two commonly applied processes are singular value rejection and regularisation.

Singular value rejection involves removal of small singular values from a matrix. These values can contribute disproportionately to levels of measurement noise. The process involves setting an

appropriate threshold value, below which small singular values are removed from the matrix and replaced with zeroes (Thite & Thompson, 2003).

Regularisation can also be performed to increase the rank of a matrix. This is a complex, established, and in-depth process, the full extent of which is beyond the scope of this project. A brief overview and discussion of the benefits is included. This is primarily based upon the work of Thite & Thompson, in the second part of their 2001 paper on the quantification of structure-borne transmission paths by inverse methods (Thite & Thompson, 2003 and 2006).

The regularisation process involves selectively removing data following eigenvalue analysis of a matrix, prioritising removal of data that has a high level of dependence, in order to identify and reduce the causes of redundancy, increasing the rank of data. This process is especially important when working with large datasets. Making sense of very large datasets can be difficult without the use of regularisation.

It is expected that the rank of an acceleration matrix for a plate would be lower than that of a simple beam. Regularisation is relevant to the analysis performed in this project because it is desirable to be able to quantify the extent of data redundancy in each case. It is likely that the multi-point interface plate system will be rank deficient due to the complexity of the system.

2.9.4 – Applying the Electro-Mechanical Round-Trip Identity to a Simple Beam with a Multi-Point Interface

A multi-DOF system is defined by Ewins as having “dynamic behaviour determined by a combination of inertia and stiffness effects” in addition to damping effects (Ewins, 2000), noting that this includes the vast majority of systems that modal analysis is required to be applied to.

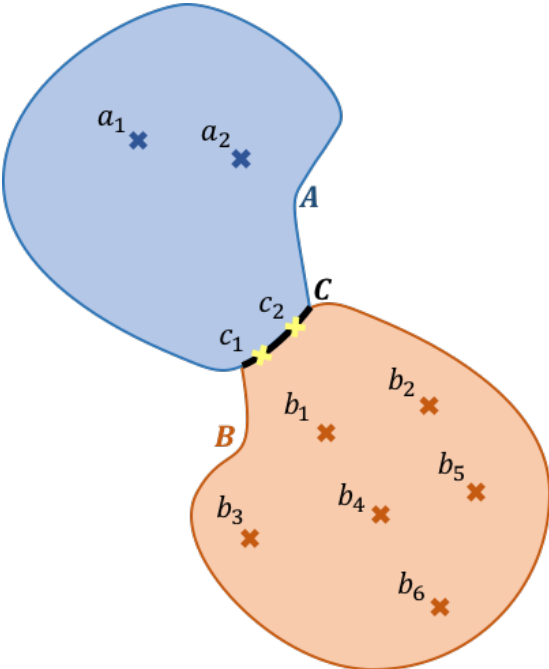
The simplest multi-DOF system is a homogenous beam that is considered to vibrate both translationally (as before), but also rotationally, adding a second degree of freedom. A modified form of the previous experimental setup would be used, with additional accelerometers connected to measure vibration in the rotational axis.

Two measurement shakers would be applied to the system. The previously excitation-only shaker would be replaced with a force hammer, as this is simpler to set up and was found previously to yield a result comparable in quality to the excitation-only shaker. This simplicity becomes more apparent as the number of interface points increases, where additional shakers would need to be powered and individually connected versus using the same force hammer.

The addition of another measurement shaker, considered as an extent into an electrical sub-system, is consistent with limitations identified by Smallwood (1997). Smallwood identifies that the two-port model of a shaker is only valid when the pair of electrical inputs corresponds to outputs that can be considered as a single pair of force and acceleration values. If motion becomes more complex, the model breaks down. Therefore, by extension, it is feasible that using multiple shakers considered as separate two-port networks would be a valid method for describing more complex motion of systems.

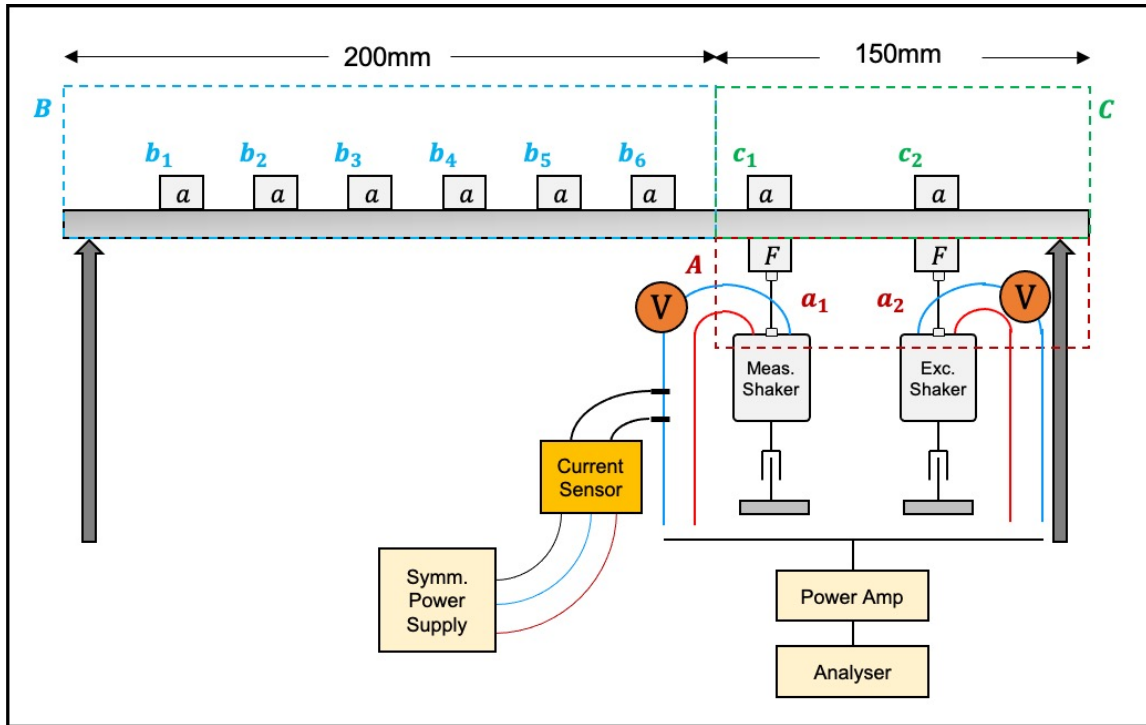
In order to over-determine the results matrix, the experimental setup detailed here consists of two a points, two interface (c) points, and six b points. This number of b points should be sufficient but adding further b points will further over-determine the system. This is illustrated in Figure 2.9.1, where region A is considered as being in the electrical domain and region B as being in the mechanical domain. The locations of points within each region are arbitrary.

Figure 2.9.1: Multi-Point Interface Block Region Diagram



The experimental setup requires eight accelerometers (with two at c positions and six at b positions) and two force transducers (one at each c point). This setup is shown in Figure 2.9.2. The channel allocation for the experiment is shown in Table 2.9.1.

Figure 2.9.2: Proposed Experimental Setup for the MDOF Experiment Applied to a Simply Supported Beam



It should be noted that the two shakers are mechanically isolated from each other.

Table 2.9.1: MDOF Experiment Analyser Channel Allocation

Channel No.	Parameter	Unit
1	Accelerometer c_1	m/s^2
2	Accelerometer c_2	m/s^2
3	Accelerometer b_1	m/s^2
4	Accelerometer b_2	m/s^2
5	Accelerometer b_3	m/s^2
6	Accelerometer b_4	m/s^2
7	Accelerometer b_5	m/s^2
8	Accelerometer b_6	m/s^2
9	Force Transducer c_1	N
10	Force Transducer c_2	N
11	Force Hammer	N/m^2
12	Voltage 1	V
13	Voltage 2	V
14	Current Sensor 1	I
15	Current Sensor 2	I

The power amp should be switched between the shakers when each is active to ensure a repeatable and coherent output. This is also needed to satisfy the open circuit boundary condition at the inactive shaker.

The measurement conditions can be broken down into three categories based on the excitation position:

- When exciting at a points, unplug the inactive shaker from the power supply and apply no external forces to the beam at b or c points.
- When exciting at c points, unplug both shakers from the power supply and apply no external forces at any b points and the other c point.
- When exciting at b points, unplug both shakers from the power supply and apply no external forces at any c or other b points.

The results matrix and full extents of the excitation conditions are shown in Table 2.9.2, where the top row indicates the variables that must be held constant during each measurement. This shows the full results matrix, identifying every data point that is obtained through the experiment and which conditions must be valid to measure them correctly.

Table 2.9.2: Multi-Point Interface Results Matrix

Hold	i_2, f_{c_1}, f_{b_n}	i_1, f_{c_2}, f_{b_n}	i_n, f_{c_2}, f_{b_n}	i_n, f_{c_1}, f_{b_n}	$i_n, f_{c_1}, f_{b_{2 \rightarrow 6}}$	$i_n, f_{c_1}, f_{b_{1,3 \rightarrow 6}}$	$i_n, f_{c_1}, f_{b_{1,2,4 \rightarrow 6}}$	$i_n, f_{c_1}, f_{b_{1 \rightarrow 3,5,6}}$	$i_n, f_{c_1}, f_{b_{1 \rightarrow 4,6}}$	$i_n, f_{c_1}, f_{b_{1 \rightarrow 5}}$
$E \rightarrow$ $R \downarrow$	a_1	a_2	c_1	c_2	b_1	b_2	b_3	b_4	b_5	b_6
a_1	Aa_1a_1	Aa_1a_2	Aa_1c_1	Aa_1c_2	Aa_1b_1	Aa_1b_2	Aa_1b_3	Aa_1b_4	Aa_1b_5	Aa_1b_6
a_2	Aa_2a_1	Aa_2a_2	Aa_2c_1	Aa_2c_2	Aa_2b_1	Aa_2b_2	Aa_2b_3	Aa_2b_4	Aa_2b_5	Aa_2b_6
c_1	Ac_1a_1	Ac_1a_2	Ac_1c_1	Ac_1c_2	Ac_1b_1	Ac_1b_2	Ac_1b_3	Ac_1b_4	Ac_1b_5	Ac_1b_6
c_2	Ac_2a_1	Ac_2a_2	Ac_2c_1	Ac_2c_2	Ac_2b_1	Ac_2b_2	Ac_2b_3	Ac_2b_4	Ac_2b_5	Ac_2b_6
b_1	Ab_1a_1	Ab_1a_2	Ab_1c_1	Ab_1c_2	Ab_1b_1	Ab_1b_2	Ab_1b_3	Ab_1b_4	Ab_1b_5	Ab_1b_6
b_2	Ab_2a_1	Ab_2a_2	Ab_2c_1	Ab_2c_2	Ab_2b_1	Ab_2b_2	Ab_2b_3	Ab_2b_4	Ab_2b_5	Ab_2b_6
b_3	Ab_3a_1	Ab_3a_2	Ab_3c_1	Ab_3c_2	Ab_3b_1	Ab_3b_2	Ab_3b_3	Ab_3b_4	Ab_3b_5	Ab_3b_6
b_4	Ab_4a_1	Ab_4a_2	Ab_4c_1	Ab_4c_2	Ab_4b_1	Ab_4b_2	Ab_4b_3	Ab_4b_4	Ab_4b_5	Ab_4b_6
b_5	Ab_5a_1	Ab_5a_2	Ab_5c_1	Ab_5c_2	Ab_5b_1	Ab_5b_2	Ab_5b_3	Ab_5b_4	Ab_5b_5	Ab_5b_6
b_6	Ab_6a_1	Ab_6a_2	Ab_6c_1	Ab_6c_2	Ab_6b_1	Ab_6b_2	Ab_6b_3	Ab_6b_4	Ab_6b_5	Ab_6b_6

The sequence of steps used to obtain these parameters is as follows:

- a columns: Excitation at a_1 and a_2 using the measurement shakers, switching the power amp connection between shakers to satisfy boundary conditions.
- b columns: Excitation using the force hammer at the six b points.
- c columns: Excitation at c_1 , then c_2 using the force hammer.

2.10 - Part 2 Summary & Conclusions

2.10.1 - Summary

Development of the Electro-Mechanical Round-Trip Identity

Following the verification of the Round-Trip Identity, network theorems were applied to the identity in order to extend it to include electrical parameters. These network theorems included equivalent circuit theory, two-port analysis and transfer matrix analysis.

Equivalent circuit theory allows representation of non-electrical systems as a series of electrical circuit elements. This can simplify calculations of system properties for hybrid systems that extend into multiple domains. This can extend to any system that is linear and time-invariant, but hybrid electrical and mechanical systems were considered as a part of this study.

Initially, the impedance analogy was considered. This equates electrical voltage with mechanical force and electrical current with velocity. This choice was made due to the logic that a both a voltage and a force being applied to a system will yield a resulting current or a velocity respectively.

Application of transfer path analysis to the electrical and mechanical variables enabled the formation of matrix equations connecting them, with variable positions in these equations based on the impedance analogy. Experimental boundary conditions that required for valid measurements were outlined.

Once transfer matrix elements had been defined, the electro-mechanical form of The Round-Trip Identity was derived from the new electro-mechanical transfer matrix. The identity features elements that are calculated from transfer functions containing both electrical and mechanical parameters.

Dimensional consistency was checked by evaluating the units of the quantities contained in the identity. These cancelled to give the expected units of acceleration per unit force, in $(\text{m/s}^2)/\text{N}$ which is consistent with the units of the mechanical Round-Trip Identity.

Single-DOF Experimental Validation

Once the Electro-Mechanical Round-Trip Identity had been derived, a simple experiment was carried out in order to show that the new form of the identity was valid in practice. This experiment featured a 350mm-long simply supported Perspex beam. The Perspex beam was supported on foam pads at either end and fitted with accelerometers in positions required by the Round-Trip Identity. A force hammer and an electrodynamic shaker were used to excite the beam at different positions, and voltage was recorded at the shaker terminals.

The results of this experiment showed that the forwards-path form of the identity was valid. The experiment was then modified to compare forwards and reverse-path measurements. This revealed difficulties with electrical measurements required for the reverse-path measurement, which requires measurement of electrical current in addition to voltage. A high-power resistor was added as a buffer between the shaker and power amp. This prevented sparking of electrical connections but did not prevent the contamination of noise on the reconstructed FRFs, likely due to low signal levels.

The experimental setup was then modified to include an additional electrodynamic shaker. This second shaker was used solely to apply an excitation at B , in order to determine if electrical measurement difficulties could be alleviated by this alternate excitation method. The results of the experiment did show an improvement over the force hammer excitation, but noise contamination on the reconstructed reverse-path FRF was still significant. The persistence of this issue suggested that an alternative method for measuring current (with a higher bandwidth, as noise was a significant problem at higher frequencies) was required.

An open-loop Hall Effect current sensor was used to measure current, providing benefits in terms of safety, ease of use and quality of reconstructed responses in comparison to the high-power resistor voltage drop method. The reasons behind this decision and extensive details regarding the implementation of this sensor can be found at Appendix B.

Changing the Electro-Mechanical Circuit Analogy

Changing electro-mechanical circuit analogy presented an improvement in the quality of FRFs that relied on current measurement. The change from the impedance analogy to the mobility analogy meant that the current measurement was made whilst the shaker was being driven, meaning that the signal was of a more easily measurable magnitude. The changes that were made to the measurement matrix are detailed in Section 2.7.3.

Identifying the optimal method of measuring current presented a challenge. Use of a simple open-loop Hall Effect sensor provided a significant improvement in the quality of reconstructed FRFs, but further experiments could benefit from the use of a zero-flux transducer, especially in the case of high-power test objects. Details of current sensor selection are provided at Appendix B.

Final SDOF Verification

Following the development of the mobility analogy forms of the identity, the Perspex beam setup was adapted in order to compare the forwards and reverse-paths. This experiment also aimed to determine which analogy was most practical to implement and gave the most accurate reconstructed FRFs.

The reverse-path mobility form of the identity provided the most accurate FRF reconstructions. There was no significant difference between hammer and shaker excitation methods. This suggests that the excitation method could be interchanged depending upon what is most practical for a given test structure.

2.10.2 - Conclusions

Theoretical Validity of the Electro-Mechanical Round-Trip Identity

The derivation of the Electro-Mechanical Round-Trip Identity was informed by a range of network theorems, each with their own requirements in terms of the systems and scenarios in which they are valid.

Boundary conditions were specified for elements of the accelerance matrix in order to ensure the validity of measured parameters. Example cases include ensuring an open or short circuit, or that no external forces are applied to the test object. The units of the reconstructed A_{cc} value were shown to be dimensionally consistent with the Round-Trip Identity.

Experimental Findings & Practical Considerations

Quality of Results

The experiments performed in Part 2 of this thesis have shown that the Electro-Mechanical Round-Trip Identity is valid both theoretically and experimentally. Reconstructed responses largely showed good agreement with measured ones, although the frequency range over which this was the case varied between experiments.

In some cases, it is likely that measurement of electrical parameters (especially current) were limited in bandwidth. This was improved when switching the current measurement method to a Hall-Effect sensor and switching the electro-mechanical circuit analogy from impedance to mobility. The switch in analogy meant that current measurement was performed whilst the shaker was actively driven, resulting in higher signal levels that were more practical to measure.

Many of the reconstructed FRFs were contaminated with noise to some extent. This largely seemed to be attributable to low signal-to-noise ratios when measuring electrical parameters, especially in the case of current measurement with the impedance analogy.

The final stage of the SDOF experimental verification (detailed in Section 2.8) obtained the highest quality results of the series of experiments, most notably with the reverse-path mobility form of the identity.

Unfortunately, it was not possible to obtain experimental data for any MDOF systems due to COVID-19 forcing closure of university facilities. Therefore, the focus has shifted to the design of a series of experiments that could be conducted to demonstrate the multiple point version of the theory.

The focus of further experimentation should be two-fold – firstly to improve the quality of results obtained for SDOF systems, and secondly to verify the identity for more complex, MDOF systems.

Practical Considerations

Difficulties and design challenges were encountered at numerous points during each stage of experimental validation. This section will identify the most significant difficulties associated with use of the identity, providing recommendations as to how these aspects can be avoided or overcome if encountered in future experiments.

Current Measurement & Back EMF

Perhaps the most notable challenge was associated with measurement of current and low signal levels due to measuring the back EMF of the electrodynamic shaker during the reverse path measurement. Realisation of this prompted the change of electro-mechanical analogy from the impedance form to the mobility form. The choice of analogy should be considered in the design of an experimental test rig, in order to ensure that signal levels are of an optimal level and minimise the chances of low signal-to-noise ratios for electrical measurements.

When using an electrodynamic shaker, the reverse path mobility form showed the most promising results, but this may vary depending on the electrical properties of the test object and the specific modal testing setup.

Experiments performed as part of this study used a LEM HX 05-P sensor to measure electrical current. This sensor was selected for several reasons:

- Galvanic isolation between the primary circuit and sensor secondary circuit to ensure safety
- Appropriate measurement range (although other sensors in the same range may be more appropriate depending on the magnitude of the current being measured)
- High level of accuracy, both in terms of magnitude and phase measurement
- Ease of implementation and low power requirements

It is recommended that further experiments should be conducted using a LEM HX SP series sensor as this requires a single positive voltage of +15v instead of a symmetrical voltage source of $\pm 15v$. This simplifies powering the sensor significantly, and this would become more apparent for more complex test rigs where a larger number of current sensors would be required.

Use of a minimum flux transducer would be recommended for future experiments, especially if they were to involve high-power test objects such as larger motors. This type of transducer offers a number of benefits compared to simple open loop current sensors such as the HX 05-P – the most relevant to this application are the eliminated gain drift with respect to sensor temperature and reduced response time. Their potential for use in environments with high levels of electrical noise could help to improve the quality of the results obtained during this study. An experiment involving a high-power test object would feature signal levels of a far greater amplitude than the experiments performed as a part of this study. As a result, it may be easier to obtain clean reconstructed FRFs in this scenario due to the increased signal-to-noise ratio.

Recommendations for Use & Limitations of the Electro-Mechanical Round-Trip Identity

Recommendations for Use of the Identity

The introduction of multiple domains to the Round-Trip Identity adds a significant amount of complexity. This comes with a number of potential pitfalls that may prevent obtaining a high-quality reconstructed FRF at a remote measurement position. As identified in the research aims, this work aims to provide recommendations that should be carried forwards as a basis for further work in the field and more complex applications of the identity.

- **Ensuring correct consideration of positions and regions**
 - Whilst there are no differences between the definitions of points in the B region and the interface C compared to the mechanical Round-Trip Identity, the physical position of the A region and enclosed a points is less obviously defined. With the mechanical form of the identity, the A region was considered as being physically positioned on the test object, adjacent to the B region, and connected by the interface, C .
 - In the Electro-Mechanical Round-Trip Identity, the A region is not considered as being in the mechanical domain, but instead as being located across the terminals of the electro-dynamic shaker.
 - The shaker and the adjacent buffer resistor were collectively considered as comprising the A region.
- **Ensuring correct boundary conditions and element definitions**

- As previously mentioned, the choice of electro-mechanical analogy will need to be considered during the design of the test rig to ensure electrical signals are of an easily measurable magnitude.
- The proposed designs of MDOF experiments featured significant numbers of boundary conditions that must be adhered to in order to obtain valid measurements. It should be determined which components are electrically and mechanically connected or provide a load or impedance in order to avoid invalidating these conditions.

Benefits and Advantages of the Identity

There are a large number of contexts where this research could be relevant, as a significant number of products where vibration is a design challenge are electrically powered. These will therefore include transduction between mechanical and electrical energy. Electrodynamic shakers being a commonly used tool used in modal analysis adds further cases where electricity and modal analysis are connected.

Performing the measurements necessary for determination of electro-mechanical quantities does not take appreciably longer versus performing solely mechanical tests and makes the give more options for analysis. If using an open-loop Hall Effect sensor for current measurement, none of the additional components that are required are particularly expensive.

The main benefit of the Round-Trip Identity is it allows computation of responses at a passive location. This passive location is often difficult to access for reasons such as not being able to disassemble the test object or the geometry of the test object impeding excitation. More options for how to experimentally reconstruct FRF responses are clearly valuable, especially so in the analysis of complex test objects.

Use of the Electro-Mechanical Round-Trip Identity in a supplementary capacity to the Round-Trip Identity could be a useful method. After measurement of all required parameters, comparison of the different forms of the identity could inform which variables provide the highest quality reconstructed FRFs.

Limitations of the Identity

As an initial investigation into the viability of this practical method, this work attempts to identify the limitations of the method in order to determine if further work should be undertaken, and if there is a significant enough a practical benefit provided for the method to potentially become adopted in industry.

Whilst the prospect of being able to reconstruct responses at remote positions using electrical and mechanical parameters is of considerable relevance to the field of structural dynamics and modal analysis, any experimental method needs to provide sufficient levels of accuracy, be easy to implement and solve or improve a problem that is not addressed by existing methods.

The original mechanical Round-Trip Identity does not require excitation at each region in order to reconstruct an FRF at a remote position. This is the case for some forms of the Electro-Mechanical Round-Trip Identity, which require excitation at positions in both regions, and at the interface

connecting them. This may mean that the electro-mechanical identity does not present a practical advantage over the original identity in certain scenarios. In some cases, there would be no reason to implement the identity if it was possible to directly excite at the position of interest, other than as a theoretical exercise to prove its validity.

Despite the improvement seen between the quality of reconstructions obtained in successive experiments, none of the experiments yielded reconstructed responses comparable in quality to those obtained by Moorhouse & Elliott in their original paper on the Round-Trip Identity.

This initial investigation has not extended to the analysis of test objects that are powered by complex signals, such as modern AC or BLDC motors, the inputs to which can be far more complex than with simpler single-phase devices. This could present difficulty in terms of how the voltage and current signals considered as a part of the Electro-Mechanical Round-Trip Identity. The position at which these signals are considered (as part of the definition of the *A* region) also becomes more complex when using multi-phase power. These aspects will be discussed, and potential solutions suggested in Part 3 of this thesis.

PART 3: PLANS FOR FURTHER EXPERIMENTATION

Part 3 Outline

As stated previously, COVID-19 forced closure of university facilities, limiting the scope of the experimental work conducted as part of this study. It had initially been planned to conduct further experiments on increasingly complex systems in order to determine if the Electro-Mechanical Round-Trip Identity could be applied to them in a valid and effective manner, and to identify difficulties associated with implementing the identity with more complex systems.

Whilst it was not possible to experimentally verify the identity in the context of MDOF systems, this work can still outline what further experiments might look like in the light of experience gained during the initial experiments. This section aims to identify difficulties that may be encountered during further experimentation and give context to the design of proposed experiments in relation to industrial practice.

Part 3: Contents

SECTION	TITLE
3.1	Applying the Electro-Mechanical Round-Trip Identity to a Plate with a Multi-Point Interface
3.1.1	Experimental Design
3.1.2	Identifying Potential Challenges
3.2	Applying the Electro-Mechanical Round-Trip Identity to a Simple DC Motor with a Multi-Point Interface
3.2.1	Motor Selection
3.2.2	Experimental Design
3.2.3	Identifying Potential Challenges
3.3	Applying the Electro-Mechanical Round-Trip Identity to More Complex Motor Designs
3.3.1	Brushless DC Motors
3.3.2	AC Induction Motors
3.3.3	Stepper Motors
3.4	Part 3: Summary, Conclusions & Further Work
3.4.1	Summary & Conclusions
3.4.2	Suggestions for Further Work

3.1 - Applying the Electro-Mechanical Round-Trip Identity to a Plate with a Multi-Point Interface

3.1.1 - Experimental Design

The aims of this experiment should be:

- To verify if the Electro-Mechanical Round-Trip Identity can be successfully applied to a plate, providing clean and accurate reconstructed acceleration FRFs
- To identify any practical issues in application of the identity to a plate
- To inform design of experiments using electric motors as test objects

The experiment proposed in this section is designed to increase the level of complexity from a multi-point interface on a simple beam by applying the identity to a more complex structure – a plate.

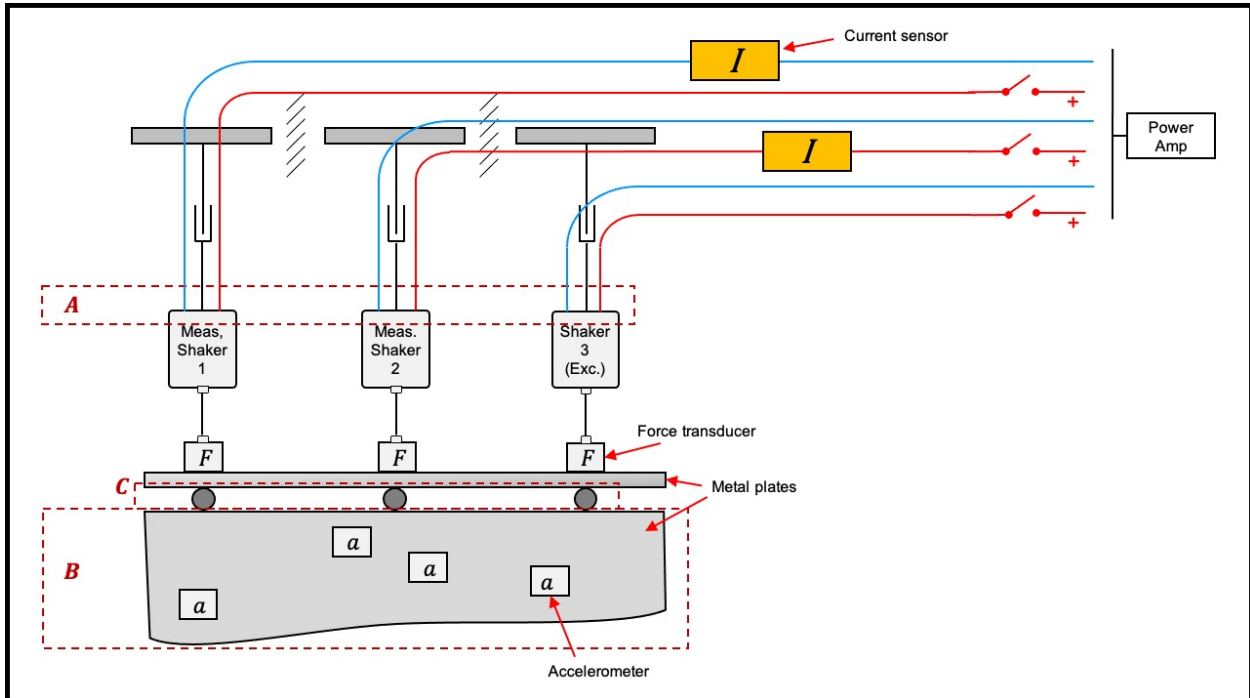
The setup and measurement procedure would be made simpler if the additional excitations were performed with a hammer, as this requires one sensor (the force hammer) that can be moved and positioned as required, instead of a potentially large number of shakers that are fixed to a certain position, and cannot be easily removed from the test structure. Use of a shaker to excite at some or all positions may be desirable in certain cases, for example with structures that would benefit from a continuous excitation method. An example of this could be a larger test structure that would not be excited to a sufficient extent by use of a force hammer.

When deciding upon the number of sensors to be applied to the test structure, there are several factors that need to be considered:

- The size of the test structure – larger structures will require more sensors
- The number of accelerometers required to over-determine the system
- The position of these sensors – these must be arranged in a manner that allows measurement of acceleration in each of the three co-ordinate axes and captures mode shapes
- Effects due to applying an increasing number of sensors (each adding a small amount of mass) – this can result in distortion of spectra when the combined weight of sensors provide a significant load to the test structure

Figure 3.1.1 shows an example experimental setup that could be used to verify if the Electro-Mechanical Round-Trip Identity can be validly applied to a plate. This consists of a plate that three shakers are coupled to, connected to a lower plate by several point connections. The regions considered in the Round-Trip Identity are indicated in Figure 3.1.1. The *A* region is difficult to represent visually, but the region should be considered to encompass electrical sensors situated between the power amp and the shaker's terminals.

Figure 3.1.1 – Proposed Experimental Design for the Analysis of a Plate with a Multi-Point Interface



It is important to ensure the isolation of shakers from each other in order to satisfy mechanical boundary conditions required for the identity. The increased number of positions also makes it more complicated to ensure that all boundary conditions are satisfied for each measurement position. For example, at some locations it will be necessary for no additional external forces to be applied to the system at any other point, excluding the required excitation at the measurement position.

3.1.2 - Identifying Potential Challenges

As a structure, a plate has low damping and a high dynamic range requirement, so getting clean reconstructed responses can be difficult - significantly more so than for a beam as in previous experiments. This will require the optimal form of the identity to be implemented, as otherwise low signal levels could lead to noise contamination of reconstructed responses. It is expected that this optimal form of the identity would be the reverse-path mobility form, consistent with the beam experiment performed following the switch to the mobility analogy (detailed in Section 2.8).

For a lightly damped structure, hammer hits must be impulsive and repeatable (with no double impacts), as random noise effects from imperfect hammer hits will be more significant.

The number of additional measurement positions makes the experimental setup significantly more complicated, requiring far more measurement channels and connected sensors. Regularisation may need to be applied to the results in order to improve the rank of the measurement matrix, reduce data redundancy and result in an over-determined matrix.

3.2 - Applying the Electro-Mechanical Round-Trip Identity to a Simple DC Motor with a Multi-Point Interface

3.2.1 - Motor Selection

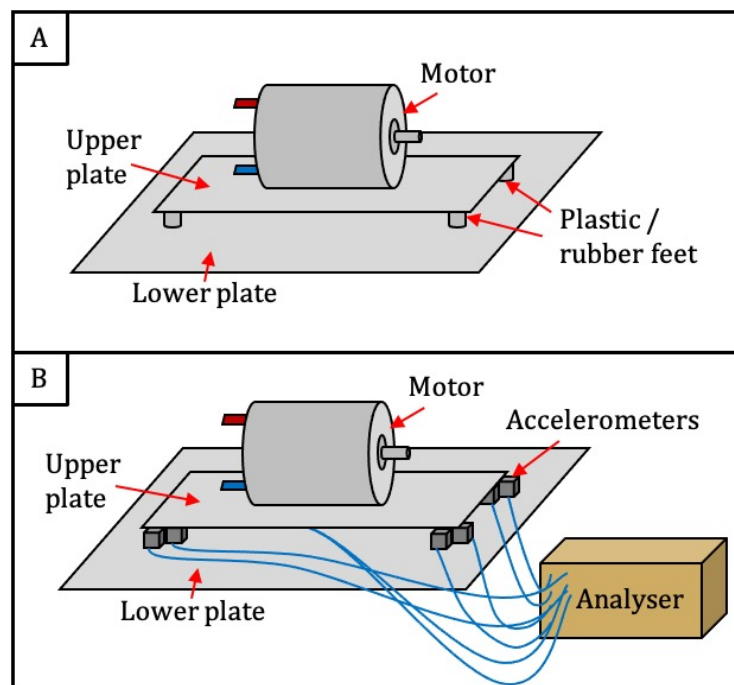
The first experiment with a motor as a test object should involve a single-phase DC motor, as this is simple to control. As identified in Section 1.3.4, the voltage input to a single-phase DC motor is proportional to the rotor speed and the current to the motor torque. Knowledge of this relationship could also allow the rotor speed and motor torque to be inferred from measurements of voltage and current respectively.

Small, low-power DC motors are readily available, simplifying the setup in terms of power requirements and reducing safety risks presented by high voltage equipment. Kim notes that although brushed DC motors are the simplest of available designs, most industries have moved away from them in favour of induction AC motors and BLDCs (Kim, 2017). The analysis of induction and BLDC motors is therefore more relevant to industrial applications.

3.2.2 - Experimental Design

A small single-phase DC motor requires a DC supply voltage in the order of magnitude of several volts. This would replace the measurement shaker used previously, and the measurement of voltage would be made across the two terminals of the motor. The motor housing would be rigidly mounted to a metal plate. Four plastic or rubber feet at the corners of this will connect this plate and another larger plate. This setup is shown in Figure 3.2.1A, with Figure 3.2.1.B showing the positions of accelerometers (which are placed around the interface feet in an arrangement that allows measurement in three co-ordinate axes).

Figure 3.2.1: Single-Phase DC Motor Experimental Setup



The *A* region can therefore be considered as being at the electrical terminals of the motor. The interface, *C* can be considered as being the points where the feet connect the two plates. The *B* region can be considered as the lower plate, with accelerometers and force transducers positioned in order to be able to describe the vibration of the test structure in three axes.

This characterisation can be achieved using multiple single axis accelerometers per position, or more ideally through the use of tri-axial accelerometers. The use of tri-axial accelerometers would add less mass to the test structure than using a large number of single axis sensors. Whilst this should not be an issue, it is important to ensure that the combined mass of the sensors applied to the test structure is significantly lower than the mass of the structure itself. This is because the boundary conditions are not satisfied due to the additional forces applied to the test structure by the combined weight of the sensors, which can result in random noise errors and distortion of reconstructed FRFs.

Voltage and current measurements can be performed in a similar manner to with the electrodynamic shaker experiments, as electrical signal paths will be similar for single-phase DC motors and shakers.

3.2.3 - Identifying Potential Challenges

With the switch of test object to an electric motor, there are several new aspects that need to be considered in order to ensure the successful implementation of the identity.

One of these is the correct positioning of accelerometers in order to accurately capture the vibration of the test object. When using an electro-dynamic shaker, the standard practice was that accelerometers were placed between the stinger and the test object. Appropriate positioning of accelerometers is important in order to obtain acceleration responses that accurately represent the test object.

The proposed experimental setup consists of a motor, the housing of which is mounted on a plate with four feet that connect the mounting plate to a second plate below it. In order to ensure an adequate signal-to-noise ratio for clean FRF reconstructions, the excitation needs to input a sufficient amount of energy to the system. This means that the motor will need to be operated in a manner that generates a vibration that is large enough in magnitude in order to be transmitted through the connected test structure and be picked up at the accelerometers in region *B* with an easily measurable amplitude. This can be solved by testing the quality of acceleration FRFs obtained by running the motor at a range of speeds.

A significant consideration when using a motor for a test object is that it may not provide enough independent excitation signals. One excitation corresponds to a single column of the measurement matrix, for example exciting with a force hammer at a particular location. To over-determine the results matrix, there must be a greater number of excitations than interface degrees of freedom. The result will be an under-determined matrix, unless further independent excitation signals can be obtained.

It is relevant to consider the mechanisms by which a motor will excite a connected structure. The mechanical forces generated by a motor can be considered in two main categories.

- Firstly, forces that arise from the generation of a changing magnetic field in the stator windings will slightly distort the motor housing and cause a vibration at the receiver
- Secondly, the motion of the rotor will result in mechanical forces that are picked up at receiver positions.

The forces due to the changing magnetic field are likely to be correlated with the input signals to the motor. There may not be any relationship between the mechanical forces and the electrical input signals to the motor.

3.3 – Applying the Electro-Mechanical Round-Trip Identity to More Complex Motor Designs

Following successful implementation of the identity to a simple single-phase DC motor, the next step should be to investigate the validity of the identity when applied to more complex motor designs. Section 1.3.4 detailed several different multi-phase motor designs. This section will detail how each of these motor types could be incorporated into an experiment that aims to reconstruct acceleration responses at passive locations by implementing the Electro-Mechanical Round-Trip Identity.

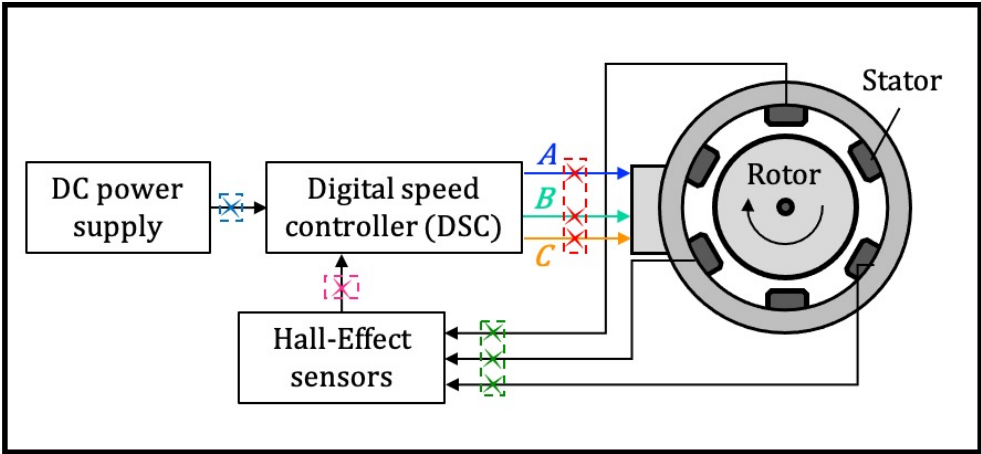
In order to determine that measurement positions selected for electrical parameters satisfy the boundary conditions that the identity requires, this section will discuss the signals that are used to power each motor type, as explained in Section 1.3.4. The nature of these signals in relation to the structure of each device will be detailed, suggesting where voltage and current sensors should be placed in each case in order to obtain a valid electrical signal.

3.3.1 - Brushless DC Motors

As explained in Section 1.3.4, a BLDC motor is controlled by stepped sequence of square digital pulses, outputted by a DSC. These sequentially excite coils on the electromagnet stator, causing the continuous motion of the permanent magnet rotor.

There are several potential positions that could be considered for measuring electrical parameters in order to implement the Electro-Mechanical Round-Trip Identity. Figure 3.3.1 shows a schematic representation of a BLDC motor, including the signal paths involved in powering and controlling the motor.

Figure 3.3.1: BLDC Motor Feedback Loop & Signal Paths



In order to determine which measurement positions satisfy the conditions required to implement the Electro-Mechanical Round-Trip Identity, the type of signal being transmitted at each point in the BLDC motor should be considered. Potential positions are indicated with coloured crosses on the paths connecting components in Figure 3.3.1. The type of signals encountered at each marked position are as follows:

- The position between the DC power supply and the DSC (marked with a blue cross) will be a DC voltage signal. For a BLDC this will be a consistent voltage level, as this power supply is only used to power the DSC itself. As a result, this is not a valid measurement position, as it will not vary as the rotational speed of the motor changes.
- The positions between the DSC outputs and the stator windings (marked with red crosses) will each be a sequence of digital square pulses with 120° phase difference between them. Even if this set of signals can be combined in order to give a value that corresponds to current, this option would be of significant complexity, and as a result this is not an ideal measurement position.
- The HE sensor will feed a signal back to the DSC (marked by either the pink or green crosses) that is proportional to the current in the stator coils. Given that a DSC is typically a microprocessor or integrated circuit that can be mounted on a printed circuit board, it would be possible to connect a wire to the pin of the DSC that receives feedback for sensing. Product datasheets will provide information as to the position of this pin, and of the scaling factor or other operations that can be applied to the feedback signal to obtain values of current. This position is likely to be the easiest position to intercept a signal, both physically in terms of attaching a wire to the circuit board, and also from a signal processing perspective, as the signal should be stationary and correspond to a value of current. Other positions may result in the measurement of a series of signals that are difficult to combine and interpret in a manner that will give a meaningful, usable signal.

3.3.2 - AC Induction Motors

AC Motor Input Signal

The input signal to an AC motor is typically a three-phase AC signal, with 120° phase difference between each successive phase.

The frequency, f_E of an AC supply is proportional to the rotational speed of the motor, as shown in Equation 3.3.1, where N_S is the synchronous speed of the rotor in ms^{-1} and N_P is the number of poles on the stator.

$$N_S = \frac{120f_E}{N_P} \quad (3.3.1)$$

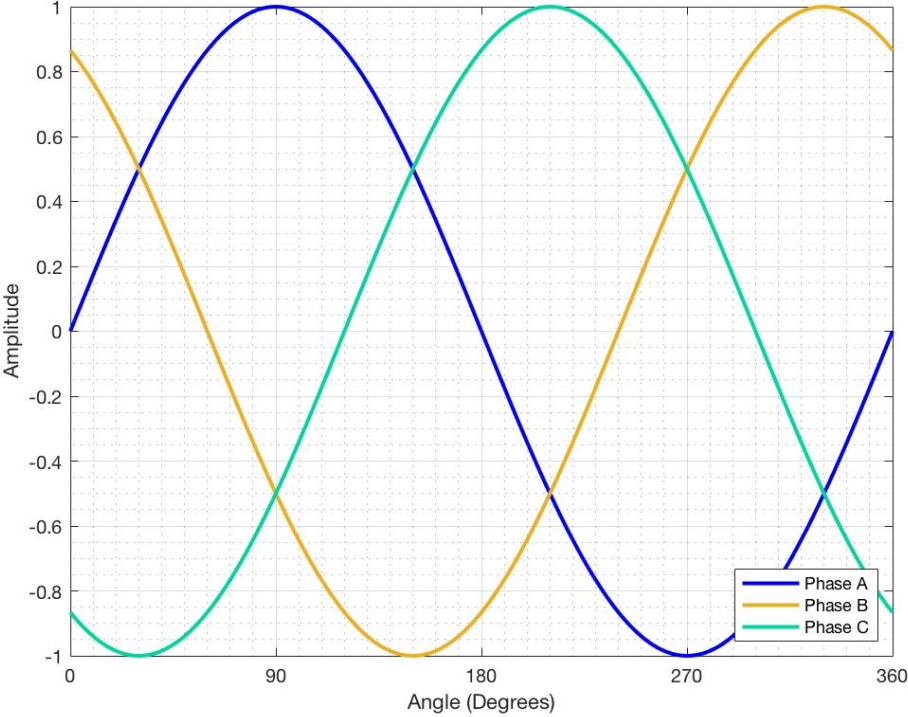
AC Motor Structure

The structure of modern AC and BLDC motors are fairly similar. Both designs are powered and controlled by the combination of a switching device (such as a DSC) and a drive unit and use feedback loops for positional control and monitoring. There are differences between the designs of the rotor and stator elements, but these do not significantly change the interactions between the other components of the motor and its control system.

As a result of this, there is significant commonality between the signals at each of the locations shown in Figure 3.3.1 between both BLDC and AC motors. One notable difference is that a BLDC motor is controlled by a set of square pulses, whereas an AC motor is controlled by three AC voltage signals,

with a 120° phase difference between them. The relationship between these signals is shown in Figure 3.3.2.

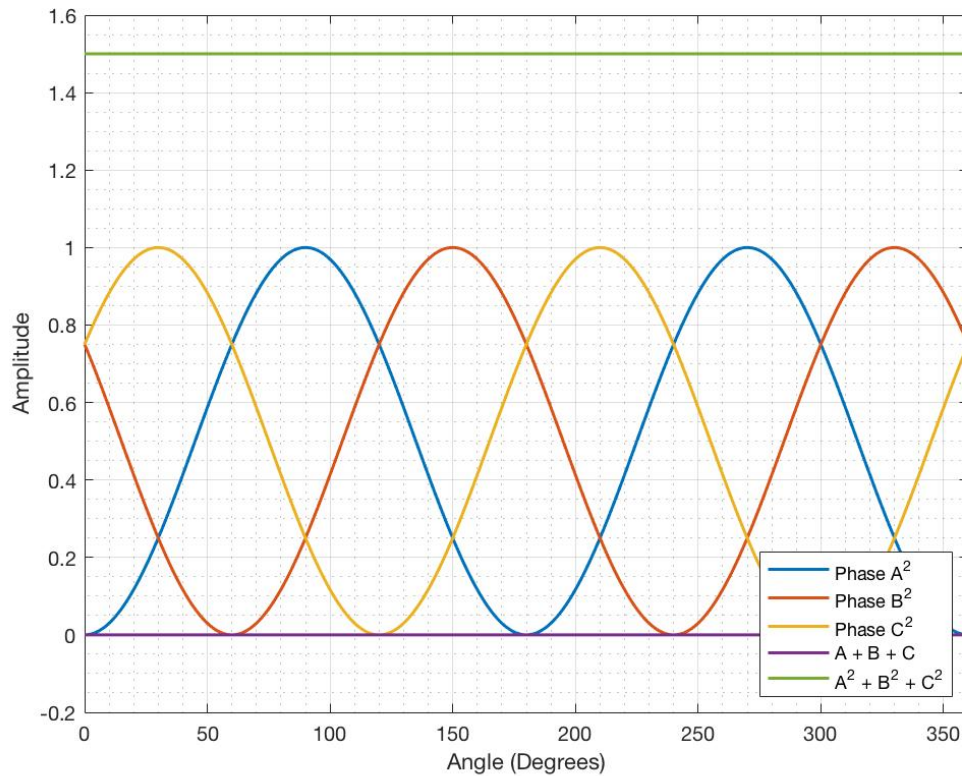
Figure 3.3.2: Three-Phase AC Supply signals



As sinusoidal signals symmetrical around the zero point on the amplitude axis, there are some interesting relationships that can be observed between individual AC power phase signals.

If squaring each individual power phase signal (shown in Figure 3.3.3), they are translated in amplitude between a minimum amplitude value of zero and a maximum value of +1v and compressed in peak-to-peak amplitude to half of their original value. The instantaneous sum of the individual squared power phases (shown in green in Figure 3.3.3) is always equal to 1.5 times the peak amplitude of an individual squared signal. The instantaneous sum of phases A, B and C is always equal to zero (shown in purple in Figure 3.3.3).

Figure 3.3.3: Squared AC Power Phases and Summations



This relationship could be used in order to combine or interpret the set of three AC signals sent from the DSC to the motor, if intercepting the electrical signals in this position to use in implementing the Electro-Mechanical Round-Trip Identity. These relationships would also allow determination of other phases or signals if a single signal was measured.

The signal fed back to the DSC from the Hall-Effect sensor used for positional control is likely to still be the most convenient option for measurement of current, as there is minimal processing of this signal required to give electrical current values (beyond applying a scaling factor to the Hall-Effect sensor output).

3.3.3 - Stepper Motors

It is expected that a stepper motor can be considered in much the same way as BLDC due to the similarity between the input signals that power the two types of motor (a series of square pulse signals). One aspect that would need to be considered is that the motion of a stepper motor, and therefore the control signals supplied to it, are likely to be far more irregular than for other motors with respect to time. This is because the use cases for stepper motors are typically environments where rapid stops, starts and direction changes are required, in contrast to other motor types that are normally operated continuously, where modifications made to rotation speed occur in a continuous manner over time. An example of this start-stop motion would be the movement of a computer-controlled robotic arm on a production line. This can be contrasted to the continuous motion of a drive unit found in an electric vehicle, which is likely to use an AC motor.

A stepper motor being subject to modal testing would need to be operated in a consistent and repeatable way throughout the measurement period. This may not be entirely representative of the standard operating conditions of a stepper motor as a result but could still give insight as to the behaviour of the motor under a range of several load conditions and rotation speeds if the motor was run continuously.

3.4 – Part 3: Summary, Conclusions & Further Work

3.4.1 - Summary & Conclusions

This section has included suggestions for conducting experiments designed to test the validity and ease of application of the Electro-Mechanical Round-Trip Identity to a range of increasingly complex systems. This initially focussed on a multi-point interface on a simple beam, then moved to a multi-point interface applied to a plate, then finally a change to using an electric motor as a test object.

A significant potential difficulty was identified with use of motors as a test object. Excitation of a structure using a motor may not result in a sufficient number of independent excitations to over-determine a measurement matrix, meaning no unique solutions would be obtainable. Two mechanisms of vibration were identified as being attributable to the changing magnetic field in the stator windings and mechanical forces due to the motion of the rotor. It was theorised that the correlation between the system inputs and the forces due to the motion of the rotor may be weak.

These two mechanisms may be able to be considered as independent excitations. This would need to be determined experimentally. Alternatively, independent excitations could be generated by controlling the signals outputted by the DSC. Sending different signals or patterns of signals to the stator windings could result in excitations considered to be independent, but again, this would need to be verified experimentally.

The simplest motor design was identified as a single-phase DC motor, so this was recommended for initial motor experiments. In terms of more complex designs, both AC and BLDC motors present their own challenges in terms of practical measurement of electrical parameters. Intercepting a signal fed back to the DSC from the Hall Effect sensors found in many BLDC and AC designs was identified as being the optimal method for determining electrical current.

Whilst the signal being measured would not itself be a current, simple scaling factors (specific to the selected Hall Effect sensor) could be applied to infer current levels. Due to the use of Hall Effect sensors, this is a safe option that should allow for high quality current responses.

Following these recommendations, there are several further aspects that could be investigated to better understand the interface between electric motors and the mechanical domain.

3.4.2 - Suggestions for Further Investigation

Equivalent circuit representations of different electric motor designs would allow for more robust analysis of the interface between an electric motor and the mechanical domain. This is because equivalent circuits are an efficient way of considering the boundaries between different domains.

These equivalent circuits could also be extended into the magnetic domain, if it was deemed beneficial to model magnetic effects as well as electrical and mechanical ones.

Blocked rotor tests can be conducted on electric motors, in order to calculate numerous electrical and magnetic parameters and determine the losses and efficiency of a motor. These parameters most notably include impedance, normal operation voltage and short-circuit current. A low-level voltage is applied in order to yield the rated current in the stator windings, then voltage and power measurements of the motor are taken (Jurkovic, 2014).

This process seems to be analogous to blocked force methods used in modal analysis. The mechanical analogy equivalent of a blocked rotor test is a short circuit test, which allows determination of variables associated with transformation type elements as described in Table 1.3.2.

The inverse of this is a no-load test. During a no-load test, the rotor is run with no resistance applied to it. This test can be used to determine the excitation current and rotational losses (Jurkovic, 2014). No load tests are equivalent to a transformer open circuit test, which is used to determine the core losses in a transformer.

When testing a motor, it is likely that blocking the motion of the rotor or conducting a no-load test would be a requirement to satisfy a boundary condition required for some elements contained in the measurement matrix. It is recommended therefore, that further research should investigate equivalent circuit representations of motors alongside the potential integration of blocked rotor and no-load tests.

As mentioned in section 3.4.1, any continuation of this research, especially if related to electric motors, would need to carefully consider methods for generating independent excitations, in order to over-determine measurement matrices.

PART 4: APPENDICES

Part 4: Contents

APPENDIX	TITLE
A	Glossary of Terms
B	Identifying the Optimal Method for Measuring Electrical Current
C	References

Appendix A: Glossary of Commonly Used Terms

This section provides explanations of the most commonly used terms in this thesis, including section references to more detailed explanations of each topic where applicable.

Accelerometer

A piezoelectric sensor used to measure acceleration at the desired position on a structure. Accelerometers can measure in a single axis, or three simultaneously. They must be rigidly coupled to a structure for accurate measurement. This is typically achieved by use of a strong adhesive or screwing onto the test structure for some models. A common model of single-axis accelerometer is the B&K Type 4507, which was used throughout this project.

Alternating Current (AC)

A method of supplying current, where the direction electron flow changes at a defined frequency. The magnitude of AC signals varies sinusoidally with respect to time. AC power often has multiple phases (most commonly three), each separated by a phase difference (120° in the case of three-phase AC power). AC power transmission is subject to lower losses over long distance transmission than direct current. As a result, alternating currents are used to transmit mains power.

Back Electromotive Force (Back EMF)

A generator can be considered as the inverse of a motor, as it converts mechanical torque into electrical energy. When a motor is spinning it will exhibit generator-like effects, inducing a current that opposes the voltage that is driving the motor. A detailed explanation of back EMF can be found at Section 2.7.2 and Appendix B.

Boundary Condition

Constraints that can be applied to the equations that describe a system in order to reflect the conditions observed at the edges of the system or component. For example, a plate that is clamped in place at its edges will behave differently when a force is applied to it compared with an identical plate that is simply supported and not held in place. For the example of a clamped plate, it can be stated that the velocity at the edges of the plate will be equal to zero.

Charge Amplifier

Piezoelectric transducers output a charge at a high electrical impedance. Frequency analysers have low impedance inputs. As such, a charge amplifier should be connected between the two devices to convert from a high-impedance charge to a low-impedance voltage and provide amplification. Most of the piezoelectric devices used during this project will include internal printed circuit board charge amplifiers so do not require external charge amplifiers. The force transducers used in some experiments require the use of external charge amplifiers.

Coherence Function

A function that indicates how closely related two signals are to each other. Coherence functions are often used to provide feedback on the repeatability of excitations in modal testing. A more in-depth explanation of coherence functions can be found at Section 1.3.2.

Determinant (of a matrix)

The determinant of a matrix is a function that is useful when trying to find the inverse of a square matrix. If the matrix is square, the determinant will be a real number. For a 2x2 square matrix, M , the determinant is as follows:

$$M = \begin{bmatrix} a & b \\ c & d \end{bmatrix} \qquad \text{Det}(M) = ad - bc$$

Direct Current (DC)

A method of supplying current where the direction of the electron flow is constant. This is in contrast to alternating current, where direction changes over time.

Electric Motor

An electric motor is a device that transduces electrical energy into mechanical torque. Electric motors are used in the design of countless products and machines in many industries across society. There are many different types of motor that offer advantages in different use cases and applications. A detailed explanation of different motor types, their structures, advantages and disadvantages can be found at Section 1.3.4.

Electrodynamic Shaker

A linearly reciprocating electrical device used in modal testing to excite structures. Electrodynamic shakers can be operated using numerous different signal types. Amongst the most common excitation signals are random noise (white, or other spectral variants), swept sine or burst random signals. Shakers are connected to a test structure via a stinger to constrain vibration to a single axis. A detailed explanation of shaker design and use can be found at Section 1.3.1.

Equivalent Circuit

Equivalent circuits are a valuable tool in the analysis of networks, especially those that comprise of components in multiple different domains. They allow problems in non-electrical domains to be expressed as a series of electrical circuit components. This allows elegant descriptions of hybrid systems and greatly simplifies calculations in many cases, as electrical network theorems can be applied instead of having to solve complex differential equations.

Force Hammer

A device, often handheld, that consists of a hammer with a force transducer at its tip. A force hammer is used to impulsively excite structures during modal testing and enables determination of the force applied to a structure when connected to a measurement system. The tip material of a force hammer can be changed to modify the frequency range of the device. More detail relating to force hammers can be found at Section 1.3.1.

Fourier Transform

A signal processing tool that converts time domain signals into the frequency domain (the inverse Fourier Transform converts signals in the opposite direction). When implemented on digital signals, a variant referred to as the Discrete Fourier Transform (DFT) must be used. The most commonly used

implementation of this is the Fast Fourier Transform (FFT), which presents a reduction in processing time over the standard DFT.

Frequency Response Function (FRF)

A frequency domain function that is the ratio of an output and input signal. FRFs can take many forms, but some of the most commonly used are acceleration, mobility, and impedance FRFs. An FRF can be converted into an impulse response by applying the inverse Fourier Transform. A detailed summary of FRFs, including descriptions of some of the most common forms, can be found at Section 1.3.2.

Hall Effect (HE)

An electro-magnetic principle which states that a current flowing in a wire will induce a magnetic field of proportional strength around that wire. This principle is used in current sensors, as measuring the strength of magnetic field induced around a wire enables calculation of the current. When implemented correctly, this is an accurate and safe way to measure current due to the galvanic isolation between the main circuit and the measurement device.

Impedance

Impedance is a quantity that expresses the extent to which an object resists motion when a force is applied to it. Different forms of impedance correspond to different domains. Mechanical impedance is the ratio of applied force to velocity. Electrical impedance is the ratio of voltage to current in a circuit. For mechanical circuits, the impedance analogy equates force with voltage and velocity with current.

Impulse Response

A time-domain function that describes the response of a system to an excitation. The Fourier Transform can be applied to the impulse response to give a frequency response.

Kirchhoff's Laws

Two fundamental laws relating to voltage and current in an electrical network, which underpin many other network theorems. Kirchhoff's Laws state that the net total of voltage or current flowing at an instantaneous point in a network is always equal to zero. Section 1.2.3 provides more detail regarding Kirchhoff's Laws.

Mobility

A quantity that is the ratio of velocity to applied force. Mobility is a commonly used frequency response function, where the input is the applied force and the output is the resulting velocity due to that force. Mobility is the inverse of mechanical impedance. More details on mobility and other FRF types can be found at Section 1.3.2

Point and Transfer FRFs

A point FRF refers to a function where the response and excitation positions occupy the same spatial point. Conversely, a transfer FRF refers to a function where the response and excitation positions are at different points, which are connected by a transfer path.

Principle of Reciprocity

The principle of reciprocity states that if a force of defined amplitude is applied to a system at point a , and the response measured at another point, b , the same response will be observed if exciting with this same force at b and measuring the response at a .

Round-Trip Identity

A mathematical identity that enables the reconstruction of a frequency response function at a remote position without the need to physically measure a response at that position. The identity was first published by Moorhouse & Elliot in 2013. A detailed explanation of the Round-Trip Identity can be found at Section 1.3.2.

Stinger

A component used in conjunction with an electrodynamic shaker to constrain vibration transmitted from the shaker to the test object to being solely in the axial direction. A stinger is a thin metal rod that is axially rigid, but laterally compliant. More detail regarding correct usage of stingers can be found at Section 1.3.1.

Tellegen's Theorem

A network theorem that is derivable solely from Kirchhoff's Laws. Tellegen's Theorem states that the instantaneous total power delivered to any point of a network is always equal to zero. This is an extension of Kirchhoff's Laws, as they describe similar relationships but in terms of voltage and current, the product of which is power. Tellegen's theorem can be applied to many types of system (including mechanical, acoustic, thermal or magnetic), not just electrical circuits. A detailed explanation of Tellegen's Theorem is provided at Section 1.2.3.

Transduction

The process by which energy is converted between different types. For example, an electric motor transduces electrical energy into a mechanical torque. A device that performs transduction is called a transducer. A detailed explanation of transduction with particular emphasis on electro-dynamic shakers is provided at Section 1.2.5.

Transfer Matrix

An analysis method that can be applied to the propagation of waves through materials comprised of a series of discrete layers. Each layer is described in terms of the properties of the material itself, and the interfaces between adjacent layers. Transfer matrices and transfer path analysis are explained in detail in Section 2.4.2.

Transposition (of a matrix)

A transposed matrix has had its rows geometrically switched to be its columns and vice versa. This operation is applied to some of the matrices in the implementation of the Round-Trip Identity. If the original matrix is A , the transposed form is denoted as A^T .

Two-Port Analysis

A method for analysing networks or systems in terms of their inputs and outputs, where a set of equations can be determined that connects the inputs and outputs of a system. This can be

considered as a “black box” type approach, where the properties of the system on a more precise level are arbitrary. Two-port analysis can be applied to many types of system, including mechanical, electrical and acoustic. A detailed explanation of two-port analysis can be found at Section 1.2.3.

Zero-Flux Transducer

A device that can be used to measure current. Essentially a more complex version of a simple open-loop Hall Effect Sensor, zero-flux transducers allow extremely precise measurement of current. They are also suitable for high-power applications. A detailed explanation of the design and benefits of zero-flux transducers can be found at Appendix B.

Appendix B: Identifying the Optimal Method for Measuring Electrical Current

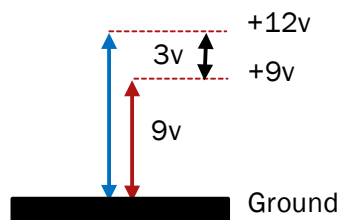
Introduction

In order to allow a high-quality reconstruction in the reverse direction, an accurate measurement of current must be made. This measurement needs to be accurate in terms of both magnitude and phase. There are two types of method for measuring current: with conductor interruption and without it.

Measurement with conductor interruption means to insert a device into the circuit in order to measure the voltage drop across it, and then infer the current using Ohm's Law. The ideal component to use for this is one that has the least footprint on the measurement circuit, so will have very low resistance. It should also be stable at an appropriate range of temperatures and have sufficiently low tolerance that the application of Ohm's Law is valid. Such a resistor is referred to as a shunt. Shunts are only usually operated at up to 60% of their stated current value, to prevent physical deformation due to increased temperature. They can be used to measure both alternating and direct currents.

One of the major issues with using a shunt or another low magnitude resistor is that high common-mode voltages can occur in the circuit, especially when a power amplifier is included in the signal path as is the case in these experiments. Common-mode voltages occur when both the positive and negative rails have a high absolute voltage relative to ground. Whilst the potential difference between the two rails is still low, the common mode voltage can be high, which can be dangerous due to the risk of electrocution. A visual representation of this is shown in Figure B.1, where the potential difference between the two rails is 3v, but the common mode voltage is given by the mean value of the two rail levels and is +10.5v:

Figure B.1: Diagrammatic Representation of Common-Mode Signals



This was an important consideration when designing experiments where current measurement was required, as in some cases common mode voltage can rise to be as high as the mains supply voltage, presenting a significant safety issue.

Measurement without conductor interruption is performed using equipment that is external to, and galvanically isolated from, the circuit, which does not interrupt the circuit in any way. A simple and inexpensive tool for this is a current clamp, which uses the principle of electromagnetic induction (also referred to as the Hall Effect) to generate a potential difference in the coils of the measurement device. The induced potential difference is proportional to the intensity of the magnetic field generated by the original circuit.

The advantages of this type of measurement method are the ease of setup and the relative safety compared to conductor interruption methods, due to the galvanic isolation between the primary experimental circuit and that of the measurement device (which will be referred to as the secondary circuit). It was decided that measurement without conductor interruption would be the safest option and would be continued with as a result.

Many of the simpler and less expensive variants of current clamps are not able to measure the magnitude or phase of the current accurately enough for high-precision applications such as modal analysis. The magnitude of this phase shift can be up to 10 degrees with some lower specification equipment, which would not be appropriate in this context. There is also scope for error in application of the clamp to a circuit in terms of its positioning and contact with experimental circuitry, which can give inconsistent or noisy readings.

In order to confirm that a basic set of current clamps were insufficient to accurately measure current, the single shaker experiment was repeated, but current clamps were applied to the circuit to measure current instead of the previously used high-power resistor. The results of the comparison are shown in Figure B.2:

Figure B.2: Electro-Mechanical Round Trip Comparison – Measured vs. Current Clamp Responses (Reverse-Path)

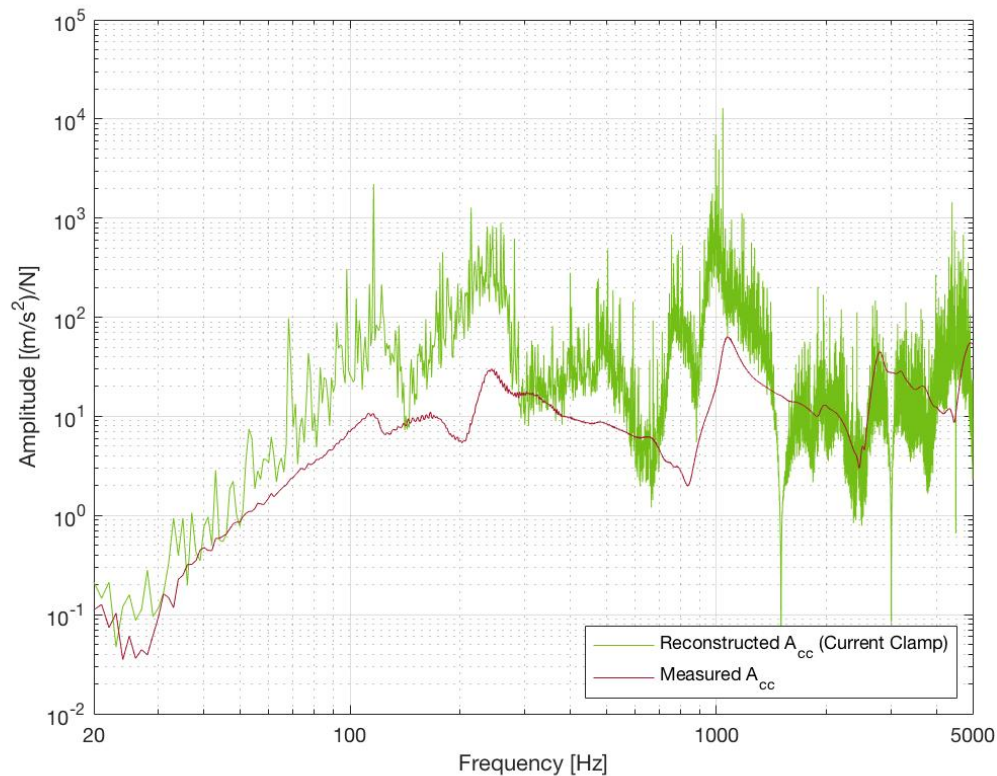


Figure B.2 shows poor agreement between the measured and reconstructed responses. The current clamp response is also contaminated with noise, far beyond an acceptable level. This test shows that the available current clamps were not an appropriate current measurement solution. An alternative

method that with lower potential for positioning error, greater stability and a lower noise floor was required.

A potentially suitable, cost-effective method was identified as using Hall Effect current sensor chips mounted on a circuit board that broke out to the rest of the experimental setup. The LEM HX 05-P was selected as its sensitivity and current measurement range were appropriate. Many similar sensors that are available are intended for measuring larger currents (as high as several thousand amps, and the HX 05-P is one of a small proportion designed for the moderately low currents likely to be measured in these experiments (in the order of magnitude of several amps).

This type of Hall Effect sensor has a significantly lower noise floor than the available current clamps and provides the previously mentioned benefit of galvanic isolation between its primary (experimental) and secondary (output) circuits, ease of setup and safety. Testing showed that its response rate and phase measurement were also sufficiently accurate for the testing requirements. Simple Hall Effect sensors are small, lightweight and also have a low power consumption, all of which contribute to their ease of use.

A significantly more accurate way to measure current with no conductor interruption is using a zero-flux current transducer (also referred to as a closed loop current transducer). These are designed for extremely precise measurement of both the magnitude and phase of the current, often in high-power scenarios, where it would be extremely dangerous to interrupt the primary circuit. They also work because of the Hall Effect, but include an additional circuit that generates a compensation current in the secondary circuit of the device, creating a magnetic flux that is equal in magnitude but opposite in direction to the magnetic flux generated by the primary current, resulting in a net flux of zero. This has several benefits over the simpler open-loop designs (LEM, 2004 and 2019):

- Eliminated gain drift with respect to temperature variation
- Significant extension of the measurement bandwidth (at high frequencies)
- Faster response time
- The output signal is easily scalable, making the devices suitable for high noise environments

The most useful benefits in relation to this application of the sensor are the lack of gain drift and reduced response time, both of which could help to provide higher quality data. Any improvement in signal to noise ratio is desirable. The extension to bandwidth is not particularly relevant in this case, as the bandwidths of Hall Effect sensors are already more than adequate given the frequency range of interest in these experiments.

Zero-flux transducers behave very linearly with extremely low phase or offset error. For example, the LEM IT 60-S zero flux transducer is capable of measuring up to 42A currents and has a stated accuracy of 0.027% (LEM, 2013). Models are available with specifications appropriate for measurement of very high currents, so it should be noted that this method would be viable if applying the Electro-Mechanical Round-Trip Identity to high-power test objects, such as large electric motors or appliances. It is also a safe option to perform due to the galvanic isolation between the sensor's primary and secondary circuits.

Despite the numerous advantages, there are several drawbacks to zero flux transducers. They require far higher supply of power, as the bias current needs to become larger with increasing primary current to ensure zero flux. This will be most significant for high-current models. The more complex construction of zero flux transducers in comparison to open-loop Hall Effect sensors also makes them considerably more expensive. Models are available that will connect directly to analyser systems with minimal setup, removing the need to design and build a printed circuit board to mount the device on.

Considering these factors, the Hall Effect sensor was deemed appropriate for initial investigations but investing in a zero-flux transducer would be beneficial for any further work.

Sensor Setup

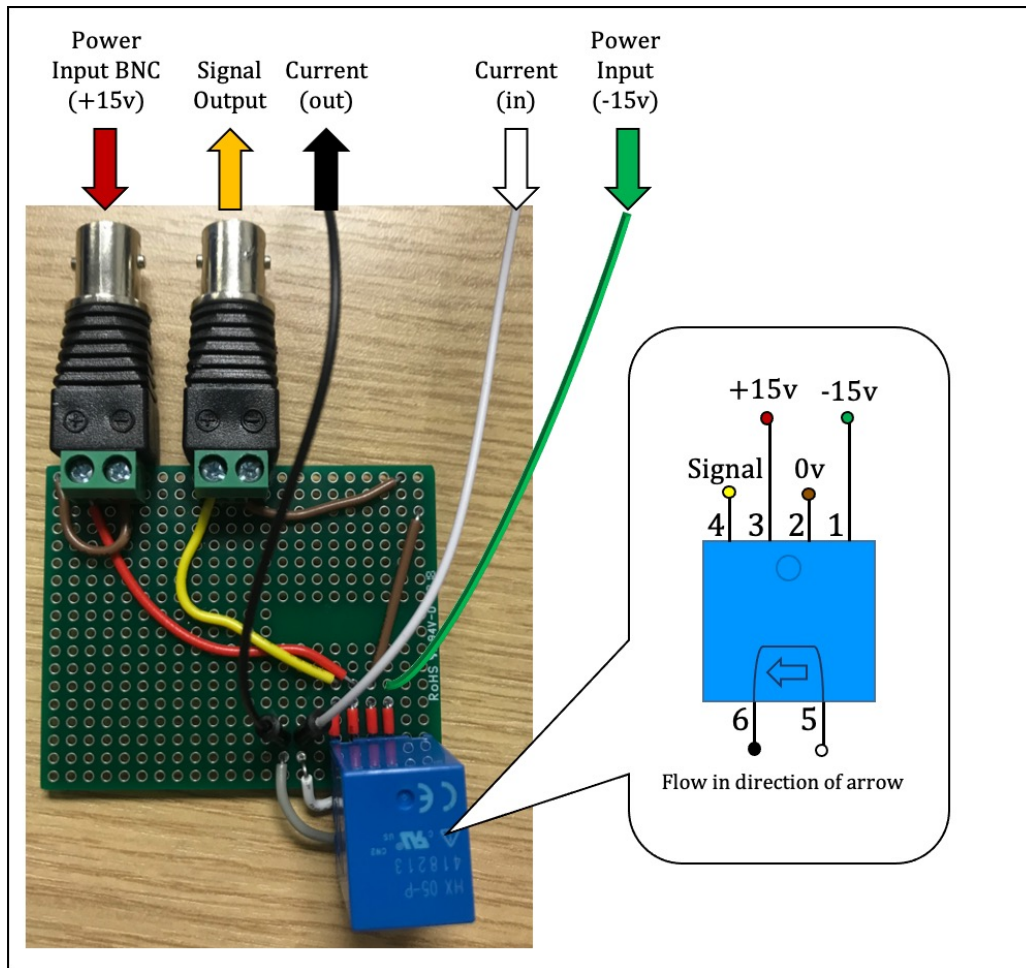
This section will outline the implementation of the LEM HX 05-P Hall Effect current sensor and its connection to the rest of the experimental setup. Relevant specifications of the sensor are shown in Table B.1.

Table B.1: Relevant LEM HX 05-P Current Sensor Specifications (LEM, 2019)

Parameter	Value
Nominal current (max.)	$\pm 15\text{A}$
Supply voltage	$\pm 15\text{V}$, 0V (Symmetrical supply required)
Frequency bandwidth	50kHz
Accuracy	$\pm 1\%$
Dimensions (L x W x H)	15.4mm x 20mm x 19mm

Figure B.3 shows the structure of the sensor with pin assignments and input and output and connections.

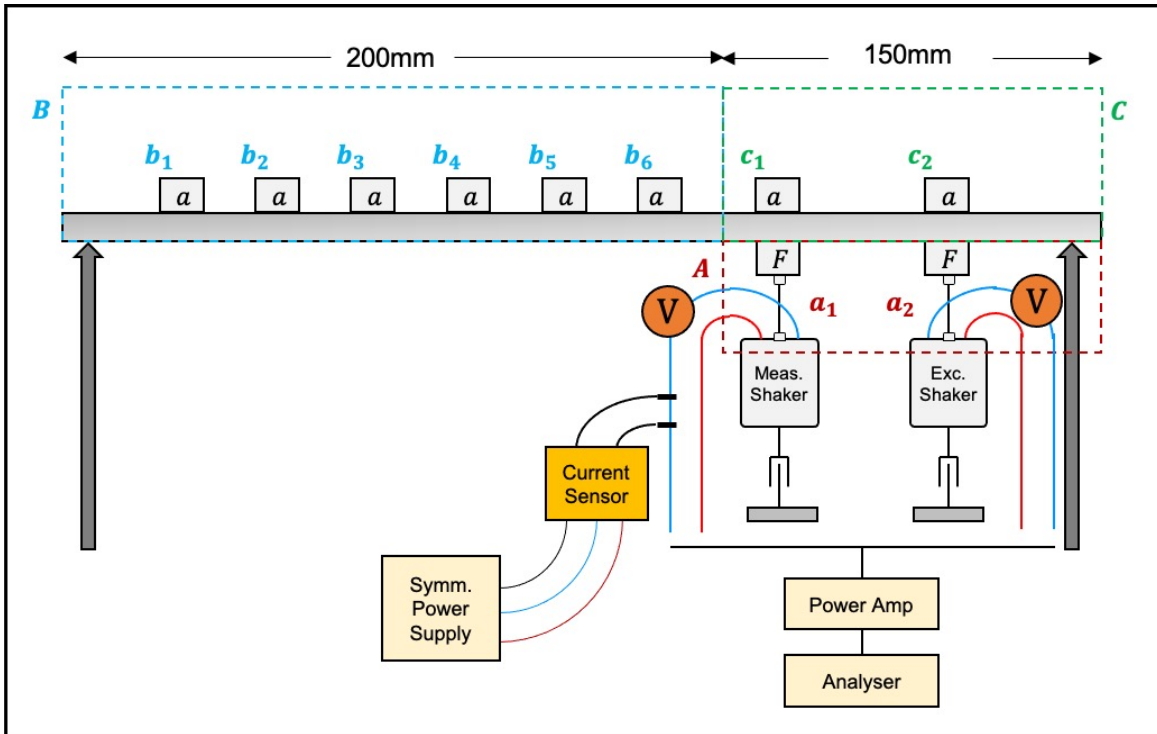
Figure B.3: Current Sensor Structure & Pin Assignments



Current Path & Connections

The primary circuit current flowed into pin 5 and out of pin 6 of the sensor. This was connected in between the shaker and the power amp, as shown in Figure B.4.

Figure B.4: Current Sensor Position Diagram



Powering the Sensor

Positive and negative voltages and a reference zero voltage are required to power the HX 05-P. The positive was at pin 3. The connection to ground was at pin 2 (ground). A symmetrical AC power supply was used for this, set to ± 15 volts.

The initial prototype used a BNC connector for the positive and zero voltage pin connections, with the negative voltage being added subsequently via the green banana cable at pin 1. Subsequent sensors used three banana connections: one positive, one negative and one connected to the common ground.

For ease of powering the sensors, it is recommended that a LEM HX SP range sensor of the appropriate measurement range is used in future experiments. This variant only requires a single positive supply voltage, instead of the symmetrical power required for the LEM HX P range. This would allow power to be provided to the sensor via a single BNC connector, reducing complexity of the device.

Signal Determination & Interpretation

The sensor signal output from pin 4 was connected to the analyser input directly via a BNC connection and also connected to the common ground.

The maximum measurable current with the HX 05-P is ± 15 A. The maximum sensor output is ± 4 v, outputted at pin 4. This will be outputted by the device when it senses a value of ± 15 A. Interpolating linearly below this allows determination of the current being measured. The linear interpolation over the measurement range is shown in Figure B.5. The scaling factor of $4/15$ ($0.2\bar{6}$) was multiplied with sensor output voltage signal to determine the current flowing through the device. This was implemented once data had been imported into MatLab.

Figure B.5: Linear Interpolation Over Sensor Measurement Range

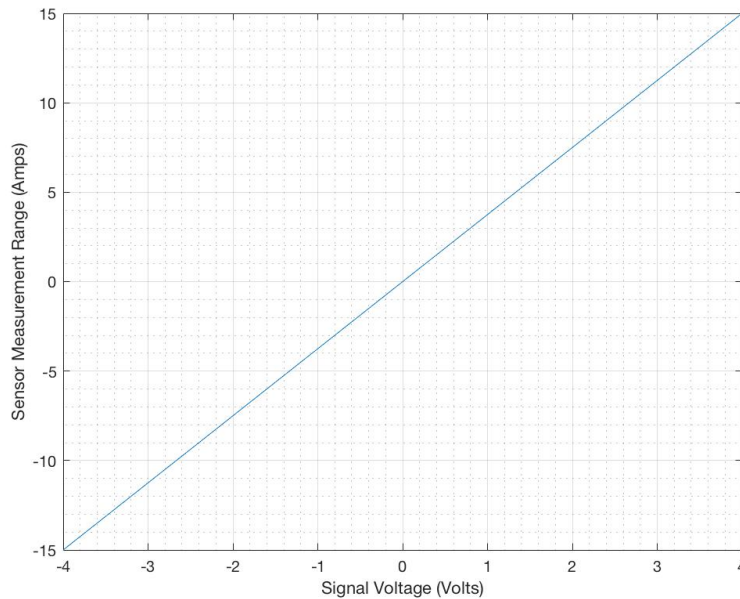


Table B.1 quotes the accuracy HX 05-P sensor as being $\pm 1\%$. The documentation for the device also states that this is the case at a nominal temperature of 25°C , with the documentation stating that generally the accuracy of an open-loop Hall Effect sensor is in the region of several percent, limited by the following factors (LEM, 2004 and 2019):

- The DC offset of the device at zero current flow
- The DC magnetic offset
- Gain error
- Linearity
- Output noise floor
- Bandwidth limitations

Shifts in temperature can also cause drift in DC offset and the gain of the device.

Conclusions

This appendix has discussed the viability of several options for measurement of electrical current with sufficient accuracy to allow high-quality reconstructed responses when implementing the Electro-Mechanical Round-Trip Identity.

Use of an open-loop Hall Effect sensor was identified as being most appropriate for this initial investigation, but with the recommendation that a zero-flux transducer (or closed-loop Hall Effect sensor) would be a higher-precision option if pursuing further work in this area. A zero-flux transducer was not selected for these initial investigations due to the significant cost of these sensors.

Appendix C: References

- Ashory, M. (1999). *High quality modal testing methods*. Doctoral dissertation, University of London.
- Avitabile, P. 2017, *Modal Testing: A Practitioner's Guide*, John Wiley & Sons Incorporated, Newark.
- Beranek, L. (1996). *Acoustics*. Michigan: American Inst. Of Physics.
- British Standards Institution (2009). BS61094-2: *Electroacoustics – Measurement microphones – Part 2: Primary method for pressure calibration of laboratory standard microphones by the reciprocity technique*.
- Brown, D. and Allemang, R. (2007). *The Modern Era of Experimental Modal Analysis - One Historical Perspective*. Cincinnati: Sound & Vibration, pp16-25
- Brown, D. and Peres, M. (2008) *Impedance Modelling of Modal Exciters*. Proceedings of The International Conference on Noise and Vibration Engineering 2008.
- Campa, G. and Camporeale, S. (2010). *Application of Transfer Matrix Method in Acoustics*. European COMSOL Conference 2010.
- Cloutier, D., Avitabile, P., Bono, R. and Peres, M. (2009), *Shaker/stinger effects on measured frequency response functions*. Proceedings of the 27th International Modal Analysis Conference (Vol. 122)
- Della Flora L. and Gründling, H. (2008), *Time domain sinusoidal acceleration controller for an electrodynamic shaker*, IET Control Theory Appl., 2008, 2(12), pp. 1044–1053
- Elliott, A. and Moorhouse, A. (2017), *Application of The Round-Trip Theory for the Indirect Measurement of Point Impedance by Air-Borne Excitation*, ICSV24, London, 23-27 July 2017
- Ewins, D. (2000). *Modal Testing. 2nd ed.* Baldock, England: Research Studies Press.
- Firestone, F. (1933), *A New Analogy Between Mechanical & Electrical Systems*, The Journal of The Acoustical Society of America, 4(249), pp.249-267
- Firestone, F. (1938), *The Mobility Method of Computing the Vibration of Linear Mechanical and Acoustical Systems: Mechanical-Electrical Analogies*. Journal of Applied Physics, 9(373)
- Green, G. (1828), *An Essay on the Application of Mathematical Analysis to the Theories of Electricity and Magnetism*, Nottingham: T. Wheelhouse
- Halvorsen, W. and Brown, D. (1977). *Impulse technique for structural frequency response testing*. Sound and Vibration, 11(11), pp.8-21.
- Helmholtz, H. and Nagel, W. (1909). *Handbuch Der Physiologischen Optik*. Hamburg: Voss.
- Jurkovic, S. (2014). *Induction motor parameters extraction*. Educyclopedia-Electronics.

Karakan, E. (2008), Estimation of Frequency Response Function for Experimental Modal Analysis, MSc Thesis, Izmir Institute of Technology, p81.

Kim, S. (2017). *Electric Motor Control: DC, AC, and BLDC Motors*. Elsevier

LEM Components (2004), *Isolated Current and Voltage Transducers: Characteristics – Applications – Calculations*, 3rd Edition

LEM Components (2019), *Current Transducer HX 03 ... 50-P (Datasheet)*. Version 15.

LEM Components (2013), *Current Transducer IT 60-S ULTRASTAB (Datasheet)*. Version 2.

Manik, D. (2017), *Vibro-Acoustics: Fundamentals and Applications*, Boca Raton: CRC Press, p241.

Marudachalam, K. (1991), *An attempt to quantify errors in the experimental modal analysis process*. International Modal Analysis Conference (IMAC), Florence, Apr. 15-18. Vol. 2, pp. 1522-1527.

Meggitt, J. (2017), *On In-situ Methodologies for the Characterisation and Simulation of Vibro-Acoustic Assemblies*. PhD Thesis. Acoustics Research Centre, The University of Salford

Moorhouse, A. and Elliott, A. (2013), *The “round trip” theory for reconstruction of Green’s functions at passive locations*, J. Acoust. Soc. Am. 134 (5), pp.3605-3612

Moorhouse, A., Elliott, A. and Evans, T. (2009), *In situ measurement of the blocked force of structure-borne sound sources*, Journal of Sound and Vibration 325, pp.679-685

Moorhouse, A., Evans, T. and Elliott, A. (2011), *Some relationships for coupled structures and their application to measurement of structural dynamic properties in situ*, Mechanical Systems and Signal Processing 25, pp.1574–1584

Penfield, P., Spence, R. and Duinker, S. (1970), *A Generalised Form of Tellegen’s Theorem*, IEEE Transactions on Circuit Theory, 17(3), pp.302-305.

Potton, R. (2004). *Reciprocity in optics*. Reports on Progress in Physics, 67(5), pp.717-754.

Quintela, F., Redondo, R., Melchor, N. and Redondo M. (2009). *A General Approach to Kirchhoff’s Laws*, IEEE Transactions on Education, 52(2), pp.273-278

Ramachandran, R. and Ramachandran, V. (2001). *Tellegen’s Theorem Applied to Mechanical, Fluid and Thermal Systems*. American Society for Engineering Education,

Randall, A. (1987). *Frequency Analysis*. Denmark: Bruel & Kjaer.

Rayleigh, J. (1878). *The Theory of Sound, Vol 2*. Cambridge MA: Macmillan.

Rente, A., (1867). *Basis for a General Theory of Functions of a Variable Complex Quantity*, Göttingen, pp 8–9.

Schmitt, R. (2002). *Electromagnetics Explained: A Handbook for Wireless/ RF, EMC, and High-Speed Electronics*. Newnes. p.75

Smallwood, D. (1996). *Shaker force measurements using voltage and current* (No. SAND-96-1354C; CONF-961179-5). Sandia National Labs. Albuquerque, NM.

Smallwood, D. (1997). *Characterizing electrodynamic shakers* (No. SAND-96-2791C; CONF-970543-1). Sandia National Labs., Albuquerque, NM.

Strang, G. (2006). *Linear Algebra and Its Applications*. 4th Edition. Cengage Learning, p225.

Strømmen, E. (2014). *Structural Dynamics*, Springer Science & Business Media, p89

Thite, A. and Thompson, D. (2003). *The quantification of structure-borne transmission paths by inverse methods. Part 1: Improved singular value rejection methods*. Journal of Sound and Vibration, 264(2), pp.411-431.

Thite, A. and Thompson, D. (2003). *The quantification of structure-borne transmission paths by inverse methods. Part 2: Use of regularization techniques*. Journal of Sound and Vibration, 264(2), pp.433-451.

Thite, A. and Thompson, D. (2006). *Selection of response measurement locations to improve inverse force determination*. J. Applied Acoustics 67, pp.797–818